Development of Highly Durable Antifogging Materials Based on Polysilsesquioxane with Hydrophilic Groups

（親水基を有するポリシルセスキオキサンをベースとした高耐久性防曇材料の開発）

March, 2023

Tetsuya Maeda

Hiroshima University

Contents

Chapter 1: Introduction

1. Introduction to antifogging materials

In recent years, antifogging materials have been attracting attention to prevent fogging on the solid surface. Fogging occurs when atmospheric moisture in the air condenses and water droplets with a diameter of 190 nm (half of the shortest wavelength of visible light) or longer adhere to the solid surfaces (**Figure 1**) [1-4]. Fogging on the solid surface scatters light and significantly reduces transparency and results in the poor optical performance of transparent and optical materials such as eyeglasses, goggles, solar cells, microscopes, camera lenses, mirrors, automobile windshields, headlamps and other display devices [5-13]. Fogging is a serious problem affecting not only a daily comfort but also a safe life. In surgical treatment, the fogging at the lens tip of the medical endoscopes may be life-threatening [14]. In windshields of vehicles, fogging may cause serious traffic accidents due to a reduction in the driver's visibility [15, 16].

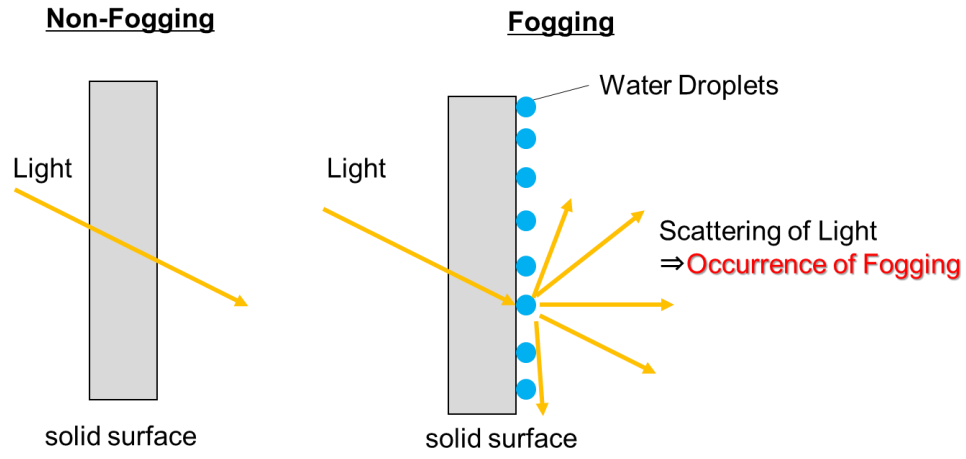

Figure 1. Mechanism of fogging occurrence.

Considering global warming and CO_2 emission, fogging has a negative effect on energy efficiency. In solar cells, fogging induces light scattering and reduces the amount of power produced [7, 17]. A standard method for preventing fogging in vehicles is to warm the cold air outside by a heater, and the

warmed and dried air is blown to the windshield to prevent fogging [18]. Operation of the defogger system, however, requires large energy consumption, leading to lower cruising distance when the defogger system is activated. This is more serious for electric vehicles that cannot utilize the waste heat from the engine [19], compared with internal combustion engine vehicles [20]. Therefore, a facility that can reduce the energy consumption for the defogger system is desired in electric vehicles. Consequently, antifogging materials have drawn attention because they can remarkably reduce the energy consumption of antifogging systems, including the defogger and a hot wire on the windshields surface.

2. Antifogging materials

There are three types of antifogging materials: (1) superhydrophilic material, (2) superhydrophobic material, and (3) water-absorbing material, as shown in **Figure 2**.

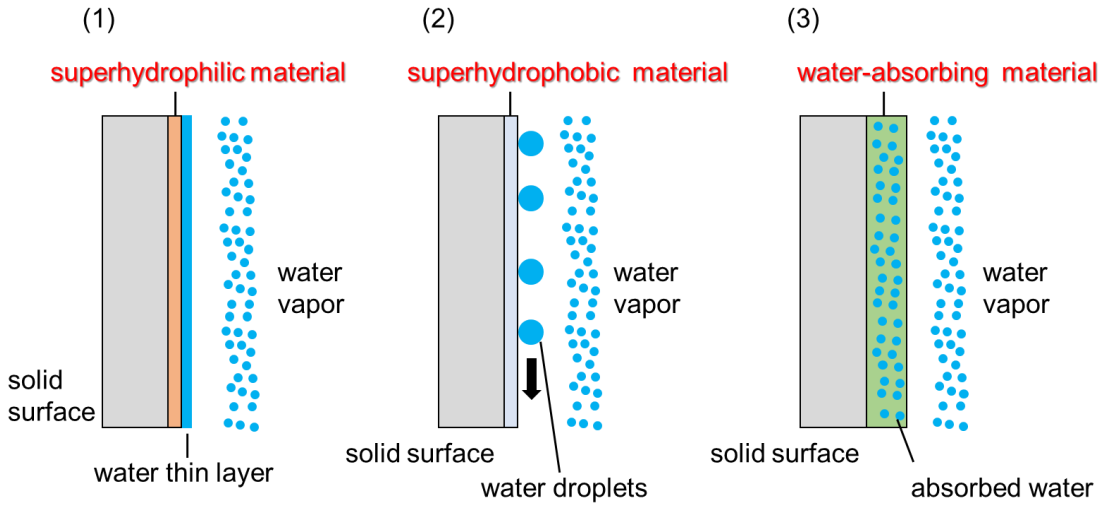

Figure 2. Antifogging mechanism of each antifogging material. (1) superhydrophilic material, (2) superhydrophobic material, and (3) water-absorbing material.

2.1 Superhydrophilic antifogging material

In the superhydrophilic material, water droplets on the superhydrophilic surface with a water contact

angle (CA) of less than 5° spread over the surface and form a thin water layer to prevent light scattering. For example, inorganic oxides such as titanium oxide (TiO_2) and silicon oxide (SiO_2) have been studied [21-24]. TiO_2 film exhibits superhydrophilicity after ultraviolet (UV) irradiation, because the concentration of OH groups on the TiO_2 surface increases by UV irradiation [25], and exhibit excellent antifogging properties. However, TiO_2 films quickly become hydrophobic in the dark, limiting their application [26]. Furthermore, the thin water layer formed on the surface of hydrophilic materials is frozen below the freezing point, resulting in a significant loss of transparency and limiting their application in environments exposed to freezing temperatures [1].

2.2 Superhydrophobic antifogging material

In the superhydrophobic antifogging material with water contact angles exceeding 150°, water droplets are repelled on the surface. Bio-inspired by the characteristic microstructure of mosquito eyes and lotus leaf, superhydrophobic antifogging material that combined nanoscale surface roughness and low surface energy has been studied [1, 2, 27, 28]. Micro/nano roughness films were fabricated by combining polydimethylsiloxane and silicon dioxide [27]. This surface exhibited excellent superhydrophobic antifogging performance with a water contact angle of 158°. However, the superhydrophobicity typically originates from the nanoscale surface roughness arising from the characteristic microstructure, leading to poor mechanical strength and transparency. Therefore, the application of superhydrophobic material as antifogging material is limited.

2.3 Water-absorbing antifogging material

Water droplets are quickly absorbed into the water-absorbing material, exhibiting antifogging properties. The water-absorbing antifogging materials have been extensively studied to overcome the disadvantages of superhydrophilic and superhydrophobic materials. The water-absorbing materials

have been reported to exhibit high antifogging properties by rapidly absorbing water in hydrophilic polymers containing hydrophilic functional groups such as hydroxyl groups, carboxyl groups, and ethylene glycol [3]. They include poly(acrylic acid) (PAA)/poly(vinyl alcohol) (PVA) [29, 30], PAA/poly(ethyleneimine) [31], PVA/Nafion [32], poly(ethylene glycol) [33], and poly(vinylpyrrolidone) [34]. The absorbed waters in hydrophilic polymers exist as nonfreezing water via strong hydrogen bonding [29]. The disadvantage of water-absorbing polymer films typically is low scratch resistance [30, 31]. The advantage and disadvantage of three types of antifogging materials are summarized in **Table 1**. This thesis focuses on the water-absorbing antifogging material, which is considered to have a wide range of applications.

Table 1. The advantages and disadvantages of three types of antifogging materials

Type of antifogging material	Examples of antifogging material	Advantage	Disadvantage
Superhydrophilic material	TiO_2, SiO_2	High antifogging	Restrictions on use in specific environments
Superhydrophobic material	Polysiloxane	No freezing	Low mechanical strength Low transparency
Water-absorbing material	PVA, PAA	High antifogging No freezing	Low scratch resistance

3. Performance required for water-absorbing antifogging material

As mentioned above, water-absorbing antifogging materials have attracted much attention in recent years, and numerous reported examples exist. Typical performance of water-absorbing antifogging materials and their respective issues are described below.

3.1 Water uptake

Numerous studies in recent years have improved the water uptake of water-absorbing antifogging

material because the more significant capacity to absorb water into the material, the higher the antifogging performance. The content of these studies can be outlined in a model equation for the swelling ratio of polymer. Various model equations have been discussed to express the swelling ratio of polymers and Flory's theory is known as one of the representative model equations [35]. According to Flory's theory, the water uptake of the polymer is related to the crosslinking density, ionic osmotic pressure, and affinity of the polymer with water. The swelling ratio Q can be expressed by Equation (1).

affinity of the polymer with water

$$Q^{\frac{5}{3}} = \left[\left(\frac{i}{2V_u S^{\frac{1}{2}}} \right)^2 + \frac{\frac{1}{2} - X_1}{V_1} \right] V_e/V_0 \qquad (1)$$

ionic osmotic pressure

crosslinking density

Q: water absorption, V_e/V_0: crosslinking density of polymer, $(1/2 - X_1)/V_1$: interaction between polymer and solution, i/V_u: fixed charge per unit volume of polymer, S: ionic strength of external solution

Previous research on achieving high water uptake in water-absorbing antifogging materials has been carried out regarding three factors of Flory's theory. Concerning water affinity of the polymer, almost all water-absorbing antifogging materials have polar hydrophilic functional groups such as hydroxyl groups, carboxyl groups, and ethylene glycol to interact with water molecules through hydrogen bonding and dipole interaction [29-33]. For ionic osmotic pressure, ionic unis such as ammonium chloride and sulfobetaine that have stronger interaction with water than neutral polar functional groups are introduced into the polymer structure [36, 37]. For crosslinking density, highly crosslinked polymers limit the amount of water absorbed into the polymer material because the higher crosslinking density results in the less swelling of polymer. Therefore, linear polymers such as PVA and PAA,

which are not crosslinked structures, are often used for antifogging materials [29-32]. These considerations indicate that the water uptake can be controlled by appropriately designing the hydrophilic groups and crosslinking structure. However, material design based on the Flory's theory often involves a trade-off between water uptake and durability such as scratch resistance and environment resistance.

3.2 Scratch resistance

As mentioned above, polymers without a crosslinked structure, such as PVA and PAA, have high antifogging performance due to their high water uptake. However, their practical application has been difficult due to low scratch resistance, which causes deterioration in transparency and antifogging properties after long-term use [32]. Therefore, many studies have discussed previously the development of new antifogging materials with high scratch resistance.

Hydrophilic organic polymers containing silica nanofillers have been investigated to improve the scratch resistance of antifogging materials [38, 39]. For example, adding SiO_2 filler into PVA can enhance the scratch resistance [5]. However, the addition of filler sometimes suppresses the antifogging performance that is usually in a trade-off relationship with the scratch resistance. Furthermore, silica nanoparticles' aggregation may reduce the transparency of antifogging films.

Self-healing materials that heal scratches by external stimuli such as heat, solvents, and light have been well studied recently and the self-healing property can improve the scratch resistance of hydrophilic organic polymers with low cross-linked structures [40-42]. Antifogging materials with self-healing ability often contain non-covalent bonding; e.g., electrostatic interactions and hydrogen bonds [43-46]. For example, antifogging copolymers based on poly(sulfobetaine methacrylate) (PSBMA) and poly(2-hydroxyethyl methacrylate) (PHEMA) can quickly heal scratches in the presence of water [43]. As the copolymer of PSBMA and PHEMA absorbs water, the electrostatic

interactions and hydrogen bonds between the PSBMA and PHEMA components weaken, and the mobility of each component increases, allowing them to diffuse easily into the scratched area. However, the healing ability of many self-healing polymers is highly dependent on the environment in which they are used because they require external stimuli to heal.

As described above, there are few reports of antifogging materials that have both high water uptake and scratch resistance, and breakthrough achievement is required to develop those materials.

3.3 Environment resistance

The durability of antifogging materials is essential for realizing practical applications. However, antifogging materials may deteriorate by chemical and physical changes caused by external factors such as heat and moisture, leading to the reduction of performances. For example, coloration is caused by oxidation, increasing the absorption in the visible light region. Additionally, physical property changes such as embrittlement due to chemical degradation cause cracks and an increase of surface roughness, leading to visible light scattering. These decreases in transparency cause issues in practical applications, for example, that of automobile windshield endangers the driver. Therefore, the development of antifogging materials that are stable under practical conditions is of high necessity. In particular, degradation due to chemical changes are often caused by hydrophilic groups. For example, the hydrophilic groups may accelerate the hydrolysis reaction of the main chain[47, 48]. Therefore, it is important to select appropriate hydrophilic groups to ensure environmental resistance.

4. Polysilsesquioxane (PSQ)

Organic-inorganic hybrid materials attract recent attention for the development of unconventional materials by combining both the properties of soft materials (rubber, gels, plastics) and hard materials (metals, ceramics, glass) synergistically [49-52]. They have, for instance, the high mechanical strength of inorganic materials and the flexibility of organic materials. Polysilsesquioxane (PSQ) is known as a typical organic-inorganic hybrid material, in which the inorganic Si-O-Si bonds and organic functional groups in the PSQ framework provide high mechanical strength and the high hydrophilicity, respectively (**Figure 3**) [53-55]. PSQ is readily processible to form film due to high solubility in organic solvents [56-59] and the films are used in a wide range of applications, such as optical materials [58], abrasion resistant coating [59], anti-reflective coating [60], antibacterial/antifungal coatings [61] low-dielectric materials [62], dielectric layer for organic field-effect transistor [63]. In this study, the author focuses the attention on PSQ as robust antifogging materials.

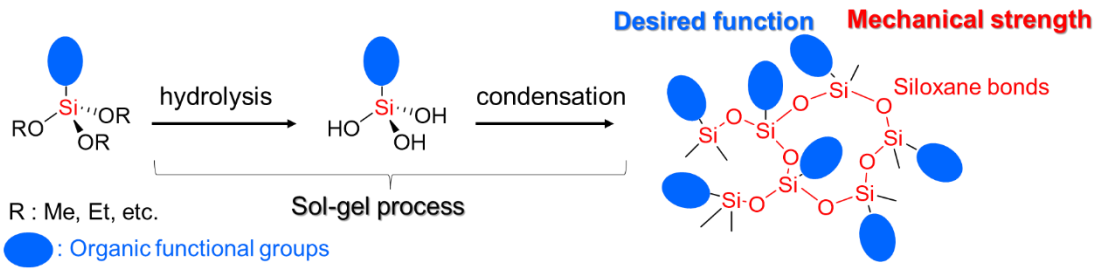

Figure 3. Structure and preparation of PSQ.

4.1 Synthesis of PSQ

PSQs are usually synthesized from alkoxysilane by the sol-gel process consisting of hydrolysis and condensation reactions forming the sol, followed by gelation of the sol (**Figure 3**) [64]. First, a solution composed of four raw materials is prepared. (1) Alkoxysilane with a selected organic group that provides the desired function, (2) Water for hydrolysis of alkoxysilane, (3) Solvent, and (4) Acid or base catalyst if necessary. Then, bulk, fiber, and thin films can be prepared by calcination of the

resultant sol after processing [58-63, 65, 66].

Hydrolysis and condensation reactions proceed by different mechanisms under acidic and basic conditions [67, 68]. In the hydrolysis reaction, there are differences in the reaction mechanism depending the catalyst used i.e., acidic or basic catalysts. Under the acidic conditions, the hydrolysis reaction giving silanol is promoted by nucleophilic attack of water with the oxonium intermediate of alkoxysilane, while hydroxide anion attacks the alkoxysilane under the basic conditions. In the condensation of silanol to form siloxane, the oxonium intermediate of silanol is attacked by another silanol unit under the acidic conditions, while the nucleophilic reaction of silanol anion with silanol is involved under the basic conditions. Because the reaction rate differs from each other under the acid and basic conditions, polymers with different shapes, such as linear polymers, crosslinked polymers, and spherical particles, are produced depending on the reaction conditions. Therefore, to obtain the desired polymer structure, the reaction conditions must be designed appropriately. For example, the method reported by Abe *et al* successfully prepared a variety of polysilsesquioxanes with controlled molecular weight by conducting the polycondensation reaction of triethoxysilanes under a nitrogen flow to remove ethanol while expelling the acid catalyst after only hydrolysis proceeds at low temperature [69].

4.2 Characterization of PSQ

Characterization of PSQs is essential for understanding the relationship between their physical properties, reactivities, structures and applications, thus gaining insights for designing new materials.

^{1}H and ^{29}Si nuclear magnetic resonance (NMR) spectroscopy is a standard spectroscopic method to analyze the structures of PSQs [70-76] by the chemical shifts that reflect the chemical environment of atoms. ^{1}H-NMR is often measured to estimate the consumption of alkoxy groups (degree of hydrolysis reaction) by the sol-gel process. For example, the ^{1}H-NMR peak derived from the methoxy group

around 3.5 ppm was reduced by the sol-gel process of trimethoxymethylsilanes. The progress of the hydrolysis reaction was calculated by comparing the integral ratios of the peaks of methyl and methoxy protons during the reaction course [75]. In the ^{29}Si-NMR, peaks are clearly separated by the number of Si bonded to OSi groups in the range of -60 to -120 ppm. For example, in the case of PSQ synthesized from methyltrialkoxysilane, the chemical shifts of T^0, T^1, T^2, and T^3 (numbers superscripted indicate the numbers of OSi bounded to the Si) are observed at -37 to -42 ppm, -47 to -51 ppm, -53 to -57 ppm, and -61 to -66 ppm, respectively [56, 57, 76]. V. Reschke *et al* reported the assignments of ^{29}Si-NMR signals of poly(methoxymethyl)siloxane as shown in **Figure 4** [77].

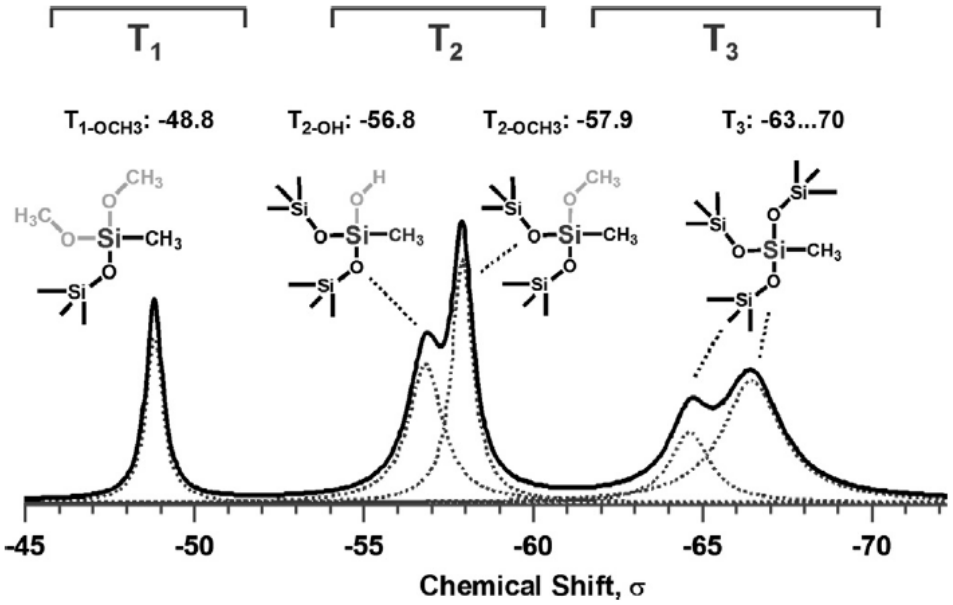

Figure 4. ^{29}Si-NMR spectra of the poly(methoxymethyl) siloxane. Reprinted from "Rheology and crosslinking of a low-viscosity SiOC preceramic polymer ", Vol 42, V. Reschke et al., p7623, Copyright 2016, with permission from Elsevier.

Infrared (IR) absorption measurements can identify substances and analyze their states by observing atomic vibrations in molecules [78, 79], which can be performed in all states, from monomer to polymer and from liquid to solid obtained during the sol-gel process. For example, the Si-OH-derived

peak near 950 cm^{-1} in a PSQ film gradually decreases as the silanol condensation proceeds when the temperature is elevated from 350 °C to 900 °C [78]. This indicates that the progress of the Si-OH condensation reaction can be analyzed quantitatively by IR measurement. GPC (Gel Permeation Chromatography) is a method of separating analytes by molecular size using a column with pores, and can measure the relative molecular weight of polymers to estimate the degree of progress of the condensation reaction. X-ray diffraction (XRD) measurements can identify and quantify the crystallization degrees and crystal structures, such as rod, ladder, and cage structures in PSQs [80, 81]. For example, PSQ with ammonium chloride groups (PSQ-$NH_3^+Cl^-$) give the diffraction peaks with the d-values consistent with the hexagonal stacking of rod-like polymers [80].

4.3 Application of PSQ to antifogging materials

Research on antifogging materials based on PSQ has been limited. In previous works, copolymers of polyhedral oligomeric silsesquioxane (POSS) and poly(2-(dimethylamino)-ethyl methacrylate)-block-poly(sulfobetaine methacrylate) exhibited excellent antifogging and anti-icing properties [82, 83]. This is because hydrophobic POSS groups aggregate on the film surface to form a self-lubricating aqueous layer by nonfreezable bound water on the surface. In addition, a POSS-linking polyamide was reported to exhibit good antifogging properties and high surface hardness [84]. The high surface hardness of this polymer film was likely due to the crosslinked structure and the rigidity of the POSS structure. However, the mechanism of effects of the siloxane network in PSQ on the scratch resistance was not adequately discussed.

5. Overview of this thesis

As described above, various studies have been conducted on water-absorbing antifogging materials to improve both water uptake and scratch resistance, which are usually in a trade-off relationship.

However, few reports succeeded in the development of high performance antifogging materials with high water uptake and scratch resistance. In this thesis, the author focuses on the antifogging materials based on PSQ containing hydrophilic groups. The effects of PSQ structures on the water uptake and scratch resistance was investigated in detail. In addition, considering the practical application of PSQ antifogging materials, the improvement of environmental resistance by designing the PSQ structures was also examined.

In Chapter 2, to investigate the potential of amine units as hydrophilic groups, solid films of poly(3-aminopropyl)silsesquioxane (PAPS) and poly(3-(2-aminoethylaminopropyl)silsesquioxane) (PAEAPS) were prepared on glass substrate by a sol-gel process, and their performance was evaluated (**Figure 5**). Furthermore, the mechanism of high scratch resistance of the PSQ films was discussed in comparison with PVA films based on the mechanical property measurement using a nanoindenter.

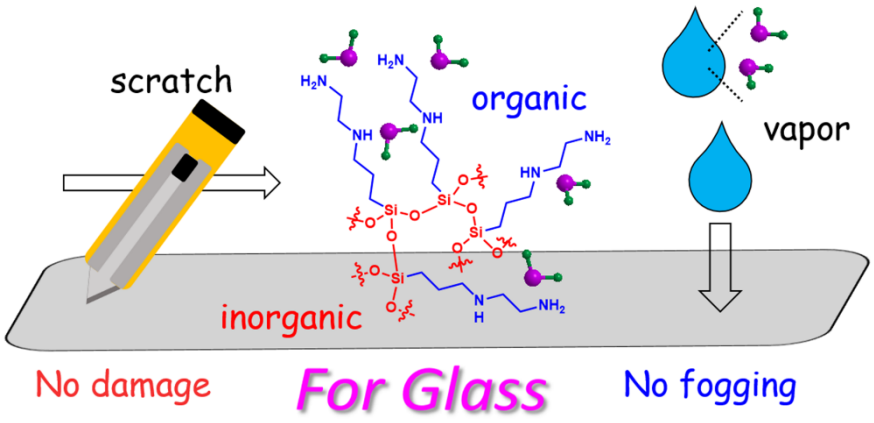

Figure 5. Schematic diagram of PAEAPS film (Chapter 2).

Chapter 3 is focused on the amine hydrochloride salt as a hydrophilic group in PSQ. It is expected that the stronger interaction of ionic units with water than neutral polar groups leads to the development of the higher performance-antifogging materials, as discussed in Equation (1). Therefore, PAEAPS film was immersed in a 0.5 mol/L hydrochloric acid (HCl) methanolic solution to prepare poly(3-(2-aminoethylamino)propyl)silsesquioxane hydrochloride (PAEAPS-Cl) film containing

amine hydrochloride salt units (**Figure 6**). The influence of amine hydrochloride salt on the antifogging properties and scratch resistance was investigated. In addition, the durability of PAEAPS and PAEAPS-Cl films under high humidity environments is also investigated to realize the practical application.

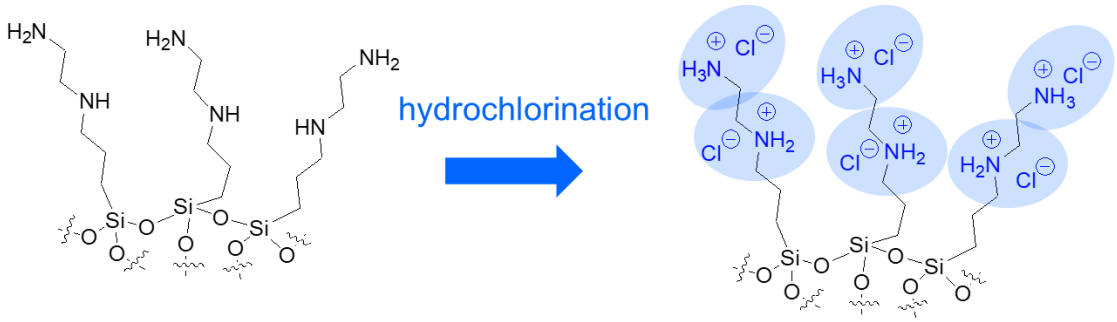

Figure 6. Schematic diagram of PAEAPS-Cl (Chapter 3).

PAEAPS and PAEAPS-Cl films were light yellow and decreased in the short wavelength range. The author hypothesized that the mechanism of yellowing was due to the oxidation of amino groups and amine hydrochloride.

In Chapter 4, hydroxyl groups are focused as hydrophilic groups in PSQ. In Chapter 2, the synthesis of amino-containing PSQs is described. Although the amino-containing PSQs show high water uptake with desirable scratch resistance, the PSQ films turn yellow upon calcination. Hydrophilic organic polymers with hydroxyl groups, such as PVA, have been widely studied and do not undergo coloration unlike polymers with amino groups. This inspired the author to prepare PSQ with hydroxy groups as colorless antifogging materials. However, synthesizing PSQ films containing hydroxyl groups is difficult due to possible side reactions between silanol and hydroxyl groups. To suppress the side reactions and to obtain a PSQ with a high concentration of hydroxyl groups (PSQ-OH), a new synthetic strategy including the preparation of PSQ with epoxy units and its hydrolysis has been developed (**Figure 7**).

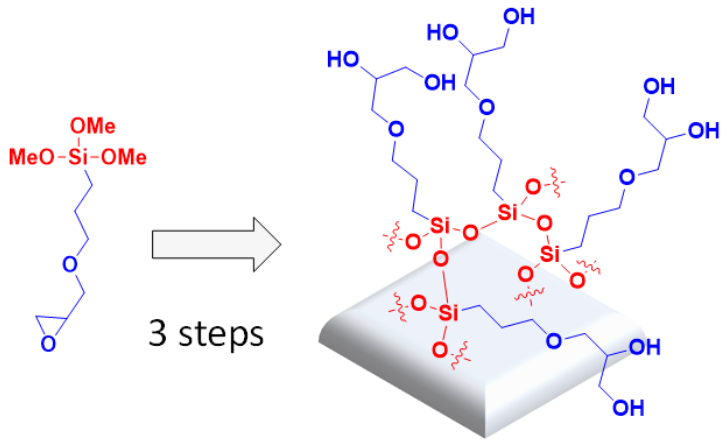

Figure 7. Schematic diagram of PSQ-OH film (Chapter 4).

Under high humidity conditions, the surface smoothness of the PSQ-OH film was significantly reduced due to surface cracking, resulting in reduced transparency. Furthermore, the water uptake of the PSQ-OH film was found to decrease by the durability test with repeated exposure of the film to high and low humidity environments. The author hypothesizes that this is due to the increased hydrophobicity of PSQ caused by polycondensation of silanols forming siloxanes in PSQ.

In Chapter 5, organically bridged PSQ synthesized from tetraethylene glycol bis(triethoxysilylpropyl)ether is described, aiming to suppress the polycondensation reaction of silanol groups due to the space effects of tetraethylene glycol units that sterically separate the silanol groups (**Figure 8**). A poly[3-(2,3-dihydroxypropoxypropyl)-co-tetraethylene glycol]silsesquioxane (PSQ-Diol/EG) film was prepared via the sol-gel reaction of 3-glycidyloxypropyltrimethoxysilane (GPTMS) and tetraethylene glycol bis(triethoxysilylpropyl)ether (BTESP-EG). The effects of introducing tetraethylene glycol chains into PSQ-OH films on the durability under high humidity conditions are discussed.

Finally, in Chapter 6, the conclusions of this thesis are described.

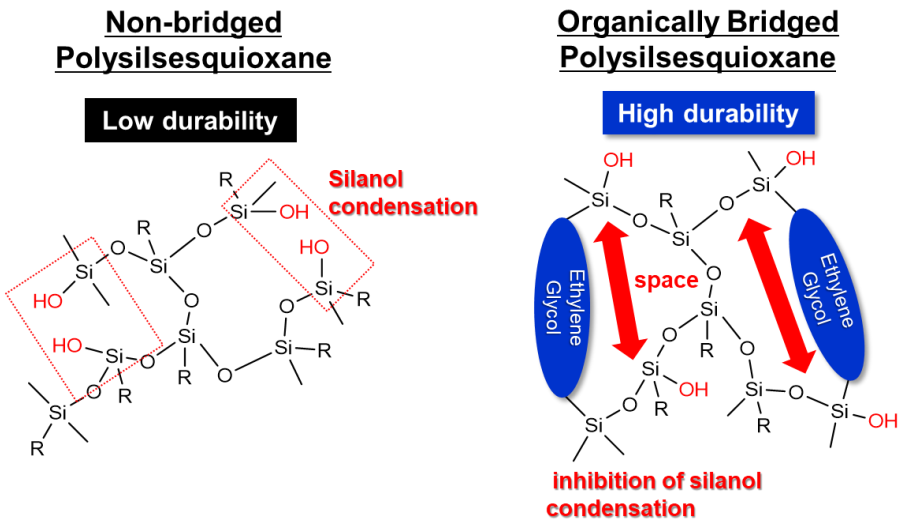

Figure 8. Schematic diagram of PSQ-Diol/EG film (Chapter 5).

6. References

[1] Z.Q. Sun, T. Liao, K.S. Liu, L. Jiang, J.H. Kim, S.X. Dou, Fly-Eye Inspired Superhydrophobic Anti-Fogging Inorganic Nanostructures, Small 10(15) (2014) 3001-3006.

[2] X.F. Gao, X. Yan, X. Yao, L. Xu, K. Zhang, J.H. Zhang, B. Yang, L. Jiang, The dry-style antifogging properties of mosquito compound eyes and artificial analogues prepared by soft lithography, Advanced Materials 19(17) (2007) 2213-2217.

[3] I.R. Duran, G. Laroche, Current trends, challenges, and perspectives of anti-fogging technology: Surface and material design, fabrication strategies, and beyond, Progress in Materials Science 99 (2019) 106-186.

[4] I.R. Duran, G. Laroche, Water drop-surface interactions as the basis for the design of anti-fogging surfaces: Theory, practice, and applications trends, Advances in Colloid and Interface Science 263 (2019) 68-94.

[5] G.Q. Wu, Y.L. Yang, Y.T. Lei, D.P. Fu, Y.C. Li, Y.H. Zhan, J.M. Zhen, M.Y. Teng, Hydrophilic nano-SiO2/PVA-based coating with durable antifogging properties, Journal of Coatings Technology and Research 17(5) (2020) 1145-1155.

[6] N. Nuraje, R. Asmatulu, R.E. Cohen, M.F. Rubner, Durable Antifog Films from Layer-by-Layer Molecularly Blended Hydrophilic Polysaccharides, Langmuir 27(2) (2011) 782-791.

[7] X.Y. Lu, Z. Wang, X.L. Yang, X. Xu, L. Zhang, N. Zhao, J. Xu, Antifogging and antireflective silica film and its application on solar modules, Surface & Coatings Technology 206(6) (2011) 1490-1494.

[8] S.J. Dain, A.K. Hoskin, C. Winder, D.P. Dingsdag, Assessment of fogging resistance of anti-fog personal eye protection, Ophthalmic and Physiological Optics 19(4) (1999) 357-361.

[9] J.M. Crebolder, R.B. Sloan, Determining the effects of eyewear fogging on visual task performance, Applied Ergonomics 35(4) (2004) 371-381.

[10] S. Kim, J.H. Park, Chemically Robust Antifog Nanocoating through Multilayer Deposition of Silica Composite Nanofilms, Acs Applied Materials & Interfaces 12(37) (2020) 42109-42118.

[11] W.H. Li, C.J. Lin, W. Ma, Y. Li, F.Q. Chu, B.L. Huang, S.H. Yao, Transparent selective photothermal coatings for antifogging applications, Cell Reports Physical Science 2(5) (2021) 100435.

[12] D.D. Wang, Y.S. Li, Y.Q. Wen, X.Y. Li, X. Du, Simple and low cost fabrication of large area nanocoatings with mechanical robustness, enhanced broadband transmittance and antifogging, Colloids and Surfaces a-Physicochemical and Engineering Aspects 629 (2021) 127522.

[13] M. Guzej, M. Zachar, CFD Simulation of Defogging Effectivity in Automotive Headlamp, Energies 12(13) (2019) 2609.

[14] L. Yang, X.C. Luo, W.L. Chang, Y.K. Tian, Z.J. Wang, J. Gao, Y.K. Cai, Y. Qin, M. Duxbury, Manufacturing of anti-fogging super-hydrophilic microstructures on glass by nanosecond laser, Journal of Manufacturing Processes 59 (2020) 557-565.

[15] P. D'Agaro, G. Croce, G. Cortella, Numerical simulation of glass doors fogging and defogging in refrigerated display cabinets, Applied Thermal Engineering 26(16) (2006) 1927-1934.

[16] Z.W. Han, X.M. Feng, Z.G. Guo, S.C. Niu, L.Q. Ren, Flourishing Bioinspired Antifogging Materials with Superwettability: Progresses and Challenges, Advanced Materials 30(13) (2018) 1704652.
[17] J.T. Park, J.H. Kim, D. Lee, Excellent anti-fogging dye-sensitized solar cells based on superhydrophilic nanoparticle coatings, Nanoscale 6(13) (2014) 7362-7368.
[18] J. Tan, P.H. Tian, M.Y. Sun, H.C. Wang, N. Sun, G.J. Chen, Y.C. Song, D.Y. Jiang, H. Jiang, M.Y. Xu, A transparent electrowetting-on-dielectric device driven by triboelectric nanogenerator for extremely fast anti-fogging, Nano Energy 92 (2022) 106697.
[19] H. Khayyam, J. Abawajy, R.N. Jazar, Intelligent energy management control of vehicle air conditioning system coupled with engine, Applied Thermal Engineering 48 (2012) 211-224.
[20] Z.G. Qi, Advances on air conditioning and heat pump system in electric vehicles - A review, Renewable & Sustainable Energy Reviews 38 (2014) 754-764.
[21] J.B. Chemin, S. Bulou, K. Baba, C. Fontaine, T. Sindzingre, N.D. Boscher, P. Choquet, Transparent anti-fogging and self-cleaning TiO2/SiO2 thin films on polymer substrates using atmospheric plasma, Scientific Reports 8 (2018) 9603.
[22] T. Huang, W.X. Huang, C. Zhou, Y. Situ, H. Huang, Superhydrophilicity of TiO2/SiO2 thin films: Synergistic effect of SiO2 and phase-separation-induced porous structure, Surface & Coatings Technology 213 (2012) 126-132.
[23] A. Tricoli, M. Righettoni, S.E. Pratsinis, Anti-Fogging Nanofibrous SiO2 and Nanostructured SiO2-TiO2 Films Made by Rapid Flame Deposition and In Situ Annealing, Langmuir 25(21) (2009) 12578-12584.
[24] F. Liu, J. Shen, W.Y. Zhou, S.Y. Zhang, L. Wan, In situ growth of TiO2/SiO2 nanospheres on glass substrates via solution impregnation for antifogging, Rsc Advances 7(26) (2017) 15992-15996.
[25] N. Sakai, A. Fujishima, T. Watanabe, K. Hashimoto, Quantitative evaluation of the photoinduced hydrophilic conversion properties of TiO2 thin film surfaces by the reciprocal of contact angle, Journal of Physical Chemistry B 107(4) (2003) 1028-1035.
[26] R. Wang, K. Hashimoto, A. Fujishima, M. Chikuni, E. Kojima, A. Kitamura, M. Shimohigoshi, T. Watanabe, Photogeneration of highly amphiphilic TiO2 surfaces, Advanced Materials 10(2) (1998) 135-+.
[27] Z.W. Han, X.M. Feng, Z.B. Jiao, Z. Wang, J.Q. Zhang, J. Zhao, S.C. Niu, L.Q. Ren, Bio-inspired antifogging PDMS coupled micro-pillared superhydrophobic arrays and SiO2 coatings, Rsc Advances 8(47) (2018) 26497-26505.
[28] K.S. Liu, X. Yao, L. Jiang, Recent developments in bio-inspired special wettability, Chemical Society Reviews 39(8) (2010) 3240-3255.
[29] H. Lee, M.L. Alcaraz, M.F. Rubner, R.E. Cohen, Zwitter-Wettability and Antifogging Coatings with Frost-Resisting Capabilities, Acs Nano 7(3) (2013) 2172-2185.
[30] X.J. Zhang, J.H. He, Hydrogen-Bonding-Supported Self-Healing Antifogging Thin Films, Scientific Reports 5 (2015) 9227.
[31] Y. Wang, T.Q. Li, S.H. Li, J.Q. Sun, Antifogging and Frost-Resisting Polyelectrolyte Coatings Capable

of Healing Scratches and Restoring Transparency, Chemistry of Materials 27(23) (2015) 8058-8065.
[32] Y.X. Li, X. Fang, Y. Wang, B.H. Ma, J.Q. Sun, Highly Transparent and Water-Enabled Healable Antifogging and Frost-Resisting Films Based on Poly(vinyl alcohol)-Nafion Complexes, Chemistry of Materials 28(19) (2016) 6975-6984.
[33] E. Nam, E.H.H. Wong, S. Tan, Q. Fu, A. Blencowe, G.G. Qiao, Antifogging Surface Facilitated by Nanoscale Coatings with Controllable Hydrophobicity and Cross-Linking Density, Macromolecular Materials and Engineering 302(1) (2017) 1600199.
[34] T. Sato, G.J. Dunderdale, A. Hozumi, Large-Scale Formation of Fluorosurfactant-Doped Transparent Nanocomposite Films Showing Durable Antifogging, Oil-Repellent, and Self-healing Properties, Langmuir 36(26) (2020) 7439-7446.
[35] B.N. Zhang, Y.D. Cui, G.Q. Yin, X.M. Li, L.W. Liao, X.B. Cai, Synthesis and Swelling Properties of Protein-poly(acrylic acid-co-acrylamide) Superabsorbent Composite, Polymer Composites 32(5) (2011) 683-691.
[36] C. Tao, S. Bai, X.H. Li, C. Li, L.X. Ren, Y.H. Zhao, X.Y. Yuan, Formation of zwitterionic coatings with an aqueous lubricating layer for antifogging/anti-icing applications, Progress in Organic Coatings 115 (2018) 56-64.
[37] S. Bai, X.H. Li, R.C. Zhang, C. Li, K.Y. Zhu, P.C. Sun, Y.H. Zhao, L.X. Ren, X.Y. Yuan, Enhancing antifogging/frost-resisting performances of amphiphilic coatings via cationic, zwitterionic or anionic polyelectrolytes, Chemical Engineering Journal 357 (2019) 667-677.
[38] C.C. Chang, F.H. Huang, H.H. Chang, T.M. Don, C.C. Chen, L.P. Cheng, Preparation of Water-Resistant Antifog Hard Coatings on Plastic Substrate, Langmuir 28(49) (2012) 17193-17201.
[39] C.C. Chang, T.Y. Tsai, L.P. Cheng, Preparation of Nanosilica/polyacrylate Antifog Coatings on Polycarbonate Substrates, Journal of Applied Science and Engineering 22(1) (2019) 153-162.
[40] T. Choung, J. Lim, D.J. Won, J. Kim, Chamber/Capsule-Integrated Self-Healing Coating on Glass for Preventing Crack Propagation, Macromolecular Materials and Engineering 303(4) (2018) 1800041.
[41] W. Li, G. Wu, J.H. Tan, X.F. Yu, G. Sun, B. You, Transparent Surfactant/Epoxy Composite Coatings with Self-Healing and Superhydrophilic Properties, Macromolecular Materials and Engineering 304(7) (2019) 1800765.
[42] Y. Du, W.Z. Qiu, Z.L. Wu, P.F. Ren, Q. Zheng, Z.K. Xu, Water-Triggered Self-Healing Coatings of Hydrogen-Bonded Complexes for High Binding Affinity and Antioxidative Property, Advanced Materials Interfaces 3(15) (2016) 1600167.
[43] B. Liang, Z.X. Zhong, E.N. Jia, G.Y. Zhang, Z.H. Su, Transparent and Scratch-Resistant Antifogging Coatings with Rapid Self-Healing Capability, Acs Applied Materials & Interfaces 11(33) (2019) 30300-30307.
[44] X.Q. Wang, S.H. Li, J.Y. Huang, J.J. Mao, Y. Cheng, L. Teng, Z. Chen, Y.K. Lai, A multifunctional and environmentally-friendly method to fabricate superhydrophilic and self-healing coatings for

sustainable antifogging, Chemical Engineering Journal 409 (2021) 128228.
[45] W. Wang, P.P. Lu, Y. Fan, L.M. Tian, S.C. Niu, J. Zhao, L.Q. Ren, A facile antifogging/frost-resistant coating with self-healing ability, Chemical Engineering Journal 378 (2019) 122173.
[46] M.W. England, C. Urata, G.J. Dunderdale, A. Hozumi, Anti-Fogging/Self-Healing Properties of Clay-Containing Transparent Nanocomposite Thin Films, Acs Applied Materials & Interfaces 8(7) (2016) 4318-4322.
[47] A. Ballara, J. Verdu, PHYSICAL ASPECTS OF THE HYDROLYSIS OF POLYETHYLENE TEREPHTHALATE, Polymer Degradation and Stability 26(4) (1989) 361-374.
[48] W.N. Ayre, S.P. Denyer, S.L. Evans, Ageing and moisture uptake in polymethyl methacrylate (PMMA) bone cements, Journal of the Mechanical Behavior of Biomedical Materials 32 (2014) 76-88.
[49] M. Faustini, L. Nicole, E. Ruiz-Hitzky, C. Sanchez, History of Organic-Inorganic Hybrid Materials: Prehistory, Art, Science, and Advanced Applications, Advanced Functional Materials 28(27) (2018) 1704158.
[50] J.Y. Yuan, A.H.E. Muller, One-dimensional organic-inorganic hybrid nanomaterials, Polymer 51(18) (2010) 4015-4036.
[51] C. Sanchez, B. Julian, P. Belleville, M. Popall, Applications of hybrid organic-inorganic nanocomposites, Journal of Materials Chemistry 15(35-36) (2005) 3559-3592.
[52] L. Nicole, C. Laberty-Robert, L. Rozes, C. Sanchez, Hybrid materials science: a promised land for the integrative design of multifunctional materials, Nanoscale 6(12) (2014) 6267-6292.
[53] R.H. Baney, M. Itoh, A. Sakakibara, T. Suzuki, SILSESQUIOXANES, Chemical Reviews 95(5) (1995) 1409-1430.
[54] N. Ahmed, H. Fan, P. Dubois, X.W. Zhang, S. Fahad, T. Aziz, J.T. Wan, Nano-engineering and micromolecular science of polysilsesquioxane materials and their emerging applications, Journal of Materials Chemistry A 7(38) (2019) 21577-21604.
[55] Y.J. Du, H.Z. Liu, Cage-like silsesquioxanes-based hybrid materials, Dalton Transactions 49(17) (2020) 5396-5405.
[56] L.H. Lee, W.C. Chen, W.C. Liu, Structural control of oligomeric methyl silsesquioxane precursors and their thin-film properties, Journal of Polymer Science Part a-Polymer Chemistry 40(10) (2002) 1560-1571.
[57] T. Gunji, Y. Iizuka, K. Arimitsu, Y. Abe, Preparation and properties of alkoxy(methyl)silsesquioxanes as coating agents, Journal of Polymer Science Part a-Polymer Chemistry 42(15) (2004) 3676-3684.
[58] W.C. Chen, L.H. Lee, B.F. Chen, C.T. Yen, Synthesis and characterization of poly(methyl silsesquioxane)titania optical thin films, Journal of Materials Chemistry 12(12) (2002) 3644-3648.
[59] E. Amerio, M. Sangermano, G. Colucci, G. Malucelli, M. Messori, R. Taurino, P. Fabbri, UV curing of organic-inorganic hybrid coatings containing polyhedral oligomeric silsesquioxane blocks, Macromolecular Materials and Engineering 293(8) (2008) 700-707.
[60] H.K. Raut, S.S. Dinachali, A.Y. He, V.A. Ganesh, M.S.M. Saifullah, J. Law, S. Ramakrishna, Robust

and durable polyhedral oligomeric silsesquioxane-based anti-reflective nanostructures with broadband quasi-omnidirectional properties, Energy & Environmental Science 6(6) (2013) 1929-1937.
[61] I.E. Bordianu, G. David, B. Simionescu, M. Aflori, C. Ursu, A. Coroaba, G. Hitruc, C. Cotofana, M. Olaru, Functional silsesquioxane-based hierarchical assemblies for antibacterial/antifungal coatings, Journal of Materials Chemistry B 3(5) (2015) 723-727.
[62] C.V. Nguyen, K.R. Carter, C.J. Hawker, J.L. Hedrick, R.L. Jaffe, R.D. Miller, J.F. Remenar, H.W. Rhee, P.M. Rice, M.F. Toney, M. Trollsas, D.Y. Yoon, Low-dielectric, nanoporous organosilicate films prepared via inorganic/organic polymer hybrid templates, Chemistry of Materials 11(11) (1999) 3080-3085.
[63] Z.N. Bao, V. Kuck, J.A. Rogers, M.A. Paczkowski, Silsesquioxane resins as high-performance solution processible dielectric materials for organic transistor applications, Advanced Functional Materials 12(8) (2002) 526-531.
[64] H. Schmidt, CHEMISTRY OF MATERIAL PREPARATION BY THE SOL-GEL PROCESS, Journal of Non-Crystalline Solids 100(1-3) (1988) 51-64.
[65] M. Nogami, Y. Moriya, GLASS-FORMATION THROUGH HYDROLYSIS OF SI(OC2H5)4 WITH NH4OH AND HCL SOLUTION, Journal of Non-Crystalline Solids 37(2) (1980) 191-201.
[66] S. Sakka, K. Kamiya, THE SOL-GEL TRANSITION IN THE HYDROLYSIS OF METAL ALKOXIDES IN RELATION TO THE FORMATION OF GLASS-FIBERS AND FILMS, Journal of Non-Crystalline Solids 48(1) (1982) 31-46.
[67] J.H. Harreld, K. Su, D.E. Katsoulis, M. Suto, G.D. Stucky, Surfactant and pH-mediated control over the molecular structure of poly(phenylsilsesquioxane) resins, Chemistry of Materials 14(3) (2002) 1174-1182.
[68] C.J. Brinker, HYDROLYSIS AND CONDENSATION OF SILICATES - EFFECTS ON STRUCTURE, Journal of Non-Crystalline Solids 100(1-3) (1988) 31-50.
[69] N. Takamura, T. Gunji, H. Hatano, Y. Abe, Preparation and properties of polysilsesquioxanes: Polysilsesquioxanes and flexible thin films by acid-catalyzed controlled hydrolytic polycondensation of methyl- and vinyltrimethoxysilane, Journal of Polymer Science Part a-Polymer Chemistry 37(7) (1999) 1017-1026.
[70] Y. Kaneko, M. Shoiriki, T. Mizumo, Preparation of cage-like octa(3-aminopropyl)silsesquioxane trifluoromethanesulfonate in higher yield with a shorter reaction time, Journal of Materials Chemistry 22(29) (2012) 14475-14478.
[71] T. Ishii, T. Mizumo, Y. Kaneko, Facile Preparation of Ionic Liquid Containing Silsesquioxane Framework, Bulletin of the Chemical Society of Japan 87(1) (2014) 155-159.
[72] T. Ishii, T. Enoki, T. Mizumo, J. Ohshita, Y. Kaneko, Preparation of imidazolium-type ionic liquids containing silsesquioxane frameworks and their thermal and ion-conductive properties, Rsc Advances 5(20) (2015) 15226-15232.
[73] A. Harada, S. Koge, J. Ohshita, Y. Kaneko, Preparation of a Thermally Stable Room Temperature Ionic

Liquid Containing Cage-Like Oligosilsesquioxane with Two Types of Side-Chain Groups, Bulletin of the Chemical Society of Japan 89(9) (2016) 1129-1135.
[74] M.C. Gravel, C. Zhang, M. Dinderman, R.M. Laine, Octa(3-chloroammoniumpropyl) octasilsesquioxane, Applied Organometallic Chemistry 13(4) (1999) 329-336.
[75] R. Hayami, Y. Ideno, Y. Sato, H. Tsukagoshi, K. Yamamoto, T. Gunji, Soluble ethane-bridged silsesquioxane polymer by hydrolysis-condensation of bis(trimethoxysilyl)ethane: characterization and mixing in organic polymers, Journal of Polymer Research 27(10) (2020) 316.
[76] R.H. Glaser, G.L. Wilkes, C.E. Bronnimann, SOLID-STATE SI-29 NMR OF TEOS-BASED MULTIFUNCTIONAL SOL-GEL MATERIALS, Journal of Non-Crystalline Solids 113(1) (1989) 73-87.
[77] V. Reschke, R.K. Bordia, F. Scheffler, M. Scheffler, Rheology and crosslinking of a low-viscosity SiOC preceramic polymer, Ceramics International 42(6) (2016) 7620-7625.
[78] J. Gallardo, A. Duran, D. Di Martino, R.M. Almeida, Structure of inorganic and hybrid SiO2 sol-gel coatings studied by variable incidence infrared spectroscopy, Journal of Non-Crystalline Solids 298(2-3) (2002) 219-225.
[79] A. Duran, C. Serna, V. Fornes, J.M.F. Navarro, STRUCTURAL CONSIDERATIONS ABOUT SIO2 GLASSES PREPARED BY SOL-GEL, Journal of Non-Crystalline Solids 82(1-3) (1986) 69-77.
[80] Y. Kaneko, H. Toyodome, M. Shoiriki, N. Iyi, Preparation of Ionic Silsesquioxanes with Regular Structures and Their Hybridization, International Journal of Polymer Science 2012 (2012) 684278.
[81] Y. Kaneko, Ionic silsesquioxanes: Preparation, structure control, characterization, and applications, Polymer 144 (2018) 205-224.
[82] C. Li, X.H. Li, C. Tao, L.X. Ren, Y.H. Zhao, S. Bai, X.Y. Yuan, Amphiphilic Antifogging/Anti-Icing Coatings Containing POSS-PDMAEMA-b-PSBMA, Acs Applied Materials & Interfaces 9(27) (2017) 22959-22969.
[83] S. Bai, X.H. Li, Y.H. Zhao, L.X. Ren, X.Y. Yuan, Antifogging/Antibacterial Coatings Constructed by N-Hydroxyethylacrylamide and Quaternary Ammonium-Containing Copolymers, Acs Applied Materials & Interfaces 12(10) (2020) 12305-12316.
[84] T. Kozuma, A. Mihata, Y. Kaneko, Preparation of Soluble POSS-Linking Polyamide and Its Application in Antifogging Films, Materials 14(12) (2021) 3178.

Chapter 2: Antifogging Polysilsesquioxane Film Containing an Amino Group with High Scratch Resistance

1. Introduction

As described in Chapter 1, polysilsesquioxanes (PSQ) are organic−inorganic hybrid materials that consist of a siloxane network with organic functional groups covalently linked to the silicon atoms [1-5]. The properties of organic−inorganic hybrid materials based on polysilsesquioxanes depend on the siloxane network structure and the choice of the organic functional group, where the inorganic Si−O−Si network structure provides thermal and mechanical stability and the organic functional group may be chosen depending on the intended application of the material [1]. Thus, a polysilsesquioxane with appropriate organic groups may be a good antifogging coating material because polysilsesquioxane films typically exhibit high scratch resistance and good transparency. However, films prepared from typical poly(alkylsilsesquioxane)s exhibit high water contact angles because the alkyl group covalently linked to the silicone atom is hydrophobic [6-9]. However, the author anticipated that a polysilsesquioxane prepared from a trialkoxysilane bearing a hydrophilic amino group would exhibit both high scratch resistance and hydrophilicity imparted by the siloxane network and the amino groups, respectively. Accordingly, in this chapter, the author describes the preparation of poly(3-aminopropyl)silsesquioxane (PAPS) and poly(3-(2-aminoethylaminopropyl)silsesquioxane) (PAEAPS) by sol−gel reactions of aminofunctionalized trialkoxysilanes and the antifogging and mechanical properties of the PSQ films. Furthermore, the mechanism of high scratch resistance of the PSQ films is discussed based on the difference in scratch behavior between poly(vinyl alcohol) (PVA) and PAEAPS films by the nanoscratch test.

2. Experimental

2.1 Materials

3-Aminopropyltriethoxysilane, 3-(2-aminoethylamino)propyltriethoxysilane, and poly(vinyl alcohol) (n = ca. 2000; degree of saponification = ca. 80 mol%) were purchased from Tokyo Chemical Industry Co., Ltd. and used as received. Ethanol (super dehydrated) was purchased from FUJIFILM Wako Pure Chemical Co., Ltd. and used as received. All other solvents were of the highest grade commercially available and used without further purification. The water used for the sol-gel reaction was purified by a Millipore Mill-Q UV system and had a resistance of 18.2 MΩ cm.

2.2 Synthesis of poly(3-(2-aminoethylaminopropyl)silsesquioxane) (PAEAPS)

In a 100 mL round-bottom flask, 3-(2-aminoethylaminopropyl)triethoxysilane (2.649 g, 10.00 mmol) and ethanol (4.605 g, 100.0 mmol) were mixed and cooled using an ice bath. Water (0.5411 g, 30.00 mmol) was slowly added and the reaction mixture was stirred at 0 °C for 10 min. Then, the reaction mixture was stirred at room temperature for 10 min and refluxed for 5 h. Finally, ethanol was removed under reduced pressure at 60 °C to obtain PAEAPS as a viscous liquid. The obtained PAEAPS was diluted with ethanol to a concentration of 20 wt% and stored in a refrigerator at ca. 4 °C prior to further use.

2.3 Synthesis of poly(3-aminopropyl)silsesquioxane (PAPS)

PAPS was prepared from 3-aminopropyltriethoxysilane in the same way and obtained as a glass-like solid. PAPS was also diluted to a concentration of 20 wt% in ethanol and stored in a refrigerator.

2.4 Preparation of film coatings

A glass substrate was cleaned using detergent and then washed successively with distilled water, acetone, and 2-propanol. The 20 wt% ethanolic polymer solution prepared above was coated onto the glass substrate using an applicator. The film was heated at 60 °C for 2 h, and then heated at 180 °C for 0.5, 1, or 2 h in air to form a gel film.

For comparison, PVA films were prepared. PVA (2 g) was added to 20 mL of distilled water and stirred for 30 min, and then the obtained solution was coated onto a glass substrate using an applicator. Finally, the PVA film was heated at 70 °C for 3 h.

2.5 Characterization

^{1}H nuclear magnetic resonance (NMR) measurements were performed using a Varian 400 MHz spectrometer and ^{29}Si NMR spectra were obtained using a Varian 500 MHz spectrometer. The samples were dissolved in deuterium chloroform ($CDCl_3$) and tetramethylsilane was used as an internal standard. Fourier transform infrared (FTIR) spectra were recorded on a Shimadzu IR Affinity-1 spectrometer equipped with an attenuated total reflectance (ATR) unit. Transmittance measurements were performed on a HITACHI U-2910 spectrophotometer. X-ray diffraction (XRD) analysis was performed on a Rigaku Ultima IV diffractometer using Cu Kα radiation (λ= 1.54 Å) generated at 40 kV and 45 mA. Samples were scanned in the 2θ range 5°–40°. Thermogravimetric analysis (TGA) was performed using a SII EXSTAR TG-DTA6200 thermal analyzer at a heating rate of 10 °C/min under air flow at 100 mL/min. The contact angle was measured with KYOWA DM 300 contact angle meter.

To measure water absorption, the films were placed in a humidity-controlled chamber at different relative humidities (RHs) at 30 °C for 1–2 h, and the weight changes were measured using a microbalance. Water uptake was calculated using Equation (1):

$$Water\ uptake\ (\%) = \frac{W_{95\%RH} - W_{20\%RH}}{W_{20\%RH}} \times 100 \quad (1)$$

where $W_{20\%RH}$ is the weight of the film after exposure to 20% RH at 30 °C for 1–2 h and $W_{95\%RH}$ is the weight of the film after exposure to 95% RH at 30 °C for 1–2 h.

The scratch resistances, elastic moduli, and elastic part of indentation work (η) of the films were

measured using an Agilent Technologies Nano Indenter G200. Scratch resistance was measured by the G-series ramp load scratch method with a cube corner diamond tip and calculated according to Equation (2) and (3). Elastic moduli and elastic part of indentation work (η) were measured with a Berkovich diamond tip in accordance with ISO 14577-1 [10].

$$Scratch\ resistance = log\ \frac{test\ load\ (N) \times 10^{-9}}{2.5981 \times (plastic\ deformation\ depth)^2\ (m)^2} = log\ \frac{test\ load\ (N) \times 10^{-9}}{contact\ area\ (m^2)} \quad (2)$$

$$Plastic\ deformation\ depth = (\text{displacement depth into surface at postscratch}) - (\text{displacement depth into surface at prescratch}) \quad (3)$$

3. Results and discussion

3.1 Synthesis of amino-functionalized polysilsesquioxane

For the preparation of amino-functionalized polysilsesquioxanes, the author used 3-aminopropyltriethoxysilane and 3-(2-aminoethylaminopropyl)triethoxysilane as the monomers. The sol-gel reactions of 3-aminopropyltriethoxysilane and 3-(2-aminoethylaminopropyl)triethoxysilane are shown in **Scheme 1**. Sol-gel reactions are typically accelerated under acidic or basic conditions, and hydrochloric acid is typically used as a catalyst [1, 2]. However, 3-aminopropyltriethoxysilane and 3-(2-aminoethylaminopropyl)triethoxysilane have basic amino groups. Thus, the amino groups in the monomer catalyze the hydrolysis and polycondensation reactions.

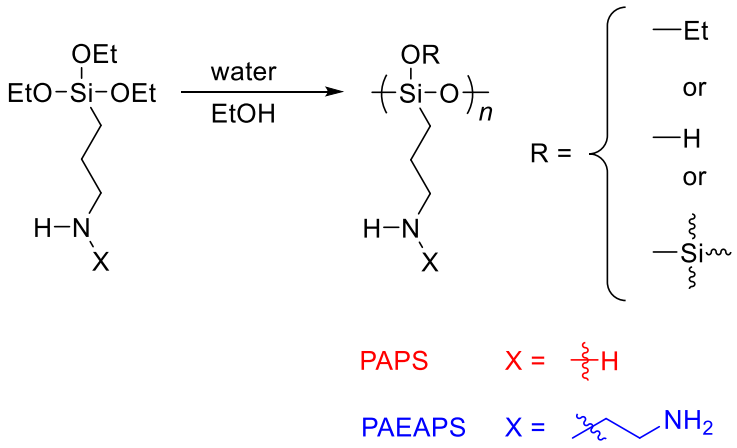

Scheme 1. Preparation of PAPS and PAEAPS by sol-gel reactions in ethanol.

First, the hydrolysis of 3-aminopropyltriethoxysilane and 3-(2-aminoethylaminopropyl)triethoxysilane was conducted at 0 °C for 10 min and then at room temperature for 10 min. Then, polycondensation was conducted under reflux for 5 h. PAPS and PAEAPS were obtained as a glass-like solid and a viscous liquid without gelation after the removal of ethanol, respectively. PAEAPS exhibits good solubility in organic solvents such as THF, ethanol, and chloroform, whereas PAPS does not easily dissolve in organic solvents, taking several hours to fully dissolve in ethanol.

The structures of PAPS and PAEAPS were investigated using ^{1}H NMR and ^{29}Si NMR analysis. **Figure 1** shows the ^{1}H NMR spectra of PAPS and PAEAPS in $CDCl_3$. For PAPS, the broad signals observed at 0.51, 1.42, and 2.57 ppm are attributed to the propyl side chains. The amino group signal overlaps with that for the propyl group at 1.42 ppm. The ethoxy group signals around 1.10 and 3.70 ppm are barely observed. Accordingly, the degree of hydrolysis of the ethoxy group was estimated to be over 99%. Thus, the starting monomer is almost completely converted by hydrolysis, even though no catalyst was added.

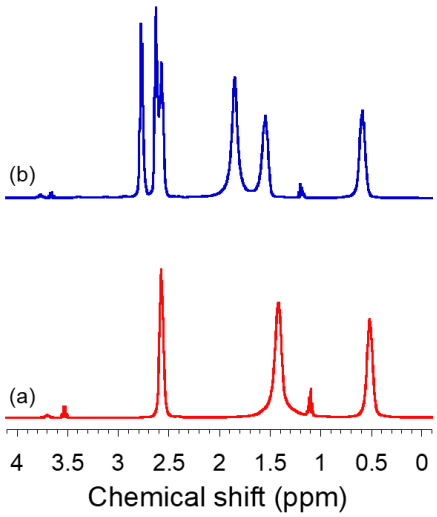

Figure 1. ^{1}H NMR spectra of (a) PAPS and (b) PAEAPS in $CDCl_3$.

Similarly, in the ^{1}H NMR spectrum of PAEAPS, broad signals attributed to propyl groups are observed at 0.58, 1.54, and 2.60 ppm, and ethyl group signals are observed at 2.60 and 2.77 ppm. The two amino group signals overlap at 1.85 ppm. Again, the ethoxy group signals around at 1.20 and 3.80 ppm are almost completely absent following hydrolysis, and the estimated conversion is over 99%. As expected, the amino groups in the starting monomer efficiently autocatalyze the sol-gel reaction. Although the autocatalyzed sol-gel by nitrogen flow method was reported [11], the synthesized PAPS and PAEAPS contained not ethoxy group, namely, the hydrolysis of ethoxy group efficiently proceeded by autocatalyzed sol-gel reaction. In the nitrogen flow method, water was removed by the flow together with ethanol to make the fine control of the reaction possible. However, in the present system, the staying water in the mixture accelerated further hydrolysis and polycondensation reaction. The autocatalyzed sol-gel reaction is useful method to prepare polysilsesquioxane not containing alkoxy group without adding catalyst. This is advantage of investigating the antifogging and mechanical property for avoiding the influence of alkoxy group because the remaining alkoxy group is hydrophobic in nature and also sometimes affects the physical property such as thermal and mechanical property.

Figure 2 shows the ^{29}Si NMR spectra of PAPS and PAEAPS in $CDCl_3$. The ^{29}Si NMR spectrum of PAPS features multiple sharp signals and small signals ranging from −65.7 to −70.8 ppm and −57.8 to −60.6 ppm, respectively. These signals are attributed to T^3 and T^2, where T^n denotes the siloxane structural unit $RSi(OSi)_n(OR)_{3-n}$ (n = 1–3, R = organic group). Although the author tried to estimate the amount of silanol groups in PAPS by the ^{29}Si NMR, it was difficult to detect the silanol groups because their signals were considerably small, as shown in **Figure 2**. This result indicates that PAPS is mainly composed of T^3 structures. Thus, the results of ^{1}H and ^{29}Si NMR analyses for PAPS indicate that the hydrolysis and polycondensation efficiently proceed under autocatalysis by the amino group, and that PAPS has highly network-like structure with a low content of ethoxy groups.

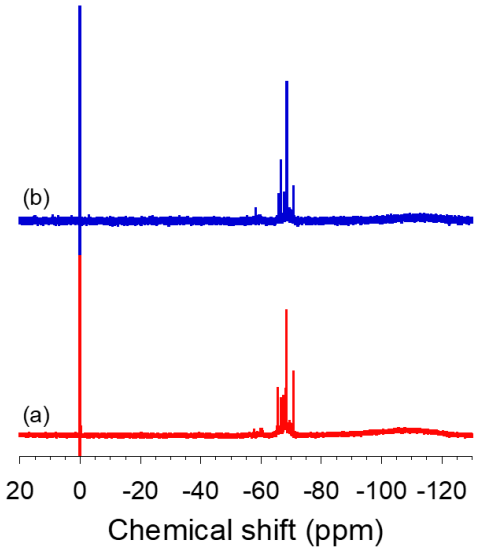

Figure 2. ^{29}Si NMR spectra of (a) PAPS and (b) PAEAPS in $CDCl_3$.

Similarly, the ^{29}Si NMR spectrum of PAEAPS features multiple sharp signals in the range from −65.8 to −71.0 ppm attributed to T^3 structures and small signals around at −58.4 ppm assigned to T^2 structures. Thus, both PAPS and PAEAPS are mainly composed of T^3 structures, demonstrating that the amino-functionalized polysilsesquioxanes adopt highly networked structures.

Kaneko *et al*. reported similar behavior for the acid-catalyzed sol-gel reactions of 3-aminopropyltrimethoxysilane and 1-methyl-3-[3-(triethoxysilyl)propyl]imidazolium chloride, where cage-type oligosilsesquioxanes were afforded as the main products [12-15]. Furthermore, the sol-gel reaction of aminopropyltrimethoxysilane in a mixture of methanol and HCl at room temperature affords a cage-like octa(3-aminoporpyl)silsesquioxane in the low yield of ca. 30% [16]. However, in the case of PAPS and PAEAPS, polycondensation effectively proceeds by the catalytic effect of the amino group, and these sol-gel reactions not only form highly cross-linked structures, they may also form partially condensed polysilsesquioxanes.

Regrettably, the molecular weights of PAPS and PAEAPS could not be measured by gel permeation chromatography because the polymers adsorb onto the column resin through the polar amino group.

3.2 Preparation of polysilsesquioxane films

To assess the antifogging and mechanical properties of the polysilsesquioxane films, ethanolic solutions of PAPS and PAEAPS were coated onto glass substrates and heated at 60 °C for 2 h to remove the ethanol. Then, the films were heated at 180 °C for 0.5, 1, or 2 h to promote gelation. To investigate the structural changes in the PAEAPS film during heating, the reaction progress was monitored using ATR–FTIR measurements. **Figure 3** shows the ATR–FTIR spectra of PAEAPS films after drying at 60 °C for 2 h and heating at 180 °C for 0.5, 1, and 2 h. For the PAEAPS film dried at 60 °C for 2 h, absorption peaks at 1093 and 1045 cm^{-1}, which are attributed to the Si-O-Si bond, are observed. Furthermore, a weak peak that corresponded to the silanol group appears around 900 cm^{-1}. As shown in **Figure 3**, the absorption peak around 900 cm^{-1} decreases with increasing heating time at 180 °C. Furthermore, the absorption peak at 1045 cm^{-1} gradually increases in intensity with increasing heating time and also shifts to 1020 cm^{-1}. Thus, the Si-O-Si bond changes during heating at 180 °C. This indicates that PAEAPS forms a highly cross-linked network upon film formation. Indeed,

PAEAPS film did not peel off from glass substrate by tape testing and showed good adhesion probably because of the formation of Si-O-Si bonds between PAEAPS and glass substrate. Accordingly, the obtained PAEAPS films are insoluble in ethanol and water. The obtained PAEAPS films are uniform, transparent, and pinhole-free according to laser microscopy observation (**Figure 4**). Moreover, the PAEAPS film has a smooth surface and a root-mean-square (RMS) roughness of 68 nm, also determined by laser microscopy (**Figure 4**). Similarly, PAPS also forms a highly cross-linked network after heating at 180 °C for 2 h. However, the PAPS films become turbid upon cooling to room temperature, even though they are prepared by the same procedure as the PAEAPS films. The PAPS film has a rougher surface and RMS roughness was 679 nm estimated by laser microscopy (**Figure 4**). One possibility is that the surface roughness caused PAPS film turbid.

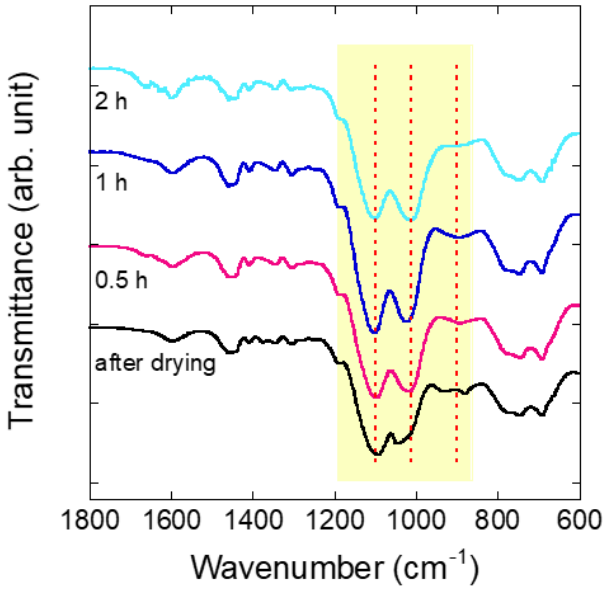

Figure 3. ATR–FTIR spectra of PAEAPS film after heating at 180 °C.

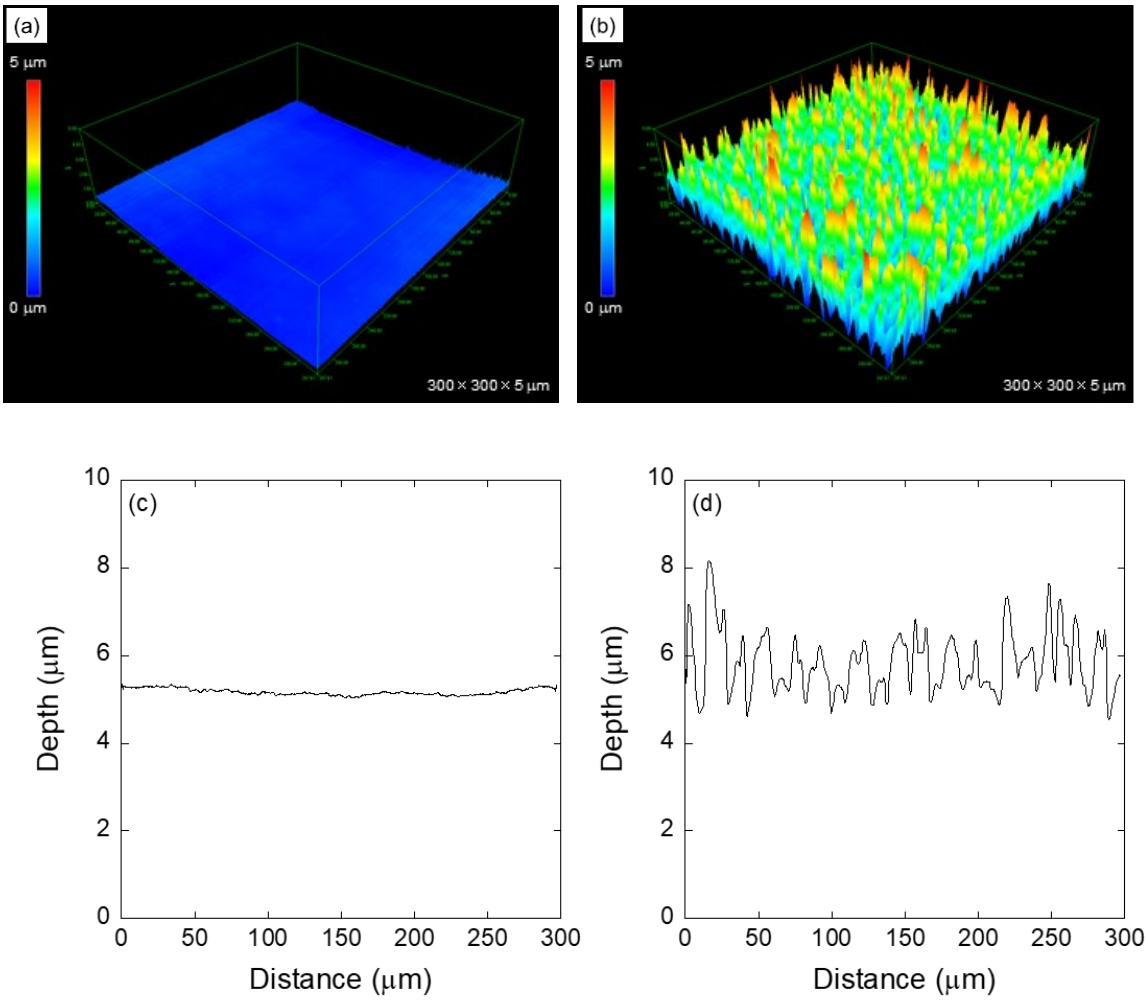

Figure 4. Laser microscopy image of (a) the PAEAPS film after heating at 180 °C for 1 h and (b) the PAPS film after heating at 180 °C for 1 h. Surface profile of (c) the PAEAPS film after heating at 180 °C for 1 h and (d) the PAPS film after heating at 180 °C for 1 h.

3.3 XRD analysis of PAPS and PAEAPS films

The PAEAPS film could have ladder-like or cage-like structures because its ^{29}Si NMR spectrum mainly shows multiple T^3 peaks. Furthermore, the PAPS film may also comprise ladder-type or cage-type structures because it becomes a whitish solid upon curing. In other words, PAPS might form a highly crystalline gel film. Therefore, XRD analysis of the PAPS and PAEAPS films was conducted

to elucidate their structures. The XRD pattern of the PAPS film features distinct broad peaks at 8.08° and 21.13°, as shown in **Figure 5**. Unlike the cage-type silsesquioxane amine salt [12-15], the PAPS film is amorphous, as evidenced by the lack of sharp diffraction peaks in its XRD pattern. However, some distinct peaks can be observed, and the d-spacings were calculated to be 1.09 (d_1) and 0.42 nm (d_2). Thus, the XRD pattern of the PAPS film indicates the formation of ordered domains, namely, ladder-like structures. According to previous reports, the d_1-spacing corresponds to the intramolecular chain-to-chain distance, i.e., the width of each double siloxane chain [17, 18]. Taken together, the XRD pattern and ^{29}Si NMR spectrum indicate that the PAPS film has not only amorphous structure but also a partial ladder-like structure because the broad peak at 8.08° corresponding to the d_1-spacing is relatively narrow and sharp and the T^3 peak for the fully condensed silicon atom in the $SiO_{3/2}$ unit is predominant.

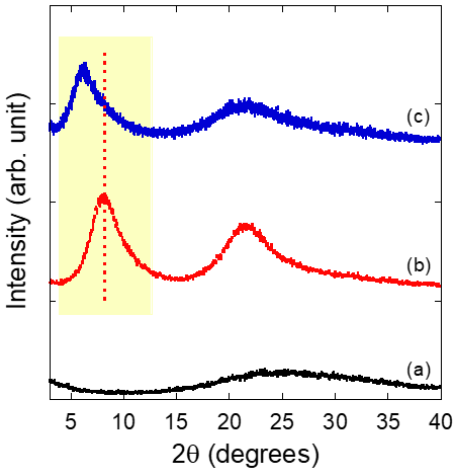

Figure 5. XRD patterns of (a) glass substrate, (b) PAPS film and (c) PAEAPS film after heating at 180 °C for 1 h.

Similarly, the PAEAPS film shows distinct broad peaks at 6.24° and 21.38°, as shown in **Figure 5**. Although PAEAPS is a viscous liquid, the obtained PAEAPS film shows diffraction peaks. The d-spacings were calculated to be 1.41 (d_1) and 0.42 nm (d_2). Interestingly, the broad peak, corresponding to d_1-spacing, is presented at a lower angle compared with that of the PAPS film. This is due to the

different sizes of the substituent groups in the side chains of the PAPS and PAEAPS films. According to a previous report, for octakis(dimethylsiloxy)octasilsesquioxanes having alkyl chains, the diffraction peak at 8° shifts to lower angles with increasing alkyl chain length [19]. In the case of the PAEAPS film, the longer side chain leads to a longer intermolecular distance between neighboring double siloxane chains.

3.4 Transparency of PAEAPS films

The transparencies and colors of antifogging materials are crucial parameters for their application to optical lenses and vehicle windshields. However, PAPS films turn whitish and turbid upon cooling to room temperature. Therefore, only the optical properties of PAEAPS-coated glass were evaluated. Accordingly, **Figure 6** shows the UV-Vis transmission spectra of a glass substrate and PAEAPS films heated at 180 °C for 1–2 h. The glass substrate shows high transmittance in the wavelength range 400–800 nm. Similarly, the PAEAPS film heated at 180 °C for 1 h exhibits a transmittance of over 88% in the wavelength range 400–800 nm, as shown in **Figure 6**. However, when the heating time is increased, the transmittance of the PAEAPS film decreases. After heating at 180 °C for 2 h, the transmittance of the PAEAPS film at 400 nm decreases to 76% accompanied by a color change from colorless to light-yellow. This may be due to some denaturation such as oxidation of the amino groups in the side chains, even though no structural changes in the amino groups are indicated by the ATR–FTIR spectra of the PAEAPS film.

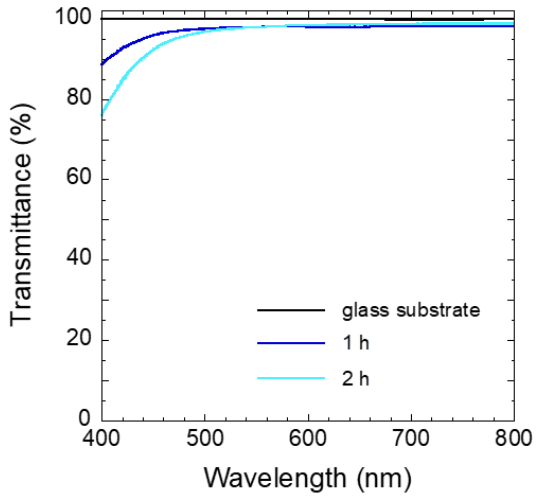

Figure 6. UV-Vis spectra of a glass substrate and PAEAPS films prepared by heating at 180 °C for 1 and 2 h.

3.5 Antifogging abilities of PAPS and PAEAPS films

To evaluate their antifogging properties, the water uptakes of PAEAPS, PAPS, and PVA films were compared. Water uptake is defined by the weight difference at 20% RH and 95% RH, and it is typically used to evaluate the water absorption materials. It is enough to discuss the antifogging property of films even though the water uptake might be not necessarily equal to antifogging property. PAEAPS was coated onto a glass substrate and heated at 60 °C for 2 h, and then at 180 °C for 0.5–2 h. For measuring water uptake, the films with similar thickness of 8.4–14.9 μm were measured for excluding the influence of film thickness. The author has also confirmed that the water uptake reached equilibrium after 1–2 h after placing in a humidity-controlled chamber at different RHs at 30 °C. The water uptake of the PAEAPS film increases with increasing RH in the range 20%–95%. For the PAEAPS film prepared by heating at 180 °C for 0.5 h, the water uptake at 95% RH was calculated to be 52%. The water uptakes of the PAEAPS films decrease from 52% to 22% with increasing the heating time from 0.5 to 2 h, as shown in **Table 1**. As discussed above, PAEAPS forms a highly cross-linked network when the heating time is increased from 0.5 to 2 h. The formation of network Si-O-Si

bonds restricts the mobility of the polymer chains, decreasing water uptake. Furthermore, the PAEAPS film before heating at 180 °C contains hydrophilic silanol groups, which also absorb water, resulting in a higher water uptake. As shown in **Figure 3**, the abundance of silanol groups decreases with increasing heating time, and the water uptake of the PAEAPS films decreased from 52% to 22% at 95% RH. Conversely, the PAPS film prepared by heating at 180 °C for 1 h exhibits a water uptake of 34%, which is lower than that of the PAEAPS film prepared under the same conditions, as shown in **Table 1**. This is due to the difference in the hydrophilicities of the side chain in the polymer units, where the PAEAPS film has two amino groups in each side chain. Although the author tried to estimate the swelling ratio of PAEAPS film after exposure to 95% RH at 30 °C, the swelling change, unfortunately, was not observed because the thickness of PAEAPS film was thin to observe their change. However, the wight change of PAEAPS film obviously indicated that PAEAPS film has the ability to absorb the water.

Table 1. Antifogging and mechanical properties of PAEAPS and PAPS films

	Curing time (h)	WU[a] (%)	Scratch resistance	Elastic modulus (GPa)	η^b (%)
PAEAPS film	0.5	52	2.3	1.2	54
PAEAPS film	1	42	2.8	2.0	58
PAEAPS film	2	22	3.2	3.7	61
PAPS film	1	34	-	1.4	22
PVA film	-	27	0.5	9.0	20

[a]Water uptake. [b]Elastic part of indentation work.

The water uptake of the PAEAPS film prepared by heating at 180 °C for 0.5 h is 1.9-times higher than that of the corresponding PVA film (27%). For the PAEAPS films, the 3-(2-

aminoethyl)aminopropyl groups act as hydrophilic moieties and absorb water under high RH conditions. The hydrophilic amino group is separated from the siloxane network by the alkyl chain and the aminoethylaminopropyl group is flexible and easily rotates in the film state. Therefore, PAEAPS films more effectively absorb water. In contrast, the water molecules cannot diffuse into the PVA film because it has high crystallinity imparted by strong hydrogen-bonding interactions.

As mentioned above, PAEAPS films exhibit high water uptake. Thus, PAEAPS films have the ability to prevent fog formation. To investigate the antifogging ability of PAEAPS, a bare glass substrate and a PAEAPS-coated substrate were cooled to 4 °C in a refrigerator and then exposed to ambient air. The glass substrate immediately fogged in the air, while the PAEAPS-coated substrate retained its transparency. Furthermore, a glass substrate and a PAEAPS-coated substrate were exposed to water vapor at 50 °C for several seconds. Again, while the glass substrate quickly fogged, the PAEAPS film retained its transparency, as shown in **Figure 7**. This indicates that the PAEAPS film quickly absorbs water and prevents the formation of fog. Interestingly, PAEAPS film exhibited antifogging ability for several ten times when it was exposed to exhaled breath. In addition, PAEAPS film has kept the antifogging ability for at least one month, showing the long-term stability.

To understand the mechanism of antifogging in PAEAPS film, water contact angle on the surface was measured. Compared with superhydrophilic material, PAPS film and PAEAPS film exhibited high water contact angles of 68° and 61°. However, PAEAPS film interestingly exhibited high water uptake and ability to prevent fog formation. Therefore, the mechanism of antifogging in PAEAPS film was totally different from superhydrophilic material. The water droplet contacted the surface of PAEAPS film and then water molecules were gradually drawn by the amine moieties and permeated into PAEAPS film. Thus, PAEAPS films exhibit high transparency even under humidified conditions and show good antifogging ability.

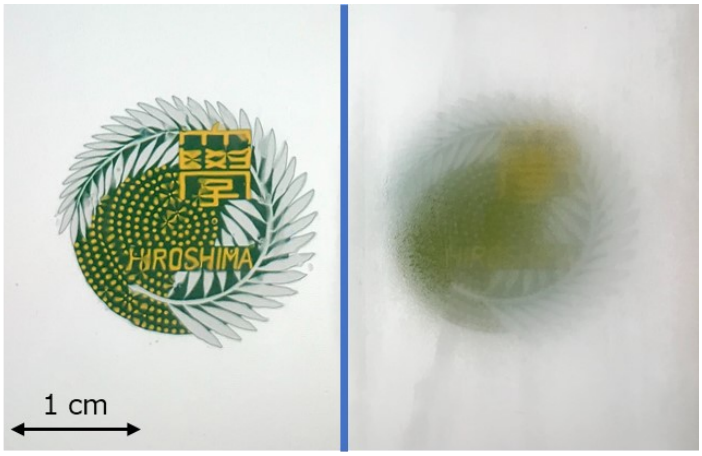

Figure 7. Photographs of a PAEAPS film on the glass substrate (left) and a glass substrate (right) exposed to water vapor.

3.6 Thermal stability of PAPS and PAEAPS films

Thermal stability is not necessarily an important property for antifogging materials, but it is of interest in the field of materials chemistry. Thus, the thermal stabilities of PAPS and PAEAPS films were evaluated using TGA. To investigate the nature of antifogging materials exposed to atmospheric water vapor, PAPS and PAEAPS films heated at 180 °C for 2 h were left in ambient conditions for several days before measurement. As shown in **Figure 8**, TGA revealed a two-step weigh loss for PAPS and PAEAPS films. The first weight loss (up to 180 °C) is attributed to 8 and 14 wt% losses of water for PAPS and PAEAPS films, respectively. Interestingly, the loss of water weight for the PAEAPS film is higher than that for the PAPS film. This is due to the difference in hydrophilicities of the films, i.e., the PAEAPS film has two amino groups in its side chains and tends to absorb and retain water. Indeed, the water uptake of the PAEAPS film is higher than that of the PAPS film, as shown in **Table 1**, and the weight loss is in good agreement with water uptake. The second weight loss starts at around at 400 °C and is assigned to the decomposition of the side chains (i.e., the aminopropyl group and (2-aminoethyl)aminopropyl group). It should be noted that these hybrid-type antifogging materials

exhibit considerable thermal stabilities compared with those of organic polymers.

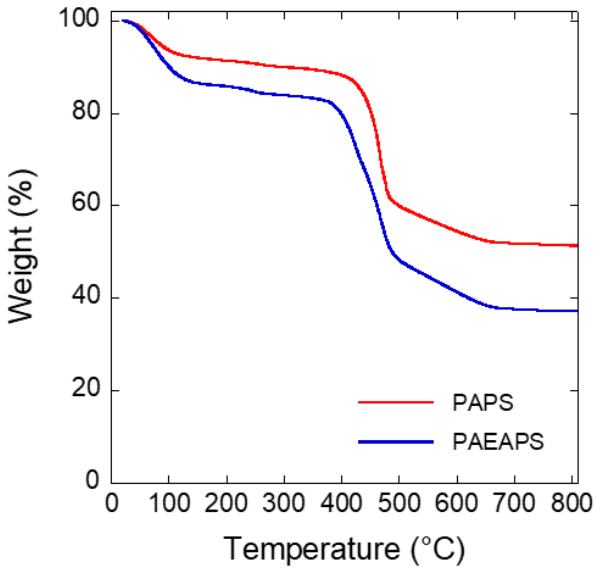

Figure 8. TGA curves for PAPS and PAEAPS measured at a heating rate of 10 °C/min under air.

3.7 Mechanical properties of PAPS and PAEAPS films

The scratch resistances of PAPS, PAEAPS, and PVA films were measured using a nanoindenter. First, scratch profiles were obtained at a scan range of 1200 μm and a scratch speed of 50 μm/s by a ramp loading of 0–20 mN on the surface of the film (**Figure 9**), and the scratch resistance was calculated according to Eq. 2. PAEAPS films prepared by heating at 180 °C for 0.5 h exhibit a scratch resistance of 2.3. The scratch resistance of the PAEAPS films increases with increasing heating time and reaches 3.2 after heating for 2 h. This increase in scratch resistance is attributed to the progress of the cross-linking reaction, as evidenced by the ATR–FTIR spectra of the PAEAPS films (**Figure 3**). Although the scratch resistance of the PAPS film was expected to be similar to that of the PAEAPS film, it was not measured because the film was not uniform. The PVA film exhibits a low scratch resistance of 0.5. Thus, the scratch resistance of the PAEAPS film is 4–6 times higher than that of the

PVA film. It has been reported that a Si-O-Si inorganic backbone structure imparts improved abrasion resistance to a material [20]. Furthermore, it is reported that polyoctahedral silsesquioxanes exhibit enhanced scratch resistance [21]. Therefore, the Si-O-Si network structure of the PAEAPS film endows it with enhanced scratch resistance.

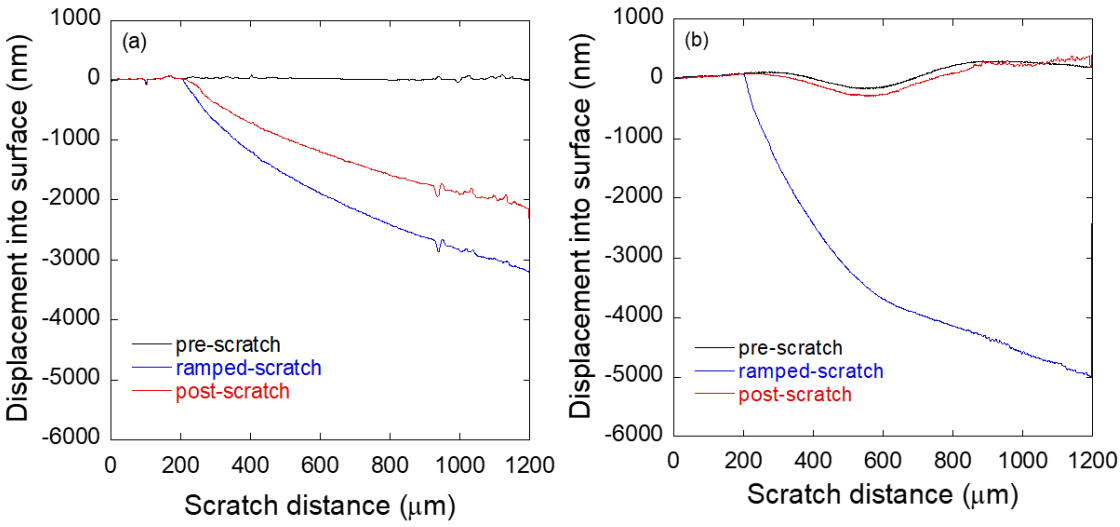

Figure 9. Scratch profile of (a) a PVA film and (b) a PAEAPS film prepared by heating at 180 °C for 1 h.

To improve the scratch resistance of antifogging materials such as PVA and polyacrylate, silica nanoparticles were introduced into their film [22-24]. Indeed, the hardness of films increased with increasing the amount of silica nanoparticles. In some cases, the trade-off relationship between the antifogging ability and the scratch resistance occurred by their strategy. Furthermore, the addition of silica nanoparticles decreases the transparency of antifogging film because of the aggregation of silica nanoparticles. However, PAEAPS film exhibited the excellent antifogging ability and scratch resistance without the additive because the PAEAPS films composed of the siloxane network and hydrophilic amino group. Furthermore, the decrease of transparency did not occur because there is not necessarily to add the silica nanoparticles. These are good advantages for antifogging materials. Recently, hybrid-type antifogging material also has been reported and this polyhedral oligomeric

silsesquioxane-poly(quaternary ammonium-*co*-2-aminoethyl methacrylate hydrochloride) showed excellent antifogging performance [25]. The content of polyhedral oligomeric silsesquioxane in the polymer was considerably low and, unfortunately, their mechanical property of hybrid-type antifogging material has not been mentioned. In contrast, the content of siloxane network in PAEAPS film was considerably high, and it might enhance the scratch resistance.

To explore the high scratch resistance of the PAEAPS films, their mechanical properties were also measured using the nanoindenter in accordance with ISO 14577-1. The elastic moduli and elastic part of indentation work (η) of PAEAPS films heated at 180 °C are shown in **Table 1**. The elastic modulus increases with increasing heating time and reaches 3.7 GPa after heating at 180 °C for 2 h. This is because the cross-linking and formation of Si-O-Si bonds enhances the elastic modulus. However, the elastic modulus of PVA is 9.0 GPa, which is higher than that of the PAEAPS film prepared at 180 °C for 2 h. It should be noted that the PAEAPS films exhibit high scratch resistances even though their elastic moduli are lower than that of the PVA film. The elastic part of indentation work (η) of the PAEAPS and PVA films was calculated from the plastic deformation work and elastic deformation work [10]. The η of the PAEAPS films was higher than that of the PVA film. The PVA film exhibited a low elastic deformation work of 20%, indicating that the film showed low elastic recovery. In contrast, the PAEAPS films exhibited a high elastic deformation work of 54−61%; in particular, they easily recovered from deformation after nanoindentation, unlike the PVA film. Actually, when the PAEAPS film surface was scratched in the range of 0−1200 μm using a ramp loading of 0−20 mN, the postscratch test showed an almost completely recovered surface from the ramped-scratch test, as shown in **Figure 9**. On the other hand, the PVA scratch test showed slight recovery from deformation during the lamp scratch test. These results indicate that a characteristic feature of polysiloxanes whereby flexible Si-O bonds help to recover from deformation and thus enhance scratch resistance.

4. Conclusions

PAPS and PAEAPS were successfully prepared by sol-gel reactions autocatalyzed by the amine moieties of the monomers. ^{1}H and ^{29}Si NMR analyses indicated that the hydrolysis and polycondensation proceed efficiently, forming amine-functionalized polysilsesquioxanes with highly cross-linked T^3 structures. PAPS and PAEAPS showed good film-form ability, and the obtained films were found to be uniform and pinhole-free. The XRD patterns of the PAPS and PAEAPS films indicated the formation of ladder-like structures. The PAPS and PAEAPS films exhibit high water uptakes of 34% and 42%, which are 1.2- and 1.5-times higher than that of the typical hydrophilic polymer PVA. The optimal PAEAPS film showed the high scratch resistance of 3.2, which is 6–7-times higher than that of a corresponding PVA film. Furthermore, a PAEAPS-coated glass substrate demonstrated excellent transparency and antifogging property. Thus, PAEAPS is a promising candidate as an antifogging material that demonstrates both excellent antifogging property and appropriate scratch resistance simultaneously.

5. References

[1] R.H. Baney, M. Itoh, A. Sakakibara, T. Suzuki, SILSESQUIOXANES, Chemical Reviews 95(5) (1995) 1409-1430.

[2] J.Y. Wen, G.L. Wilkes, Organic/inorganic hybrid network materials by the sol-gel approach, Chemistry of Materials 8(8) (1996) 1667-1681.

[3] R. Ciriminna, A. Fidalgo, V. Pandarus, F. Beland, L.M. Ilharco, M. Pagliaro, The Sol-Gel Route to Advanced Silica-Based Materials and Recent Applications, Chemical Reviews 113(8) (2013) 6592-6620.

[4] N. Ahmed, H. Fan, P. Dubois, X.W. Zhang, S. Fahad, T. Aziz, J.T. Wan, Nano-engineering and micromolecular science of polysilsesquioxane materials and their emerging applications, Journal of Materials Chemistry A 7(38) (2019) 21577-21604.

[5] Y.J. Du, H.Z. Liu, Cage-like silsesquioxanes-based hybrid materials, Dalton Transactions 49(17) (2020) 5396-5405.

[6] Z.N. Bao, V. Kuck, J.A. Rogers, M.A. Paczkowski, Silsesquioxane resins as high-performance solution processible dielectric materials for organic transistor applications, Advanced Functional Materials 12(8) (2002) 526-531.

[7] T. Nagase, T. Hamada, K. Tomatsu, S. Yamazaki, T. Kobayashi, S. Murakami, K. Matsukawa, H. Naito, Low-Temperature Processable Organic-Inorganic Hybrid Gate Dielectrics for Solution-Based Organic Field-Effect Transistors, Advanced Materials 22(42) (2010) 4706-4710.

[8] T. Hamada, T. Nagase, T. Kobayashi, K. Matsukawa, H. Naito, Effective control of surface property on poly(silsesquioxane) films by chemical modification, Thin Solid Films 517(4) (2008) 1335-1339.

[9] M. Watanabe, K. Muro, T. Hamada, T. Tamai, A. Masuyama, H. Naito, K. Matsukawa, Surface Modification of Organic-Inorganic Hybrid Insulator for Printable Organic Field-effect Transistors, Chemistry Letters 38(1) (2009) 34-35.

[10] E. Borisenko, D. Borisenko, I. Bdikin, A. Timonina, B. Singh, N. Kolesnikov, Mechanical characteristics of gallium sulfide crystals measured using micro- and nanoindentation, Materials Science and Engineering a-Structural Materials Properties Microstructure and Processing 757 (2019) 101-106.

[11] T. Gunji, S. Itagaki, T. Kajiwara, Y. Abe, T. Hatakeyama, R. Aoki, Preparation and Properties of Siloxane/Epoxy Organic-Inorganic Hybrid Thin Films, Self-Standing Films, and Bulk Bodies, Polymer Journal 41(7) (2009) 541-546.

[12] Y. Kaneko, M. Shoiriki, T. Mizumo, Preparation of cage-like octa(3-aminopropyl)silsesquioxane trifluoromethanesulfonate in higher yield with a shorter reaction time, Journal of Materials Chemistry 22(29) (2012) 14475-14478.

[13] T. Ishii, T. Mizumo, Y. Kaneko, Facile Preparation of Ionic Liquid Containing Silsesquioxane Framework, Bulletin of the Chemical Society of Japan 87(1) (2014) 155-159.

[14] T. Ishii, T. Enoki, T. Mizumo, J. Ohshita, Y. Kaneko, Preparation of imidazolium-type ionic liquids containing silsesquioxane frameworks and their thermal and ion-conductive properties, Rsc Advances 5(20)

(2015) 15226-15232.
[15] A. Harada, S. Koge, J. Ohshita, Y. Kaneko, Preparation of a Thermally Stable Room Temperature Ionic Liquid Containing Cage-Like Oligosilsesquioxane with Two Types of Side-Chain Groups, Bulletin of the Chemical Society of Japan 89(9) (2016) 1129-1135.
[16] M.C. Gravel, C. Zhang, M. Dinderman, R.M. Laine, Octa(3-chloroammoniumpropyl) octasilsesquioxane, Applied Organometallic Chemistry 13(4) (1999) 329-336.
[17] C.Q. Liu, Y. Liu, Z.R. Shen, P. Xie, R.B. Zhang, J.L. Yang, F.L. Bai, Study of the steric tacticity of novel soluble ladderlike poly(phenylsilsesquioxane) prepared by stepwise coupling polymerization, Macromolecular Chemistry and Physics 202(9) (2001) 1581-1585.
[18] Y.C. Sheen, C.H. Lu, C.F. Huang, S.W. Kuo, F.C. Chang, Synthesis and characterization of amorphous octakis-functionalized polyhedral oligomeric silsesquioxanes for polymer nanocomposites, Polymer 49(18) (2008) 4017-4024.
[19] F.X. Perrin, T.B.V. Nguyen, A. Margaillan, Linear and branched alkyl substituted octakis(dimethylsiloxy)octasilsesquioxanes: WAXS and thermal properties, European Polymer Journal 47(7) (2011) 1370-1382.
[20] J. Wen, V.J. Vasudevan, G.L. Wilkes, Abrasion resistant inorganic organic coating materials prepared by the sol-gel method, Journal of Sol-Gel Science and Technology 5(2) (1995) 115-126.
[21] E. Amerio, M. Sangermano, G. Colucci, G. Malucelli, M. Messori, R. Taurino, P. Fabbri, UV curing of organic-inorganic hybrid coatings containing polyhedral oligomeric silsesquioxane blocks, Macromolecular Materials and Engineering 293(8) (2008) 700-707.
[22] C.C. Chang, F.H. Huang, H.H. Chang, T.M. Don, C.C. Chen, L.P. Cheng, Preparation of Water-Resistant Antifog Hard Coatings on Plastic Substrate, Langmuir 28(49) (2012) 17193-17201.
[23] C.C. Chang, T.Y. Tsai, L.P. Cheng, Preparation of Nanosilica/polyacrylate Antifog Coatings on Polycarbonate Substrates, Journal of Applied Science and Engineering 22(1) (2019) 153-162.
[24] G.Q. Wu, Y.L. Yang, Y.T. Lei, D.P. Fu, Y.C. Li, Y.H. Zhan, J.M. Zhen, M.Y. Teng, Hydrophilic nano-SiO2/PVA-based coating with durable antifogging properties, Journal of Coatings Technology and Research 17(5) (2020) 1145-1155.
[25] S. Bai, X.H. Li, Y.H. Zhao, L.X. Ren, X.Y. Yuan, Antifogging/Antibacterial Coatings Constructed by N-Hydroxyethylacrylamide and Quaternary Ammonium-Containing Copolymers, Acs Applied Materials & Interfaces 12(10) (2020) 12305-12316.

Chapter 3: Enhancing Antifogging Property of Polysilsesquioxane Film via an Amine Hydrochloride Salt

1. Introduction

As described in Chapter 2, the PAEAPS film absorbs water owing to hydrophilicity and flexibility of 3-(2-aminoethyl)aminopropyl group , and the siloxane network enhances their mechanical properties. As a result, the PAEAPS film exhibited high water uptake and scratch resistance. Antifogging materials based on PSQ may replace traditional antifogging materials. Therefore, further investigation of the structure and antifogging properties of PSQ films is required to develop high-performance antifogging materials.

Previously, ionic units such as ammonium chloride and sulfobetaine that have stronger interaction with water than polar functional groups were introduced into the polymer as hydrophilic groups [1, 2]. This is easily understood considering that ammonium salts are usually readily dissolved in water by hydration of the ionic units. For example, the polymer containing 2-(methacryloyloxy)ethyltrimethylammonium chloride and sulfobetaine methacrylate exhibited high water-absorbing capacity due to strong polymer-water interactions by strong hydrogen bonds [2]. In Chapter 3, the author describes the preparation of amine salt-containing PSQ films, expecting that the amine hydrochloride salt could provide high water uptake. The influence of amine hydrochloride salt of PSQ on the antifogging properties and scratch resistance was investigated. In addition, the durability of PAEAPS and PAEAPS-Cl films under high humidity environments is also investigated to explore the potential for practical application.

2. Experimental

2.1 Materials

PAEAPS was synthesized as described in Chapter 2. 3-(2-Aminoethylaminopropyl)triethoxysilane and methyltriethoxysilane were purchased from Tokyo Chemical Industry Co. Ltd. (Tokyo, Japan) and used as received without further purification. Ethanol (superdehydrated) and 0.5 mol/L hydrochloric acid (HCl) methanolic solution were purchased from FUJIFILM Wako Pure Chemical Co. Ltd. (Osaka, Japan). Water was purified using a Millipore Milli-Q UV system and showed resistance and total organic carbon content values of 18.2 MΩ·cm and <10 ppb, respectively. To clean the glass substrates using an alkaline solution, KOH (50 g) was first dissolved in a mixture containing 2-propanol (600 mL) and water (100 mL). Then, the glass substrates were immersed in this mixture for at least 15 h. The cleaned glass substrates were washed with water twice and immersed in a 0.2 M HCl solution. Finally, the cleaned glass substrates were rewashed with water and dried under an argon flow. The water contact angle of the glass substrates was confirmed to be ~28°. The cleaned glass substrates were immediately used for film preparation.

2.2 Measurements

^{1}H nuclear magnetic resonance (NMR) measurements were performed on a Varian 400 MHz spectrometer in deuterium chloroform ($CDCl_3$) or deuterium oxide (D_2O) using residual chloroform or water as internal standards (7.26 ppm and 4.79 ppm) for chemical shift referencing. ^{13}C and ^{29}Si solid-state NMR experiments were performed using a Varian System 600 spectrometer by magic-angle spinning. For the ^{13}C and ^{29}Si solid-state NMR spectra, hexamethylbenzene and 3-(trimethylsilyl)-propionic acid were used as external standards for chemical shift referencing. Fourier-transform infrared (FTIR) spectroscopy was conducted in the transmittance mode on a Shimadzu IR Affinity-1 spectrometer. Size exclusion chromatography (SEC) was performed on a Shimadzu Prominence HPLC System with triply connected Shodex OHpak SB-G/SB-805HQ/SB-804HQ columns calibrated

using poly(ethylene oxide). 0.2 mol/L sodium nitrate ($NaNO_3$) solution was used as the eluent at a flow rate of 0.5 mL/min at 40 °C. Scanning electron microscopy (SEM) and energy-dispersive X-ray spectroscopy (EDX) was performed using an EDX (GENESIS, EDAX) attached to a high-resolution SEM (HITACHI S-5200). The PSQ film prepared on the Kapton film was coated with carbon by sputtering to prevent charging. The scratch resistance and the elastic modulus of the PSQ film containing the amine hydrochloride salt were measured by indentation and scratch tests using a Nano Indenter G200 (the detailed procedure is provided in Chapter 2).

To measure the water uptake (WU) of the film, the 12.5-μm-film Kapton film was used as a substrate to reduce the influence of the substrate weight error. The PSQ-OH film coated on the Kapton film prepared using the aforementioned procedure was placed in a temperature- and humidity-controlled chamber, and the weight of the polymer film coated on the Kapton film was measured at 20% and 95% relative humidity (*RH*) for 2 h at 30 °C. The WU was calculated using Equation (1):

$$WU\ (\%) = \frac{W_{95\%RH} - 0.024 \times W_{Kapton} - W_{20\%RH}}{W_{20\%RH}} \times 100, \quad (1)$$

where $W_{20\%\ RH}$ and $W_{95\%\ RH}$ denote the weight of the polymer film after exposure to 20% and 95% relative humidity, respectively, at 30 °C for 2 h. W_{Kapton} denotes the weight of the Kapton film as the substrate and is corrected by taking into consideration the water absorbed by the Kapton film. The Kapton film absorbed ~2.4 wt% water relative to its weight of the Kapton film under 95% relative humidity at 30 °C.

2.3 Preparation of poly[3-(2-aminoethylamino)propyl-co-methyl]silsesquioxane (P(AEAP-co-Me)S)

P(AEAP-co-Me)S was synthesized by the reflux method described in Chapter 2. In a 100-mL round-bottom flask equipped with a Dimroth condenser, 3-(2-aminoethylaminopropyl)triethoxysilane

(5.289 g, 20.00 mmol), methyltriethoxysilane (1.783 g, 10.00 mmol), and ethanol (13.82 g, 300.0 mmol) were mixed in an ice–water bath for 10 min. Water (1.081 g, 60.00 mmol) was slowly added, and the reaction mixture was stirred at 0 °C for 10 min. Then, the mixture was stirred at room temperature for 10 min and refluxed for 5 h. Finally, ethanol was removed under reduced pressure at 60 °C to obtain P(AEAP-co-Me)S as a viscous liquid. The obtained P(AEAP-co-Me)S was diluted with ethanol to a concentration of 20 wt% and stored in a refrigerator at ca. 4 °C prior to further use.

^{1}H NMR (400 MHz, $CDCl_3$, ppm): δ = 0.08 (1.1H, brs, $SiCH_3$), 0.55 (2H, brs, $SiCH_2$), 1.41–1.59 (5.2H, brm, CH_2, amino group, $OCH_2C\underline{H}_3$), 2.54–2.74 (6H, brm, CH_2 (adjacent to nitrogen atoms)), 3.76 (0.4H, m, $OC\underline{H}_2CH_3$).

2.4 Preparation of poly[3-(2-aminoethylamino)propyl]silsesquioxane hydrochloride (PAEAPS-Cl) and poly[3-(2-aminoethylamino)propyl-co-methyl]silsesquioxane hydrochloride (P(AEAP-co-Me)S-Cl) films by the immersion method

An ethanol solution of 20 wt% PAEAPS or P(AEAP-co-Me)S was coated on the glass substrate by an applicator with a clearance gap of 100 μm and heated at 60 °C and 180 °C for 2 h, respectively. The obtained PAEAPS or P(AEAP-co-Me)S film on the glass substrate was immersed in 0.5 mol/L HCl methanolic solution for 1 h and washed with methanol several times. Finally, the obtained PAEAPS-Cl and P(AEAP-co-Me)S-Cl films on the glass substrate were dried at 60 °C for 30 min.

2.5 Synthesis of PAEAPS-Cl by the reaction of PAEAPS with HCl

In a 50-mL round-bottom flask was placed 551 mg (3.60 mmol) of PAEAPS as a viscous liquid and 18 mL of 0.5 mol/L HCl methanolic solution was slowly added. The white solid was gradually precipitated, and the reaction mixture was stirred at room temperature for 1 h. Finally, the solvent was removed by an evaporator, and the white solid (809 mg, 99%) was dried at 100 °C for 2 h under a vacuum.

^{1}H NMR (400 MHz, D_2O, ppm): δ = 0.84 (2H, brs, CH_2), 1.84 (2H, brs, CH_2), 3.17 (2H, brs, CH_2),

3.43–3.45 (4H, brm, CH_2).

2.6 Preparation of the PAEAPS-Cl film by the coating method

PAEAPS-Cl was dissolved in water to obtain 20 wt% PAEAPS-Cl/water solution and coated on the glass substrate by the applicator with a clearance gap of 100 μm. The wet film was heated at 60 and 180 °C for 2 h, respectively, to afford the PAEAPS-Cl film.

3. Results and discussion

3.1 Preparation of the PAEAPS-Cl film by the immersion method

For the preparation of PSQ films containing amine hydrochloride salts, two methods were conducted as follows: (1) PAEAPS film was treated using a HCl methanolic solution to form the amine hydrochloride salt, and (2) PSQ having amine hydrochloride salt was synthesized, and coated on the substrate using the applicator, as shown in **Scheme 1**.

First, PAEAPS was coated on a silicon wafer and heated at 60 and 180 °C for 2 h, respectively. The obtained PAEAPS film on silicon was immersed in 0.5 mol/L HCl methanolic solution for 1 h to convert the amino group to the amine hydrochloride salt (**Scheme 1**). The chemical structures of the PAEAPS and PAEAPS-Cl films were investigated by FTIR spectroscopy and ^{13}C solid-state NMR. As shown in **Figure 1**, the PAEAPS film showed distinct peaks at 1126 cm^{-1} and 1036 cm^{-1} corresponding to the siloxane bond, and small peaks corresponding to the amino group were observed at 1666 cm^{-1} and 1603 cm^{-1} before HCl treatment. After immersion in 0.5 mol/L HCl methanolic solution, a broad peak appeared in the range of 3500–2500 cm^{-1}, and the small peaks corresponding to the amino group slightly changed [3]. Then, in the ^{13}C solid-state NMR spectrum of the PAEAPS film (**Figure 2**), signals corresponding to the methylene group were observed at 9.2, 22.2, 40.5, and 51.4 ppm. These signals shifted entirely to the upfield region after the conversion to the amine hydrochloride salt at 8.7, 19.1, 36.4, and 48.0 ppm. These results clearly supported that the amine

group was converted to the amine hydrochloride salt upon immersion in 0.5 mol/L HCl methanolic solution.

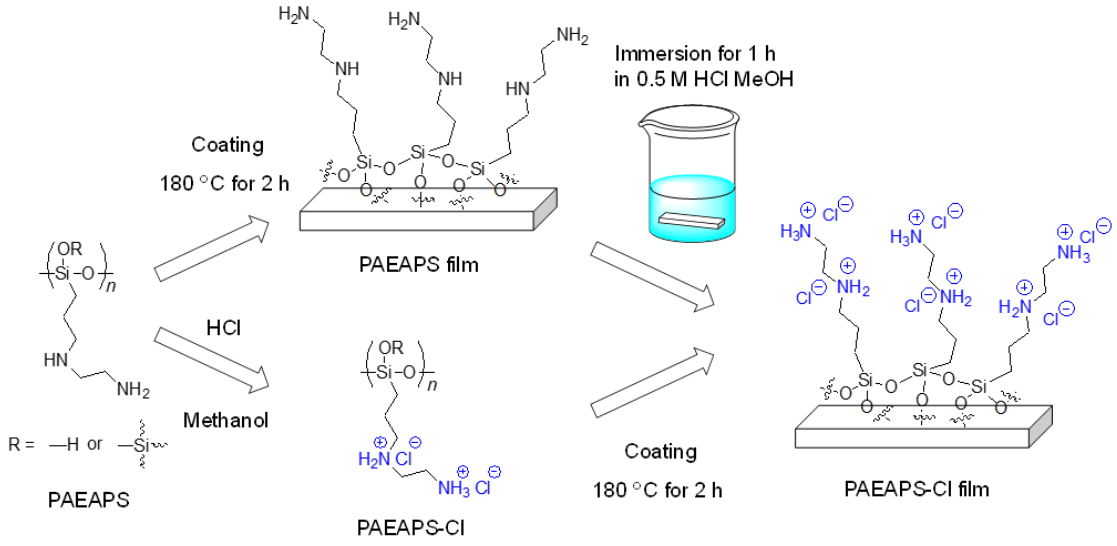

Scheme 1. Schematic illustrating the preparation of the PAEAPS-Cl film via the immersion method and the coating method.

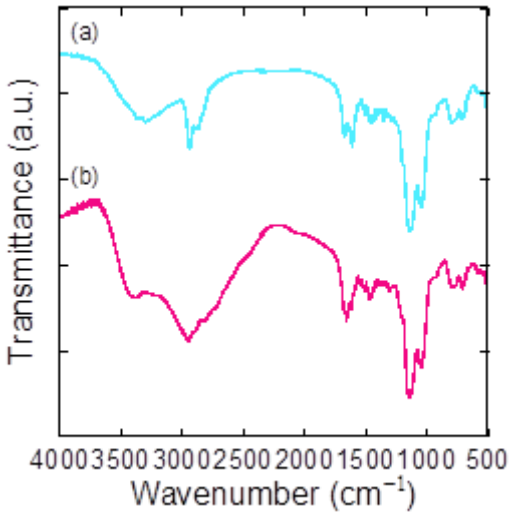

Figure 1. FTIR spectra of (a) PAEAPS film and (b) PAEAPS-Cl film prepared by immersion in 0.5 M HCl/MeOH solution for 1 h.

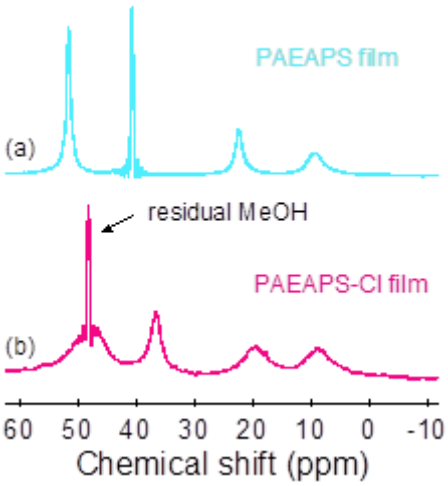

Figure 2. ^{13}C solid-state NMR spectra of (a) PAEAPS film and (b) PAEAPS-Cl film prepared by immersion in 0.5 mol/L HCl/MeOH solution for 1 h.

In addition, the introduction of chloride ions into the amino group was also confirmed by SEM-EDX spectra before and after immersion in 0.5 mol/L HCl methanolic solution. In the PAEAPS film, only the peaks attributed to carbon, oxygen, and silicon were observed at 0.25, 0.52, and 1.75 eV, respectively. A new peak at 2.63 eV corresponding to the chloride atom appeared in the SEM-EDX spectrum of the PAEAPS-Cl film after the formation of the amine hydrochloride salt **(Figure 3**). The PAEAPS-Cl film maintained a smooth surface, and cracks and pinholes were not observed on the surface and cross-sectional images of the PAEAPS-Cl film even after the formation of the amine chloride salt (**Figure 4**). Furthermore, the elemental mapping image also showed that chloride atoms were homogeneously distributed on the surface of the PAEAPS-Cl film, as shown in **Figure 4**.

Overall, FTIR, ^{13}C solid-state NMR, and SEM-EDX results showed that the amine hydrochloride salt was successfully formed by the neutralization of amino groups with HCl in the PAEAPS film.

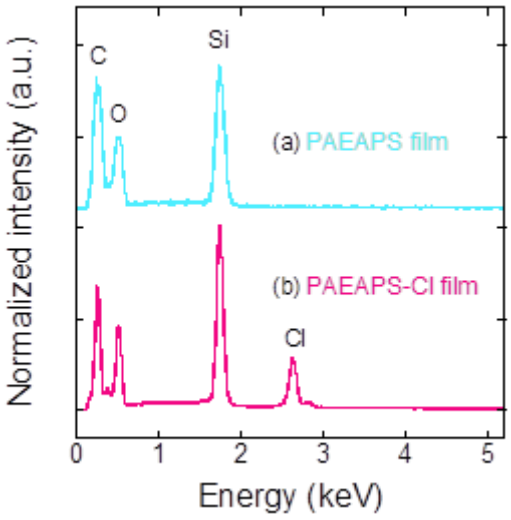

Figure 3. Scanning electron microscopy–energy-dispersive X-ray spectroscopy (SEM-EDX) spectra of (a) poly[3-(2-aminoethylaminopropyl)]silsesquioxane (PAEAPS) film and (b) poly[3-(2-aminoethylamino)propyl]silsesquioxane hydrochloride (PAEAPS-Cl) film prepared by immersion in 0.5 M HCl/methanol solution for 1 h.

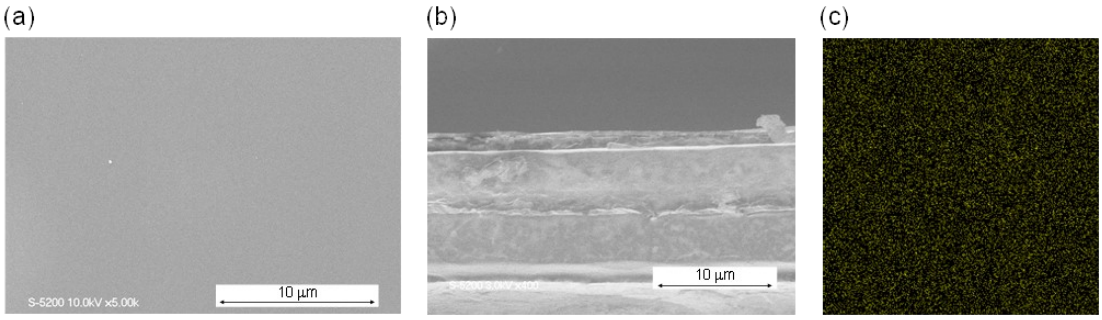

Figure 4. SEM micrograph of (a) surface and (b) cross section of the PAEAPS-Cl film on the Kapton film. (c) Elemental mapping image of chlorine atoms on the surface of the PAEAPS-Cl film.

3.2 Synthesis of PAEAPS-Cl and preparation of the PAEAPS-Cl film by the coating method

For the synthesis of PSQ having the amine hydrochloride salt, PAEAPS was reacted with HCl in methanol (**Scheme 1**). As described in Chapter 2, PAEAPS shows high solubility in organic solvents, including ethanol, chloroform, and acetone. The solubility of PSQ having the amine hydrochloride

salt was totally different, and the precipitant was obtained through the addition of an HCl methanolic solution. The reaction mixture was stirred at room temperature for 1 h to attain the quantitative reaction. PAEAPS-Cl was obtained as a white solid with a high yield (99%). The solubility of PAEAPS-Cl drastically changed, and it did not dissolve in organic solvents, such as acetone, THF, chloroform, methanol, and ethanol. Interestingly, PAEAPS-Cl dissolved in water, verifying that the amino group in PAEAPS was converted to the amine hydrochloride salt. Then, the structure of PAEAPS-Cl was confirmed using ^{1}H NMR in D_2O. All signals shifted downfield, and their signals were reasonable based on the integration of the methylene proton (**Figure 5**). In Chapter 2, the molecular weight of PAEAPS was not detected by SEC employing a polystyrene gel column in THF as an eluent because PAEAPS was adsorbed on the column via the amino group. However, the ionization of the amino group prevented the adsorption on the column, and the molecular weight of PAEAPS-Cl was estimated to be 5700 (weight-average) with a polydispersity index of 2.4 by SEC employing polyhydroxy methacrylate gel in a 0.2 mol/L $NaNO_3$ solution.

Next, the PAEAPS-Cl solution in water was coated on a silicon wafer and heated at 60 °C and 180 °C for 2 h, respectively. In the FTIR spectrum of the PAEAPS-Cl film after heating at 60 °C for 2 h, the peak of the siloxane bond was observed at 1132 cm^{-1} and 1042 cm^{-1}, as shown in **Figure 6**. After heating at 180 °C for 2 h, the intensity of the peak attributed to the siloxane bond at 1040 cm^{-1} increased (**Figure 6**), indicating that a network structure composed of siloxane bonds was formed by thermal curing, and the PAEAPS-Cl film was obtained by the coating process.

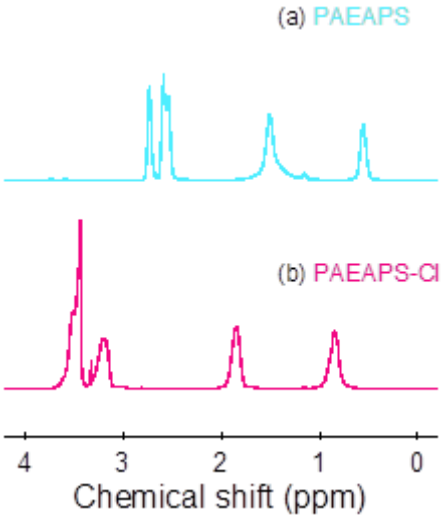

Figure 5. ^{1}H nuclear magnetic resonance (NMR) spectra of (a) PAEAPS in $CDCl_3$ and (b) PAEAPS-Cl in D_2O.

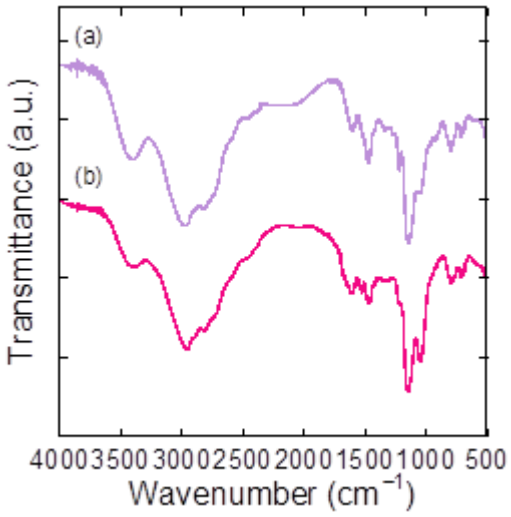

Figure 6. FTIR spectra of the PAEAPS-Cl film prepared using the coating method (a) after heating at 60 °C for 2 h and (b) after heating at 180 °C for 2 h.

3.3 Synthesis of P(AEAP-co-Me)S and preparation of the P(AEAP-co-Me)S-Cl film by the immersion method

To enhance the surface hardness of the PAEAPS film and investigate the influence of the number

of amino groups on the antifogging property, P(AEAP-co-Me)S was also synthesized at a 3-(2-aminoethylaminopropyl)triethoxysilane/methyltriethoxysilane molar ratio of 2/1 by hydrolysis and polycondensation (**Scheme 2**). As described in Chapter 2, the amino groups in 3-(2-aminoethylaminopropyl)triethoxysilane act as a catalyst for the hydrolysis and polycondensation reaction. Therefore, the hydrolysis and polycondensation of 3-(2-aminoethylaminopropyl)triethoxysilane and methyltriethoxysilane were conducted under the same conditions without adding a catalyst for the preparation of PAEAPS. After the polycondensation reaction, a viscous liquid was obtained upon the removal of the solvent. The structure of P(AEAP-co-Me)S was investigated by ^{1}H NMR. In the ^{1}H NMR spectrum of P(AEAP-co-Me)S in $CDCl_3$, the signals attributed to the propyl group were observed at 0.55, 1.51, and 2.54 ppm, and part of the signal was observed with the signal of the ethyl group in the ethoxy group at 2.54–2.74 ppm. Similarly, the signals of two amino groups at 1.29 ppm overlapped with the signal of the propyl group. In PAEAPS, over 99% of the ethoxy group was consumed because of amine autocatalyzation. In the preparation of P(AEAP-co-Me)S, the hydrolysis and polycondensation reaction effectively proceeded, and the residual ethoxy group was less than 5%. The composition of the aminoethylaminopropyl group and the methyl group was estimated to be 2.7:1 based on the integration of methylene and methyl groups. Although the number of methyl groups was slightly lower than the calculated value based on the feed ratio, P(AEAP-co-Me)S with different contents of amino groups could be prepared by copolymerization without gelation. P(AEAP-co-Me)S also showed good film-forming ability, and its film containing the amine hydrochloride salt was also prepared similarly, as shown in **Scheme 2**.

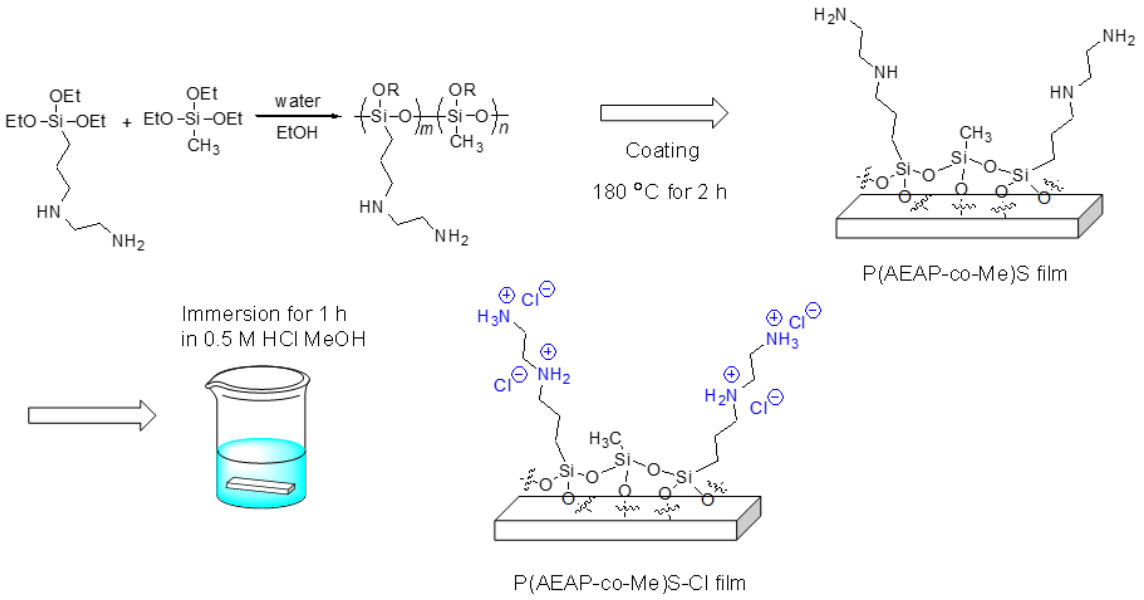

Scheme 2. Synthesis of P(AEAP-co-Me)S via the hydrolysis and polycondensation of 3-(2-aminoethylaminopropyl)triethoxysilane and triethoxymethylsilane and the preparation of the P(AEAP-co-Me)S-Cl film by the immersion method.

3.4 Antifogging and mechanical properties of the PAEAPS-Cl and P(AEAP-co-Me)S-Cl films and its stability against water vapor

To investigate the influence of the amine hydrochloride salt on the antifogging and mechanical properties of the PAEAPS film, the WU of the PAEAPS-Cl film was measured and compared with that of the PAEAPS film, along with the fog test conducted through exposure to water vapor. The surface hardness of the PAEAPS-Cl film was also evaluated based on scratch resistance and elastic modulus by the nanoindenter. The data are shown in **Table 1**. The PAEAPS film prepared by heating at 180 °C for 2 h exhibits a WU of 22%. When the PAEAPS film on the glass substrate was exposed to hot vapor at 40 °C at a distance of 2 cm, the PAEAPS film on the glass substrate became cloudy within 9 s. On the other hand, the WU of the PAEAPS-Cl film increased up to 29% upon the introduction of the amine hydrochloride salt structure. The PAEAPS-Cl film on the glass substrate

maintained transparency for 8 s, which was almost similar to the PAEAPS film on the glass substrate.

Table 1. Antifogging properties and mechanical properties of PAEAPS, PAEAPS-Cl, and P(AEAP-co-Me)S-Cl films

	WU[a] (%)	fogging test[b] (s)	scratch resistance	elastic modulus (GPa)	film state
PAEAPS	22	9	3.2	3.7	transparent
PAEAPS-Cl	29	8	4.3	3.4	transparent
P(AEAP-co-Me)S-Cl	17	7	3.7	2.6	transparent

[a]Water uptake. [b]Film was exposed to hot vapor at 40°C at a distance of 2 cm, and an average of 3 measurements was presented.

Although the introduction of the amine hydrochloride salt apparently enhanced the WU, the difference in the time of fog formation was not observed in the evaluation of the antifogging property by the fog test. In the PAEAPS film, the amino group in the side chain absorbs water via hydrogen bonding and retains it in the film. In the case of the PAEAPS-Cl film, the absorption mechanism of water might be due to the hydrate around the chloride ion, similar to the polymer electrolyte membrane [4]. The hydrophilicity of the film totally increased by the introduction of the amine hydrochloride salt structure, increasing the WU of PAEAPS-Cl. However, according to the fog test, the PAEAPS-Cl film might slowly absorb water and retain water molecules around the salt structure. It is concluded that the absorption speed due to the hydration of water molecules is slower than that due to hydrogen bonding.

As shown in **Table 1**, the PAEAPS film prepared by heating at 180 °C for 2 h showed scratch resistance and elastic modulus values of 3.2 and 3.7 GPa, respectively. Interestingly, the PAEAPS-Cl

film exhibited a high scratch resistance of 4.3. As discussed in Chapter 2, the scratch resistance of the PAEAPS film is affected by the crosslinking density of the siloxane network. Indeed, the scratch resistance of the PAEAPS film increased from 2.3 to 3.2 as the heating period increased from 0.5 h to 2 h. However, the crosslinking densities of the PAEAPS and PAEAPS-Cl films are similar because the PAEAPS-Cl film, as well as the PAEAPS film, was also prepared by heating at 180 °C for 2 h. The introduction of the amine hydrochloride salt into the PAEAPS film enhanced surface hardness. On the other hand, the elastic modulus of the PAEAPS-Cl film was similar to or slightly lower than that of the PAEAPS film, indicating that the PAEAPS-Cl film tended to deform, compared with the PAEAPS film, even though the amine hydrochloride salt structure increased the surface hardness. This may be due to the presence of water molecules in the PAEAPS-Cl film. The PAEAPS-Cl film can retain water molecules through hydration around the salt structure. Water molecules might have acted as a plasticizer, decreasing the elastic modulus of the PAEAPS-Cl film [5]. In addition, the high scratch resistance of the PAEAPS-Cl film might be derived from the effect of water molecules as a plasticizer. Importantly, both films exhibited high surface hardness compared with a (hydrophilic) poly(vinyl alcohol) film.

The long-term stability of antifogging materials is an important factor from the viewpoint of practical applications. Thus, the PAEAPS and PAEAPS-Cl films were stored at 40 °C and 95% relative humidity (RH) for 1 h for investigating film stability against water vapor. To investigate whether the structural changes occur after exposure to water vapor at 40 °C and 95% RH for 1 h, the FTIR measurements of the PAEAPS and PAEAPS-Cl films were conducted. In the FTIR spectrum of the PAEAPS film, the peak corresponding to the amino group at 1643 cm^{-1} showed almost no change after exposure to water vapor at 40 °C and 95% RH for 1 h, as shown in **Figure 7** (a). However, the peaks of the siloxane bond at 1132 cm^{-1} and 1038 cm^{-1} slightly changed. In the case of the polymethylsilsesquioxane film, the peaks at 1120 cm^{-1} and 1030 cm^{-1} were assigned to the cage and

network structures of siloxane bonds in the FTIR spectrum [6]. In the PAEAPS film, a subtle change in the ratio of two peaks was observed before and after exposure to water vapor at 40 °C and 95% RH for 1 h, indicating that the siloxane network structure attributed to the cage and network structure might be changed. On the other hand, in the FTIR spectrum of the PAEAPS-Cl film, the change in the structure of the PAEAPS-Cl film was not observed before and after exposure to water vapor at 40 °C and 95% RH for 1 h, as shown in **Figure 7** (b).

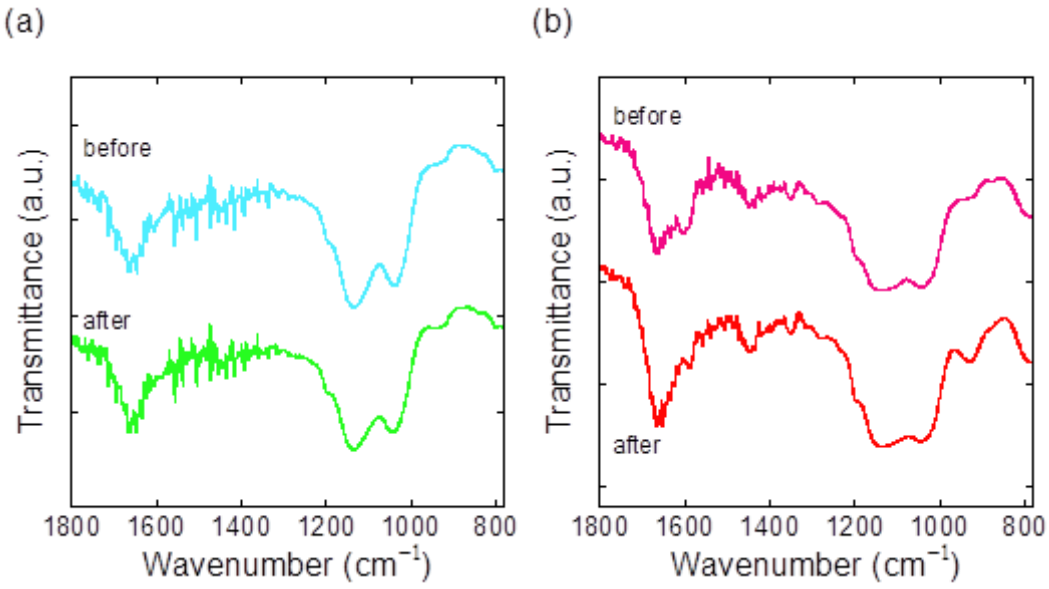

Figure 7. FTIR spectra of (a) PAEAPS film and (b) PAEAPS-Cl film before and after exposure to vapor at 40 °C and 95% for 1 h.

^{29}Si solid-state NMR afforded useful information on the structural changes of the siloxane network in the PAEAPS film. In **Figure 8** (a), the PAEAPS film mainly exhibited a strong peak at −66.9 ppm attributed to the T^3 structure, along with a small T^2 peak at −58.2 ppm. The peak corresponding to the T^3 structure decreased after exposure to water vapor at 40 °C and 95% RH for 1 h, and the peak intensities of the T^3 and T^2 structures were quite similar, indicating that the structure

changed because of hydrolysis and the cleavage of the siloxane network. As described in Chapter 2, PAEAPS was prepared by the autocatalyzed sol–gel reaction using the reflux method. In this reaction, the amino group efficiently catalyzed the hydrolysis of the ethoxy group by water and the polycondensation reaction of silanol in the polymer. Similarly, in the PAEAPS film, the amino group acted as a base catalyst to facilitate hydrolysis. On the other hand, in the PAEAPS-Cl film, the T^3 structure at −67.9 ppm was mainly observed even after exposure to water vapor at 40 °C, along with the small T^2 structure at −59.1 ppm in the ^{29}Si solid-state NMR spectrum (**Figure 8** (b)). It was concluded that the introduction of the amine hydrochloride salt prevented the decomposition of the siloxane network. As mentioned above, the siloxane network in the PAEAPS film was cleaved because of the basicity of amino groups. In the case of the PAEAPS-Cl film, the decomposition of the siloxane network upon hydrolysis was prevented because the amine hydrochloride salt was almost neutral. Therefore, the introduction of the amine hydrochloride salt structure increased the WU and prevented the decomposition of the siloxane network. This means that the stability under high humidity was also improved by the neutralization of the amino group.

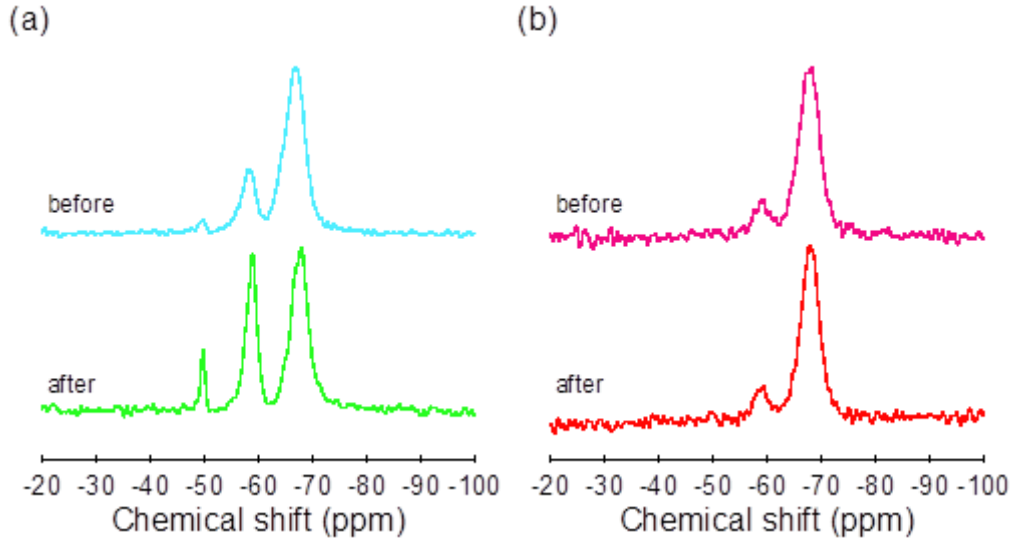

Figure 8. ^{29}Si solid-state NMR spectra of (a) PAEAPS film and (b) PAEAPS-Cl film before and after exposure to vapor at 40 °C and 95% RH for 1 h.

After exposure to water vapor at 40 °C and 95% RH for 1 h, the surface morphology of the PAEAPS film was smooth, and no cracks were observed. However, the morphology of the PAEAPS-Cl film sometimes drastically changed, and cracks and dimples were observed by laser microscopy (data shown later). Interestingly, these morphological changes did not always occur, and the PAEAPS-Cl film sometimes showed a clear appearance after exposure at 40 °C and 95% RH for 1 h. Additionally, the morphological change of the PAEAPS-Cl film prepared using the coating method was more significant than that prepared using the immersion method. When the PAEAPS-Cl film prepared using the coating method was exposed to water vapor, a crack suddenly formed during the absorption of water.

The morphological change of the PAEAPS-Cl film might be due to the hydration around hydrophilic groups. In other words, the hydrated water induced the volume change in the PAEAPS-Cl film, and their volume change was not maintained even though the siloxane network provided excellent mechanical properties. Furthermore, the PAEAPS-Cl film prepared by the coating method showed a more substantial morphological change than the PAEAPS-Cl film prepared using the immersion method. Unfortunately, the WU of the PAEAPS-Cl film prepared using the coating method could not be measured due to the strong morphological changes. In the PAEAPS-Cl film prepared using the coating method, the siloxane network might not be formed efficiently because PAEAPS-Cl contains a large side chain of the amine hydrochloride salt. As a result, the PAEAPS-Cl film prepared using the coating method easily led to a morphological change. Overall, the introduction of an amine salt structure enhanced the WU and surface hardness and prevented the hydrolysis of the siloxane network. Unfortunately, cracks and dimples sometimes formed after exposure to water vapor. This is a significant disadvantage for the practical applications of the film.

P(AEAP-co-Me)S-Cl film was synthesized to enhance the surface hardness of the PAEAPS film by the introduction of methyltrialkoxysilane, and their antifogging property and mechanical properties

were investigated. However, despite expectations, an interesting phenomenon was observed following the copolymerization of methyltriethoxysilane. The P(AEAP-co-Me)S-Cl film exhibited a WU of 17%, which was lower than those of the PAEAPS and PAEAPS-Cl films. When the P(AEAP-co-Me)S-Cl film on the glass substrate was exposed to vapor at 40 °C at a distance of 2 cm, it turned cloudy after 7 s. This is reasonable because the number of amino groups decreased because of the copolymerization of methyltriethoxysilane. However, the WU of the P(AEAP-co-Me)S-Cl film was sufficient to show considerable antifogging performance. Contrary to expectations, the surface hardness and elastic modulus of the P(AEAP-co-Me)S-Cl film were 3.7 and 2.6 GPa, respectively. As discussed in Chapter 2, the amino groups in 3-(2-aminoethylaminopropyl)triethoxysilane acted as the catalyst for the hydrolysis and polycondensation reaction, leading to a highly crosslinked network of siloxane bonds. However, the number of amino groups decreased in the presence of methyltriethoxysilane. The decrease in surface hardness might be due to the reduction in the network structure. On the other hand, the copolymerization of 3-(2-aminoethylaminopropyl)triethoxysilane and methyltriethoxysilane was effective in improving stability under high humidity. In the FTIR spectra of the P(AEAP-co-Me)S-Cl film before and after exposure to water vapor at 40 °C and 95% RH for 1 h, the structural change was not observed, similar to the PAEAPS-Cl film (**Figure 9**). The P(AEAP-co-Me)S-Cl film maintained a smooth surface even after exposure to water vapor at 40 °C and 95% RH for 1 h, and cracks were not observed. **Figure 10** shows the laser microscopy image of the P(AEAP-co-Me)S-Cl film after exposure to water vapor at 40 °C and 95% RH for 1 h, along with that of the treated PAEAPS-Cl film. The surface of the PAEAPS-Cl film was considerably rough, and its root-mean-square (rms) roughness, estimated by laser microscopy, was 773 nm after exposure to water vapor at 40 °C and 95% RH for 1 h. In contrast, the laser microscopy image of the P(AEAP-co-Me)S-Cl film showed a smooth surface even after exposure to water vapor, and an rms roughness was determined to be 71 nm (**Figure 10**). Therefore, in the P(AEAP-co-Me)S-Cl film, the volume change due to the hydration of water

molecules was prevented by the decreased amount of the amine hydrochloride salt.

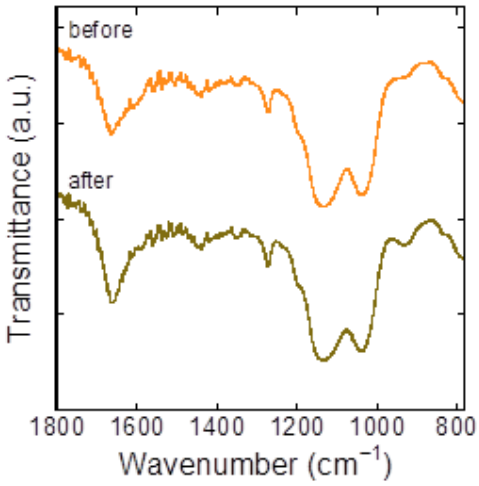

Figure 9. FTIR spectra of the P(AEAP-co-Me)S-Cl film before and after exposure to vapor at 40 °C and 95% RH for 1 h.

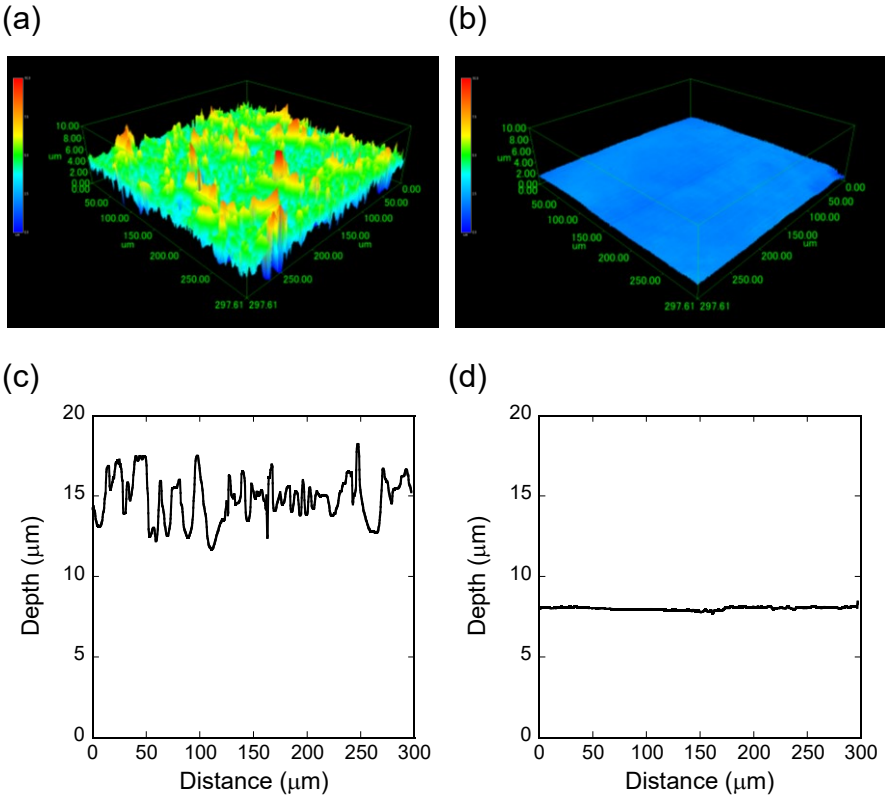

Figure 10. Laser microscopy images of (a) PAEAPS-Cl film and (b) P(AEAP-co-Me)S-Cl film after exposure to vapor at 40 °C and 95% RH for 1 h. Surface profiles of (c) PAEAPS-Cl film and (d) P(AEAP-co-Me)S-Cl film after exposure to vapor at 40 °C and 95% RH for 1 h.

The transparency and color of antifogging materials are also important factors from the viewpoint of practical applications. **Figure 11** shows the UV-vis spectra of the PAEAPS, PAEAPS-Cl, and P(AEAP-co-Me)S-Cl films. The transmittance of the PAEAPS-Cl film at 400 nm was less than 85%, which showed light-yellow. This may be due to oxidation of ammonium salts, similar to PAEAPS.

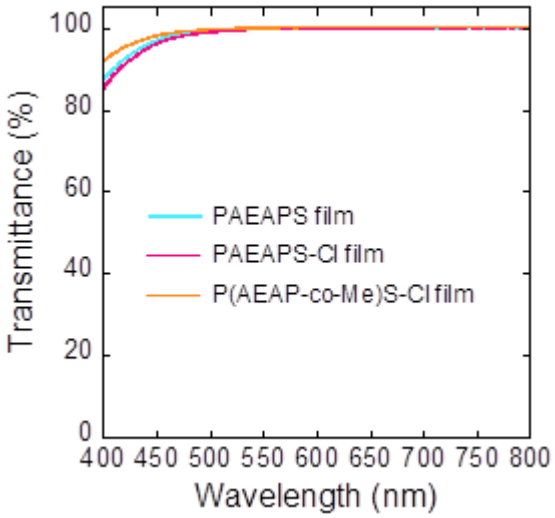

Figure 11. UV-vis spectra of PAEAPS, PAEAPS-Cl, and P(AEAP-co-Me)S-Cl films.

4. Conclusions

PAEAPS-Cl films containing amine hydrochloride salt were prepared by two methods: the immersion method and the coating method. In the immersion method, the PAEAPS film on the substrate was immersed in 0.5 mol/L HCl methanolic solution. FTIR, ^{13}C solid-state NMR, and SEM-EDX results indicated that the amino group was converted to the amine hydrochloride salt upon immersion in 0.5 mol/L HCl methanolic solution for 1 h. The PAEAPS-Cl film showed no cracks or pinholes, and chloride atoms were homogeneously distributed on the surface of the PAEAPS-Cl film. In the coating method, PAEAPS-Cl was synthesized by the treatment of PAEAPS with HCl for 1 h at room temperature, and PAEAPS-Cl was obtained as a white solid with a yield of 99%. The obtained

PAEAPS-Cl did not dissolve in organic solvents but in water. The solubility of PAEAPS-Cl drastically changed following the introduction of the amine hydrochloride salt. The PAEAPS-Cl film was also prepared by the coating method. The WU and surface hardness of the PAEAPS-Cl film prepared using the immersion method were measured to investigate the influence of the amine hydrochloride salt on the antifogging property and mechanical properties. The PAEAPS film showed a WU and scratch resistance of 22% and 3.2, respectively. The introduction of the amine hydrochloride salt into the PAEAPS film increased its antifogging property and surface hardness, and the WU and scratch resistance of the PAEAPS-Cl film became 29% and 4.3. When the PAEAPS film was exposed to water vapor at 40 °C and 95% RH for 1 h, the structural change of the siloxane network was observed because of decomposition via the hydrolysis caused by the basicity of the amino group in the FTIR and ^{29}Si solid-state NMR results. On the other hand, as the amine hydrochloride salt structure was almost neutral, it prevented the cleavage of the siloxane network. However, the amine hydrochloride salt sometimes induced the morphological change of the PAEAPS-Cl film owing to strong hydration, and cracks and dimples were observed after exposure to water vapor at 40 °C and 95% for 1 h, whereas the P(AEAP-co-Me)S-Cl film exhibited a WU of 17%, which was lower than those of the PAEAPS and PAEAPS-Cl films, but the cracks and dimples of the P(AEAP-co-Me)S-Cl films were not observed even after exposure to water vapor at 40 °C and 95% RH for 1 h. The introduction of the amine hydrochloride salt structure did not decrease transparency. These findings are promising for further design and development of antifogging materials with high-performance and long-term stability.

5. References

[1] C. Tao, S. Bai, X.H. Li, C. Li, L.X. Ren, Y.H. Zhao, X.Y. Yuan, Formation of zwitterionic coatings with an aqueous lubricating layer for antifogging/anti-icing applications, Progress in Organic Coatings 115 (2018) 56-64.

[2] S. Bai, X.H. Li, R.C. Zhang, C. Li, K.Y. Zhu, P.C. Sun, Y.H. Zhao, L.X. Ren, X.Y. Yuan, Enhancing antifogging/frost-resisting performances of amphiphilic coatings via cationic, zwitterionic or anionic polyelectrolytes, Chemical Engineering Journal 357 (2019) 667-677.

[3] Y. Kaneko, N. Iyi, T. Matsumoto, K. Kitamura, Synthesis of rodlike polysiloxane with hexagonal phase by sol-gel reaction of organotrialkoxysilane monomer containing two amino groups, Polymer 46(6) (2005) 1828-1833.

[4] J.R. Varcoe, P. Atanassov, D.R. Dekel, A.M. Herring, M.A. Hickner, P.A. Kohl, A.R. Kucernak, W.E. Mustain, K. Nijmeijer, K. Scott, T.W. Xu, L. Zhuang, Anion-exchange membranes in electrochemical energy systems, Energy & Environmental Science 7(10) (2014) 3135-3191.

[5] T.T. Duy, S. Sawada, S. Hasegawa, Y. Katsumura, Y. Maekawa, Poly(ethylene-co-tetrafluoroethylene) (ETFE)-based graft-type polymer electrolyte membranes with different ion exchange capacities: Relative humidity dependence for fuel cell applications, Journal of Membrane Science 447 (2013) 19-25.

[6] L.H. Lee, W.C. Chen, W.C. Liu, Structural control of oligomeric methyl silsesquioxane precursors and their thin-film properties, Journal of Polymer Science Part a-Polymer Chemistry 40(10) (2002) 1560-1571.

Chapter 4: Highly Transparent Antifogging Materials Based on Polysilsesquioxane Containing a Hydroxy Group

1. Introduction

As described in Chapter 2 and 3, the PAEAPS film and PAEAPS-Cl film on a glass substrate showed high transparency under humidified conditions and thus good antifogging properties. The amino and amine hydrochloride groups in the side chain effectively work to absorb water, and the siloxane network enhances the scratch resistance. However, the transmittance of the PAEAPS film and PAEAPS-Cl film decreases in the short-wavelength region and the film has a light yellow color because of denaturation, such as the oxidation of the amino group and amine hydrochloride group in the side chain. Therefore, a new design for PSQ-based antifogging materials is necessary; in particular, the hydrophilic group must be changed to another hydrophilic group. For example, hydrophilic polymers containing a hydroxy group have been widely studied as antifogging materials, although these organic polymers exhibit low scratch resistance, and the hydroxy group is typically not prone to discoloration. However, the preparation of PSQ film containing a hydroxy group is difficult because of the side reaction between silanol and hydroxy groups.

In Chapter 4, to develop a scratch-resistant, transparent, and colorless antifogging material, the author focused on 3-glycidyloxypropyltrimethoxysilane because the epoxy ring is hydrolyzed to form a hydrophilic diol group. The preparation of a PSQ film containing a high concentration of hydroxy groups while suppressing side reactions is described. The antifogging properties, mechanical properties, and transparency of the diol-containing film are discussed.

2. Experimental

2.1 Materials

Herein, 3-glycidyloxypropyltrimethoxysilane was purchased from Tokyo Chemical Industry Co. Ltd. (Tokyo, Japan) and used as received without purification. Methanol (super dehydrated), tetrahydrofuran (THF; super dehydrated), 2-propanol, 6 mol/L hydrochloric acid (HCl), 1 mol/L sulfuric acid (H_2SO_4), and potassium hydroxide (KOH) were purchased from FUJIFILM Wako Pure Chemical Co. Ltd. (Osaka, Japan) and used as received. The water used in the experiments was purified using a Millipore Milli-Q UV system and showed a resistance and total organic carbon content of 18.2 MΩ·cm and <10 ppb, respectively. Glass substrates were cleaned in an alkaline solution. The detailed procedure was described in Chapter 3. A 12.5-μm-thick Kapton film was purchased from AZ ONE Corporation (Osaka, Japan).

2.2 Synthesis of poly(glycidyloxypropyl)silsesquioxane (PGPS) by hydrolysis and polycondensation

PSQ with different molecular weights were synthesized according to the procedure described in previous studies [1-3]. In a typical synthesis using a water/monomer molar ratio of 1.2, 3-glycidyloxypropyltrimethoxysilane (4.727 g and 20.00 mmol) and methanol (6.408 g and 200.0 mmol) were added to a 100-mL four-necked flask equipped with a mechanical stirrer and a nitrogen inlet and outlet. The flask was placed in an ice-water bath, and the solution was stirred for 10 min with a rotation speed of 150 rpm. A solution of 0.3646 g of 6 mol/L HCl and 0.1403 g of water was slowly added by pipette under a nitrogen stream of 360 mL/min, and the reaction mixture was stirred at ice-water bath temperature for 10 min and at room temperature for 10 min. Then, the reaction mixture was further stirred at 80°C for 3 h with a rotation speed of 150 rpm under a nitrogen stream of 360 mL/min. PGPS was obtained as a viscous liquid and dissolved in THF to a concentration of 50 wt%, and was stored in a refrigerator until use.

The reaction ratios were estimated by the weight of the initial monomer and obtained polymer and the molecular weight (M_w) of the monomer and polymer unit ($RSiO_{1.5}$) by assuming that the hydrolysis and polycondensation proceeded quantitatively according to Equation (1).

$$Reaction\ ratio\ (\%) = \frac{weight\ of\ monomer\ - weight\ of\ obtained\ polymer}{(M_W\ of\ monomer\ - M_W\ of\ RSiO_{1.5}) \times mol\ number\ of\ monomer} \times 100 \quad (1)$$

2.3 Preparation of poly(3-(2,3-dihydroxypropoxypropyl)silsesquioxane) (PSQ-OH) film via route A

In a 50-mL flask, 0.20 g of 50 wt% PGPS solution in THF was diluted with 0.80 g of THF and stirred at ice-water bath temperature for 10 min. To hydrolyze the epoxy group, 5 g of 1 mol/L HCl (aq) was added dropwise at ice-water bath temperature, and the resulting solution was stirred at room temperature for 3 h. Finally, the reaction mixture was evaporated under reduced pressure and dried under vacuum. PSQ-OH was obtained as a viscous liquid. For the film preparation, a 50 wt% PSQ-OH solution in THF was coated on a glass substrate using an applicator with a clearance gap of 50 μm; then, the coated substrate was heated at 80 °C for 1 h and at 150 °C for 2 h.

2.4 Preparation of PSQ-OH film via route B

A 50 wt% PGPS solution in THF was coated on a glass substrate using an applicator with a clearance gap of 50 μm, and the coated glass substrate was heated at 80 °C for 1 h and at 150 °C for 0.5–2 h. Then, the obtained substrate was immersed in 0.5 mol/L H_2SO_4 for 1–15 h to hydrolyze the epoxy group. After being washed several times with water, the polymer film on the glass substrate was dried at 60 °C for 1 h.

2.5 Measurements

^{1}H and ^{29}Si nuclear magnetic resonance (NMR) spectra were recorded on Varian 400-MHz and 500-MHz spectrometers, respectively. Deuterium chloroform ($CDCl_3$) was used as the solvent, and tetramethylsilane was used as an internal standard for chemical shift reference in the ^{1}H and ^{29}Si NMR spectra. Solid-state ^{13}C and ^{29}Si NMR experiments were performed using a Varian 600-MHz spectrometer by magic-angle spinning. Hexamethylbenzene and 3-(trimethylsilyl) propionic acid were used as external standards for chemical shift reference in the ^{13}C and ^{29}Si NMR spectra, respectively. Gel permeation chromatography was performed on a Shimadzu LC-20AD equipped with a CTO-20A column oven and a RID-10A detector using triply connected TSKgel G6000H/G4000H/G2000H columns that was calibrated using polystyrene standards. THF was used as the eluent at a flow rate of 1 mL/min (40 °C). For Fourier transform infrared (FTIR) spectroscopy, the polymer was coated onto a silicon wafer and the FTIR spectrum of the polymer film on the silicon wafer was recorded in the transmittance mode on a Shimadzu IRAffinity-1 spectrometer. The water uptake (WU) of the film coated on the Kapton film was measured using a temperature- and humidity-controlled chamber. The detailed procedure was described in Chapter 3.

Indentation and scratch tests were performed to evaluate the elastic modulus, scratch resistance, elastic part of indentation work (η), using a Nano Indenter G200. The detailed procedure is available in Chapter 2.

3. Results and discussion

3.1 Synthesis of PGPS by hydrolysis and polycondensation

PGPS was synthesized by hydrolysis and polycondensation by the nitrogen flow method, as illustrated in **Scheme 1**. The nitrogen flow method is useful for controlling the molecular weight of PSQ by changing the water/monomer molar ratio, as reported in previous studies [1-5]. Therefore,

PGPS samples were synthesized by changing the water/monomer molar ratio to obtain a polymer with different molecular weights, as presented in **Table 1**. With a water/monomer molar ratio of 1.2, the weight-average molecular weight (M_w) and polydispersity index (M_w/M_n) of PGPS were 5200 and 2.0, respectively (Entry 1 in **Table 1**). The obtained PGPS was easily soluble in organic solvents, such as acetone, THF, and chloroform. The ^{1}H NMR spectrum of PGPS with M_w of 5200 and M_w/M_n of 2.0 is presented in **Figure 1**. Broad signals attributed to the propylene CH_2-CH_2-Si group were observed at 0.67 and 1.69 ppm, and signals attributed to the epoxy ring appeared at 2.60, 2.79, and 3.14 ppm. Two methylene protons adjacent to an oxygen atom and methyl proton of the residual methoxy group overlapped at 3.37–3.73 ppm. Based on the integration of the methylene protons and methoxy protons, the residual methoxy group against the methoxy group in the initial monomer was estimated to be 41%. The reaction ratio estimated based on the change in the weight of the film using Equation (1) was 63%, similar to the consumption of the methoxy group (59%) estimated using ^{1}H NMR.

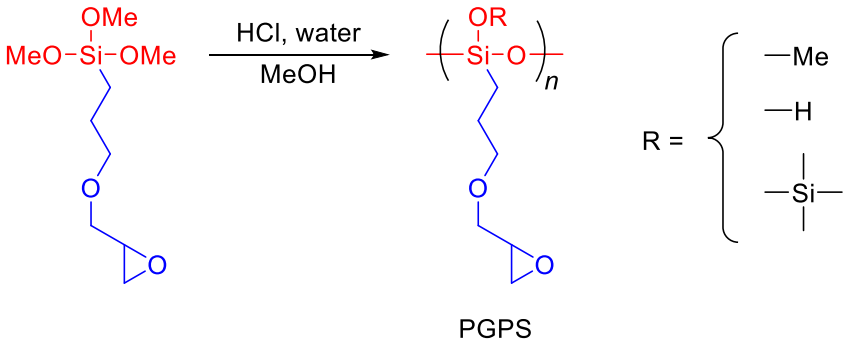

Scheme 1. Preparation of PGPS by hydrolysis and polycondensation.

When the water/monomer molar ratio was increased from 1.2 to 1.7, the molecular weight increased from M_w = 5200 to 11000 (Entries 1–6 in **Table 1**). The reaction ratio also increased from 63% to 78% with increasing the water/monomer molar ratio (**Table 1**). Finally, the formation of gel was observed with the water/monomer molar ratio of 1.8 (Entry 7 in **Table 1**). In hydrolysis and polycondensation by the nitrogen flow method, a large amount of water facilitates efficient hydrolysis and moderate polycondensation to form high-molecular-weight PGPS. Indeed, M_w linearly increased with increasing water/monomer molar ratio (**Figure 2**), indicating that the molecular weight of PGPS could be controlled by varying the amount of water. This trend is consistent with the hydrolysis and polycondensation of bis(triethoxysilyl)ethane and triethoxymethylsilane by the nitrogen flow method [1, 3, 5].

Table 1. Results on the synthesis of PGPS

Entry	Water/monomer molar ratio	M_w	M_w/M_n	Reaction ratio (%)
1	1.2	5200	2.0	63
2	1.3	7300	2.2	70
3	1.4	11000	2.7	71
4	1.5	13000	3.2	73
5	1.6	22000	4.5	75
6	1.7	110000	19	78
7	1.8	Gel		

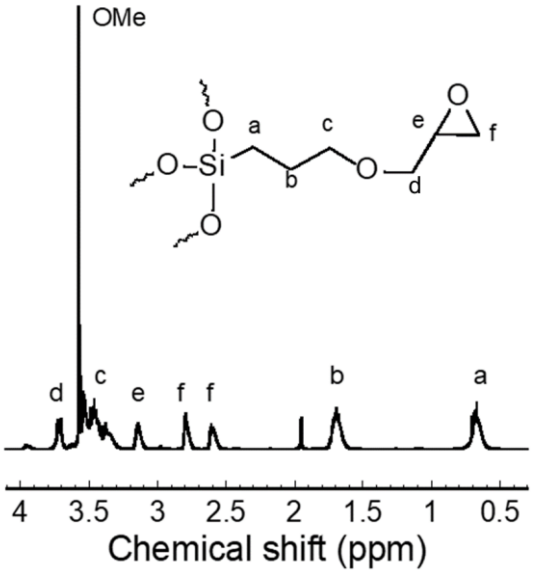

Figure 1. ^{1}H NMR spectrum of PGPS (Entry 1, Table 1) in $CDCl_3$.

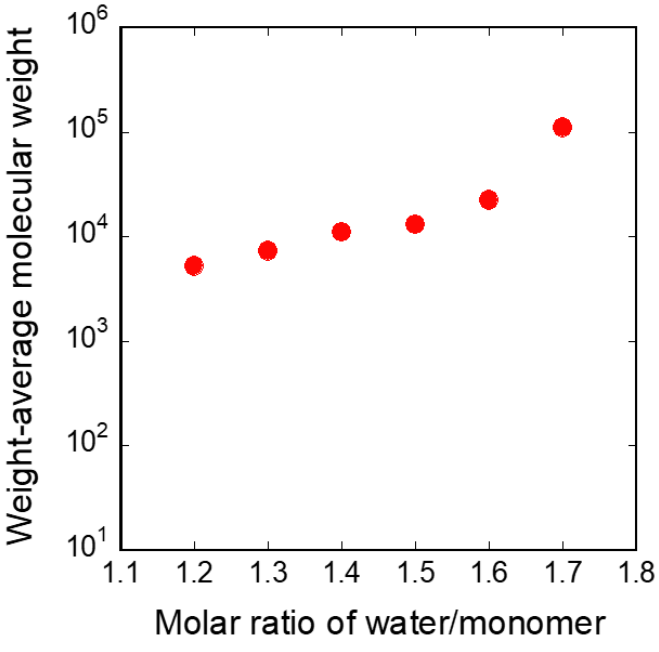

Figure 2. Influence of the water/monomer molar ratio on M_w of PGPS.

3.2 Preparation of PSQ-OH film via route A

Two routes were designed for the preparation of the PSQ-OH films (**Figure 3**). First, PGPS was hydrolyzed under acidic or basic conditions to convert the epoxy groups to diol groups. When the hydrolysis of the epoxy group was performed in a mixture containing THF and water with nitric acid or HCl, the PGPS solution remained transparent for 3 h. The polymer was isolated via extraction with brine to remove the acid; however, a gel was formed during extraction. In contrast, the hydrolysis of the epoxy group in a mixture containing THF and ammonia solution produced gel during the reaction. Therefore, HCl was used for the hydrolysis of the epoxy group by considering the removal of acid. After the hydrolysis of the epoxy group in PGPS for 3 h, HCl and solvents were removed by a vacuum pump at room temperature without extraction, and the obtained viscous liquid was dissolved in THF. The polymer/THF solution was coated onto a silicon wafer for FTIR measurements and heated at 80 °C for 1 h and 150 °C for 2 h to obtain the PSQ-OH film (route A).

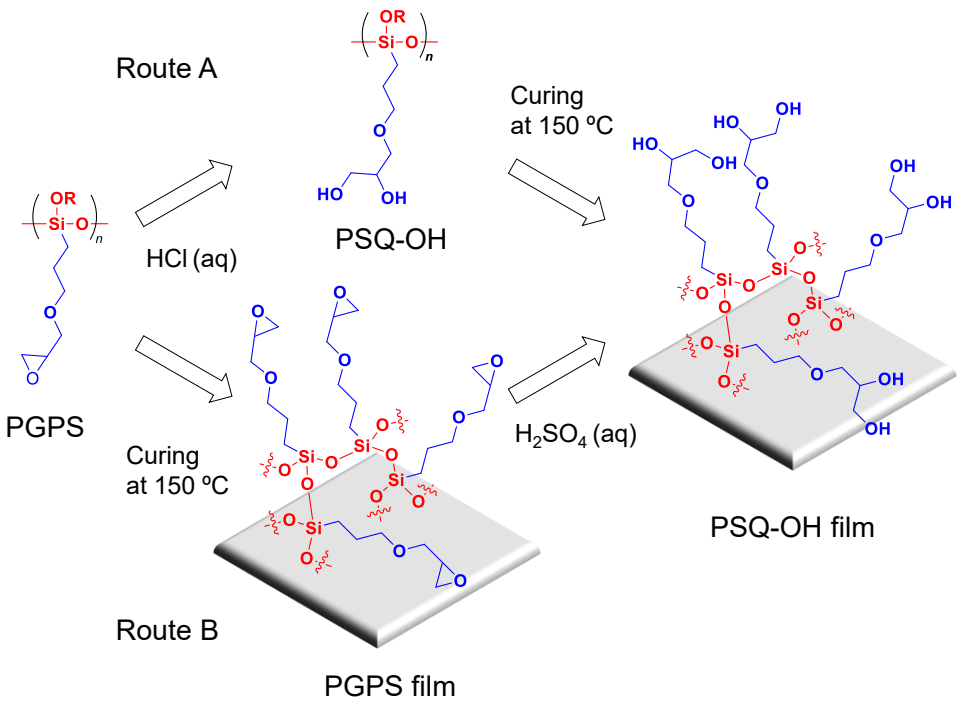

Figure 3. Preparation of the PSQ-OH film via routes A and B.

To investigate the chemical structure, the PGPS film was also prepared on a silicon wafer by heating the PGPS-coated wafer at 80 °C for 1 h and at 150 °C for 0.5 h (PGPS with M_w = 5200). For the PGPS film, distinct absorption peaks at 1100 and 3450 cm^{-1}, corresponding to the Si–O–Si bond and silanol group, respectively, were observed (**Figure 4**). A weak peak at ~900 cm^{-1}, corresponding to the epoxy ring, overlapped with the absorption peak of the silanol group. For the PSQ-OH film prepared via route A, the absorption peak at ~3450 cm^{-1} increased by the formation of the diol group by hydrolysis. However, it was difficult to quantify the formation of the diol group by FTIR measurement due to the overlapping of the silanol and hydroxyl groups.

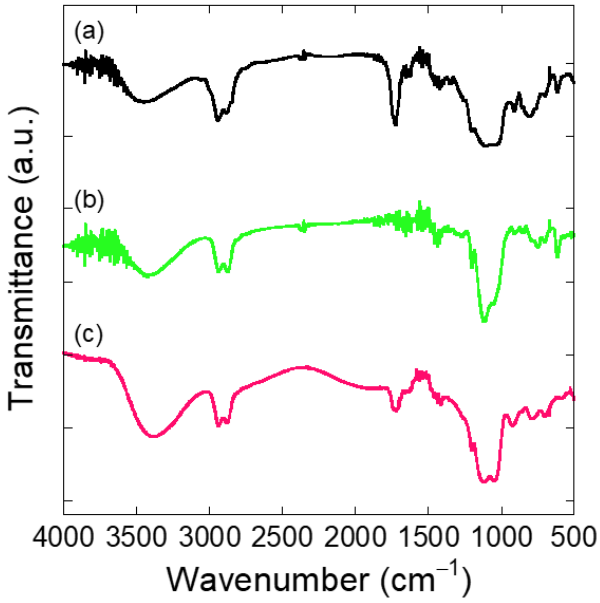

Figure 4. FTIR spectra of (a) PGPS film, (b) PSQ-OH film prepared via route A, and (c) PSQ-OH film prepared via route B (immersion for 15 h).

To obtain further information, the hydrolyzed PGPS/THF solution was poured into a poly(tetrafluoroethylene-co-perfluoroalkyl vinyl ether) (PFA) vial, and a free-standing gel film of PSQ-OH was prepared by heating at 80 °C for 1 h and 150 °C for 3 h for solid-state ^{13}C NMR

spectroscopic measurements. Similarly, a free-standing gel film of PGPS was prepared by heating at 80 °C for 1 h and 150 °C for 3 h. The solid-state ^{13}C NMR spectra before and after the hydrolysis of PGPS are presented in **Figure 5**. In the spectrum of the PGPS film before hydrolysis, signals attributed to the propylene group were observed at 7.5, 22.5, and 72.5 ppm. The peak at 70.9 ppm was attributed to methylene carbon adjacent to an oxygen atom. Furthermore, peaks attributed to the epoxy ring were observed at 42.9 and 49.9 ppm. In the PSQ-OH film prepared via route A, the peaks attributed to the epoxy group at 42.9 and 49.9 ppm completely disappeared, and new peaks corresponding to the carbon atom in the diol were observed at 62.8 and 69.3 ppm. It was observed that an unknown peak appeared at 45.6 ppm in the solid-state ^{13}C NMR of PSQ-OH film prepared via route A. This may be due to a side reaction between the epoxy and silanol groups. For example, PSQ containing a hydroxy group was prepared from hydroxymethyl(triethoxy)silane by hydrolysis and polycondensation [6]. In this reaction, the condensation reaction of C–OH and Si–OH bonds occurred to form Si–O–C bonds at high temperature. In the PSQ-OH film prepared via route A, a similar reaction may have occurred by heating the hydrolyzed film at 150 °C. If this peak was attributed to the Si–O–C bond formed by the side reaction of the epoxy and silanol groups, the Si–O–C bond should have been easily hydrolyzed. However, the unknown peak did not disappear even after further hydrolysis of the PSQ-OH film. However, FTIR and solid-state ^{13}C NMR spectroscopy indicated that the epoxy group was fully converted to a diol group by hydrolysis, which was sufficient to investigate the antifogging properties of the film.

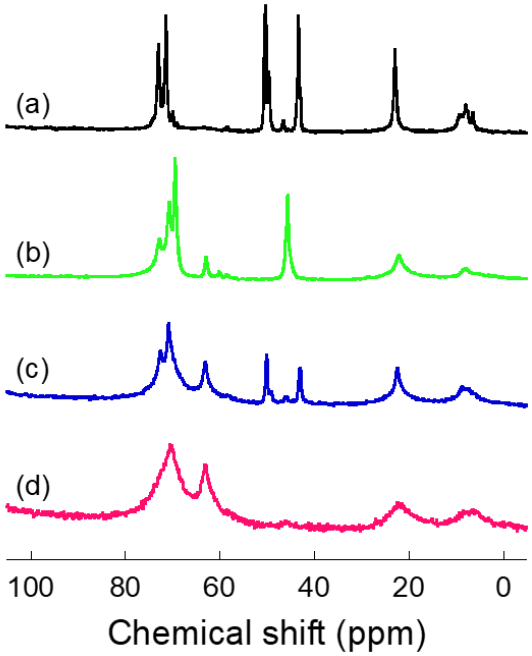

Figure 5. Solid-state ^{13}C NMR spectra of (a) PGPS film, (b) PSQ-OH film prepared via route A, (c) PSQ-OH film prepared via route B (after immersion for 7 h), and (d) PSQ-OH film prepared via route B (after immersion for 15 h).

Finally, to prepare the PSQ-OH film on a glass substrate via route A, a 50 wt% PSQ-OH solution in THF was coated onto an alkali-washed glass substrate and heated at 80 °C for 1 h and 150 °C for 2 h. The obtained PSQ-OH film was uniform and transparent.

3.3 Preparation of PSQ-OH film via route B

Next, a PSQ-OH film was prepared via route B (**Figure 3**). To prepare the PGPS film, a solution containing PGPS with M_w = 5200 in THF was coated onto a glass substrate and heated at 80 °C for 1 h and 150 °C for 0.5–2 h. The obtained PGPS film was completely stiff and transparent without cracks. When PGPS films were prepared using PGPS with M_w = 13000 and 22000 (water/monomer molar ratio = 1.5 and 1.6), cracks were partially observed after heating at 150 °C for 3 h. This may be

attributed to the high cross-linking ratio of the siloxane bond (**Figure 6**). The main signal at −66 ppm attributed to the T^3 structure was observed in the solid-state ^{29}Si NMR of the PGPS films, where T^n denotes the siloxane structural unit. The calculated cross-linking ratios of the PGPS films based on T^3/T^{total} ranged from 82% to 88%, which increased in the following order: water/monomer molar ratio = 1.2, 1.5, and 1.6. PGPS with a high molecular weight formed a cross-linked network, and the obtained film was too stiff, resulting in crack formation. Therefore, PGPS with an M_w of 5200 (water/monomer molar ratio = 1.2) was used for PSQ-OH film preparation.

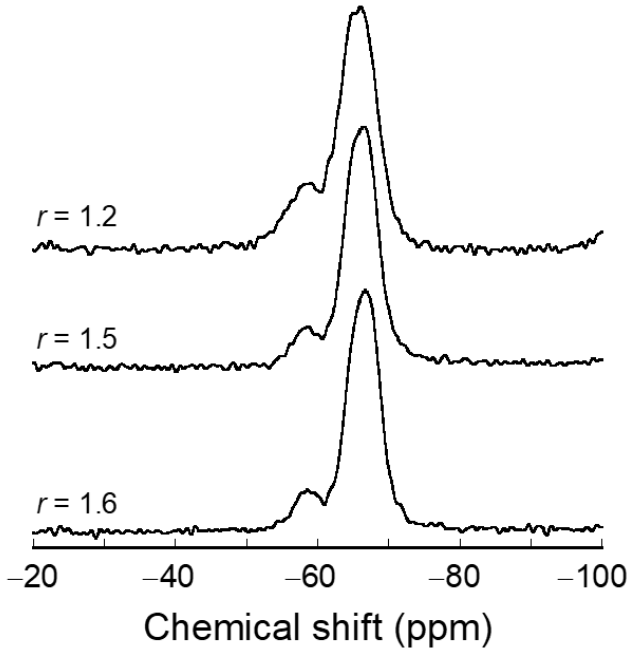

Figure 6. ^{29}Si solid-state nuclear magnetic resonance (NMR) spectra of poly(glycidyloxypropyl)silsesquioxane (PGPS) films prepared by heating the polymer samples at 150 °C for 3 h. PGPS prepared by water/monomer molar ratio (r) = 1.2, 1.5, and 1.6 was used for film preparation.

To investigate the reaction progress, the free-standing gel film of PGPS and the PGPS film on the silicon wafer were immersed in a 0.5 mol/L H_2SO_4 aqueous solution for 1–15 h for the ring-opening reaction of the epoxy group. As illustrated in **Figure 4**, a distinct broad peak corresponding to the hydroxy group was observed at ~3400 cm^{-1} in the IR spectrum, after immersion in the 0.5 mol/L H_2SO_4 solution, indicating the formation of the diol group by hydrolysis. However, the conversion of the epoxy group to the diol group could not be estimated using FTIR measurements because the peak of the hydroxy group overlapped with the absorption peak of the silanol group. However, solid-state ^{13}C NMR spectroscopy successfully estimated the yield of the diol group formation. **Figure 5** presents the solid-state ^{13}C NMR spectra of the PGPS and PSQ-OH films after immersion in 0.5 mol/L H_2SO_4 (aq) for 7 and 15 h. The peaks at 42.9 and 49.9 ppm, corresponding to the epoxy ring carbons, decreased after immersion in 0.5 mol/L H_2SO_4 (aq) for 7 h. In addition to the reduction of the epoxy ring signals, a new peak ascribed to one of the carbon atoms in the diol unit was observed at 63 ppm. Another carbon atom in the diol overlapped with the methylene carbon adjacent to the ether group. The peaks at 42.9 and 49.9 ppm completely disappeared after immersion in 0.5 mol/L H_2SO_4 (aq) for 15 h; in other words, the hydrolysis of the epoxy group quantitatively proceeded in this process. Unlike the PSQ-OH film prepared via route A, no unidentified peak was observed in the solid-state ^{13}C NMR spectrum of the free-standing gel film of PSQ-OH. Overall, a PSQ-OH film containing a diol group could be successfully prepared via route B (**Figure 3**). The PSQ-OH film was uniform and transparent, similar to the PSQ-OH film prepared via route A. Furthermore, the PSQ-OH film did not peel off after tape testing and exhibited good adhesion to the glass substrate owing to the formation of Si–O–Si bonds, similar to the PAEAPS film.

3.4 Antifogging and mechanical properties of PSQ-OH film via routes A and B

To compare the antifogging and mechanical properties of the PSQ-OH films prepared via routes A and B, the WU and scratch resistance were investigated; the results are presented in **Table 2**. The WU of the PSQ-OH film prepared via route A was only 5%, whereas that of the PSQ-OH film prepared via route B was 5%–19%. As mentioned in the section Preparation of PSQ-OH film via route A, a side reaction occurred during preparation, which may be responsible for the decrease in WU because the amount of hydrophilic materials in the film decreased by the reaction of C–OH and Si–OH that formed a Si–O–C bond. In the PSQ-OH film prepared via route B, the WU increased from 5% to 19% as the immersion time was increased from 1 to 15 h. As shown in **Figure 5**, the epoxy ring was completely hydrolyzed after immersion in 0.5 mol/L H_2SO_4 (aq) for 15 h. Therefore, the WU of the PSQ-OH film depended on the number of diol groups. Furthermore, the WU of the PSQ-OH film decreased from 19% to 14% as the curing time increased from 0.5 to 2 h at 150 °C before immersion in 0.5 mol/L H_2SO_4 (aq), likely because the enlargement of the PSQ-OH film by swelling with water was suppressed by the enhanced cross-linking provided by the siloxane bond.

Table 2. Antifogging and mechanical properties of PSQ-OH film prepared via route A and route B

Film	Route	Curing time (h)	Immersion time (h)	WU[c] (%)	Scratch resistance	Elastic modulus (GPa)	η^d (%)
PSQ-OH film	A[a]	2		5	1.6	0.2	94
PSQ-OH film	B[b]	0.5	1	5	3.6	0.9	70
PSQ-OH film	B[b]	0.5	9	12	2.7	1.5	72
PSQ-OH film	B[b]	0.5	15	19	2.7	1.1	76
PSQ-OH film	B[b]	2	15	14	3.5	1.9	61
PAEAPS film		2		22	3.2	3.7	61
PVA film				27	0.5	9.0	20

[a]PGPS was hydrolyzed in an aqueous HCl/THF solution to form a diol group; the hydrolyzed polymer was coated on a glass substrate and heated at 150 °C for 2 h. [b]PGPS was coated on a glass substrate and immersed in a 0.5 mol/L H_2SO_4 solution for the ring-opening reaction of the epoxy group. [c]Water uptake. [d]Elastic part of indentation work.

As described in Chapter 2, the PAEAPS film with an amino group in the side chain exhibited high WU. The WU of the PSQ-OH film was lower than that of the PAEAPS film (**Table 2**) owing to the hydrophilicity of the side chain in the polymer. In other words, the amino groups in the side chain of PAEAPS effectively absorbed more water than the hydroxy group in the side chain of PSQ-OH. Similarly, the WU of the PSQ-OH film was lower than that of the PVA film. However, the PSQ-OH film exhibited a WU of 5%–19%, which is sufficiently high for antifogging properties. Indeed, when the PSQ-OH film with a WU of 19% and an average thickness of 5.3 μm coated on a glass substrate was exposed to water vapor at 40 °C at a distance of 2 cm, it retained transparency for 13–16 s. In the PSQ-OH film coated on the glass substrate, fogging was prevented by the absorption of water (**Figure 7**).

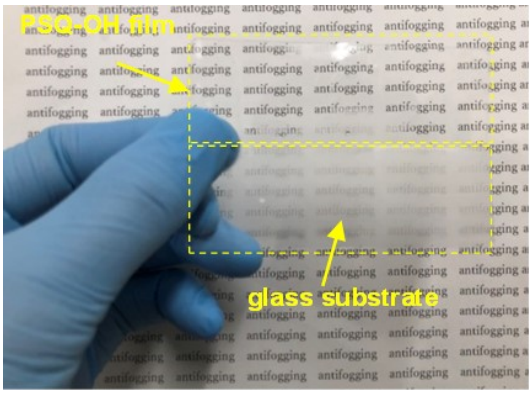

Figure 7. Photographs of the PSQ-OH film on a glass substrate (top) and a glass substrate without the PSQ-OH film (bottom) exposed to water vapor.

The mechanical properties of the PSQ-OH film were evaluated using a nanoindenter, and the data were compared with those of the PAEAPS and PVA films. The PSQ-OH film prepared via route B exhibited a high scratch resistance of 2.7–3.6, similar to that of the PAEAPS film and 5–7 times higher than that of the PVA film. However, the elastic moduli of the PSQ-OH films were 0.9–1.9 GPa, 5–10

times lower than those of the PVA film. The high scratch resistance was attributed to the highly cross-linked siloxane network. Moreover, the flexible siloxane bond helped the film to recover from deformation, as described in Chapter 2. When the PSQ-OH film surface was scratched in the range of 0–1200 μm using a ramp loading of 0–20 mN, the post-scratch test revealed an almost completely recovered surface from the ramped-scratch test (**Figure 8**). A similar phenomenon was observed in the scratch profiles of PAEAPS film. Although the PVA film exhibited a high elastic modulus of 9 GPa, its scratch resistance was considerably low due to the lack of a restorative effect.

Furthermore, the PSQ-OH film exhibited a high elastic part of indentation work (η) of 67%–94%, similar to that of the PAEAPS film. These results indicate that the siloxane network can recover from deformation in PSQ-OH films as well as in PAEAPS films.

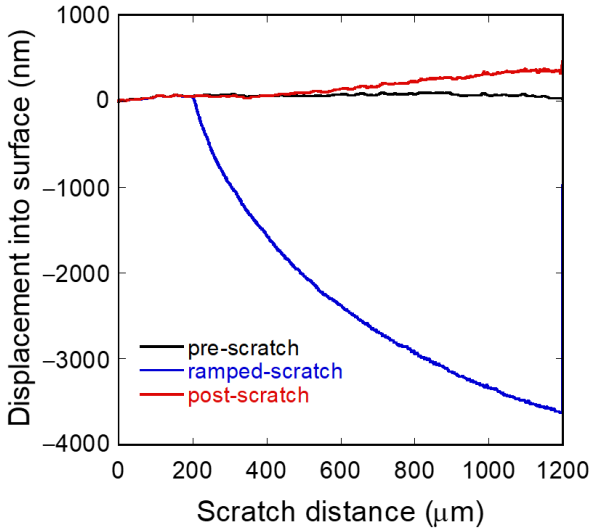

Figure 8. Scratch profiles of PSQ-OH film prepared via route B (immersion for 15 h).

3.5 Surface morphology and transparency of PSQ-OH film prepared via route B

The surface morphology of the PSQ-OH film prepared via route B was investigated using laser microscopy. The PSQ-OH film prepared by immersion in 0.5 mol/L H_2SO_4 (aq) for 15 h was uniform, and pinholes and cracks were not observed (**Figure 9**). The root-mean-square (rms) roughness was determined to be 54 nm using laser microscopy. The PSQ-OH film exhibited a smooth surface, similar to that of the PAEAPS film (rms = 68 nm).

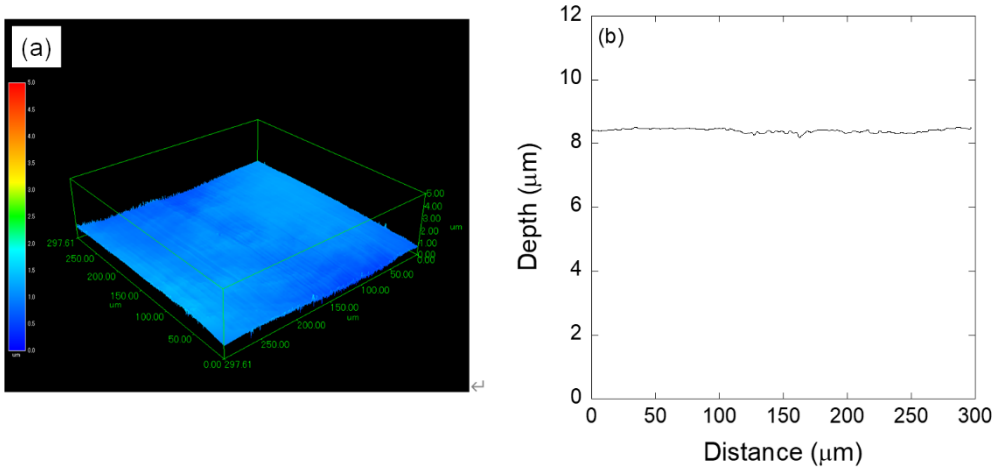

Figure 9. Poly(3-(2,3-dihydroxypropoxypropyl)silsesquioxane) (PSQ-OH) film prepared by route B. (a) Laser microscopy image, and (b) surface profile of PSQ-OH film prepared by route B.

The transparency of antifogging materials is also important for practical applications. **Figure 10** presents the UV–visible transmission spectra of a glass substrate, PAEAPS film, and PSQ-OH film prepared via routes A and B. The glass substrate exhibited a high transmittance of 100% in the wavelength range of 400–800 nm. The PAEAPS film prepared by heating at 180 °C for 1 h exhibited a high transmittance of >88% in the wavelength range of 400–800 nm (**Figure 10**). However, the transmittance of the PAEAPS film prepared by heating at 180 °C for 2 h decreased sharply to 76% at 400 nm. This indicates that the amino group in the side chain was unstable at high temperatures owing to denaturation, such as oxidation. Alternatively, the PSQ-OH films prepared via routes A and B were

highly transparent and colorless. In particular, the PSQ-OH film prepared via route B exhibited a high transmittance of >98% in the wavelength range of 400–800 nm. The color of the PSQ-OH film did not change even after several months. Unlike the amino group, the hydroxy group in the side chain of the PSQ-OH film was stable at high temperatures because oxidation does not occur in ambient atmosphere.

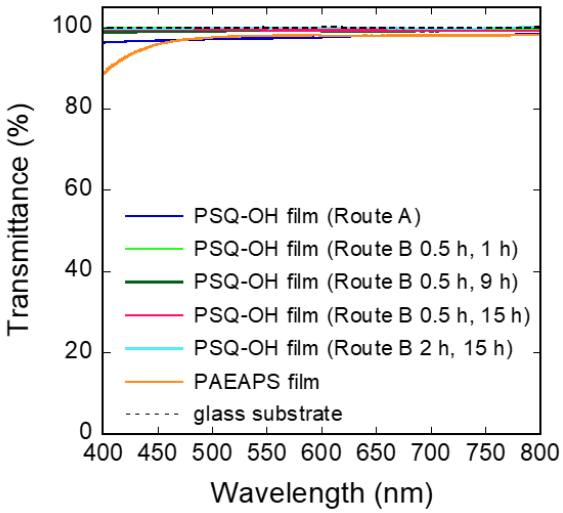

Figure 10. UV–visible spectra of a glass substrate, PSQ-OH film prepared via route A, PSQ-OH film prepared via route B (where the PGPS film was prepared by heating at 150 °C for 0.5 or 2 h, and the obtained film was immersed in 0.5 mol/L sulfuric acid for 1, 9, and 15 h), and PAEAPS film.

4. Conclusions

PGPS was successfully synthesized by hydrolysis and polycondensation using the nitrogen flow method. The molecular weight M_w of PGPS was controlled at 5200–110000 by changing the water/monomer molar ratio from 1.2 to 1.7. PSQ-OH films containing a hydroxy group were prepared via two routes. In route A, PGPS was hydrolyzed in an aqueous HCl/THF solution to form a diol group; the hydrolyzed polymer was coated on a glass substrate and heated at 150 °C for 2 h. The

obtained PSQ-OH film exhibited a low WU of 5% and a scratch resistance of 1.6 because of the formation of the Si–O–C bond via the side reaction between the silanol and hydroxy groups. In route B, PGPS was coated on a glass substrate and immersed in a 0.5 mol/L H_2SO_4 solution for the ring-opening reaction of the epoxy group. The hydrolysis of the epoxy group was confirmed using solid-state ^{13}C NMR, and the epoxy group was completely hydrolyzed after immersion in the 0.5 mol/L H_2SO_4 solution for 15 h. The WU of the PSQ-OH film prepared via route B increased from 5% to 19% as the immersion time increased from 1 to 15 h and was higher than that of the PSQ-OH film prepared via route A. The WU of the PSQ-OH film was 12%–19%, lower than those of the PAEAPS and PVA films but sufficiently high to prevent fogging. Indeed, the PSQ-OH film on a glass substrate retained transparency when exposed to water vapor at 60 °C. The PSQ-OH film prepared via route B exhibited a high scratch resistance of 2.7–3.6, similar to that of the PAEAPS film. Surprisingly, the scratch resistance of the PSQ-OH film was 5–7 times higher than that of the PVA film. The PSQ-OH film prepared via route B was uniform, and no pinholes and cracks were observed using laser microscopy. The PSQ-OH film on a glass substrate was highly transparent and colorless and exhibited a high transmittance of >90% in the wavelength range of 400–800 nm. Thus, this study presents a convenient procedure for preparing a PSQ film containing a hydroxy group. The PSQ-OH film prepared via route B is demonstrated to be an excellent antifogging material.

5. Reference

[1] T. Ishimoto, S. Tsukada, S. Wakitani, K. Sato, D. Saito, Y. Nakanishi, S. Takase, T. Hamada, J. Ohshita, H. Kai, Model-based research toward design of innovative materials: molecular weight prediction of bridged polysilsesquioxanes, Rsc Advances 10(48) (2020) 28595-28602.

[2] S. Tsukada, Y. Nakanishi, T. Hamada, K. Okada, S. Mineoi, J. Ohshita, Ethylene-bridged polysilsesquioxane/hollow silica particle hybrid film for thermal insulation material, Rsc Advances 11(40) (2021) 24968-24975.

[3] T. Hamada, T. Goto, S. Takase, K. Okada, A. Uedono, J. Ohshita, Structure-Thermal Property Relationships of Polysilsesquioxanes for Thermal Insulation Materials, Acs Applied Polymer Materials 4(4) (2022) 2851-2859.

[4] N. Takamura, T. Gunji, H. Hatano, Y. Abe, Preparation and properties of polysilsesquioxanes: Polysilsesquioxanes and flexible thin films by acid-catalyzed controlled hydrolytic polycondensation of methyl- and vinyltrimethoxysilane, Journal of Polymer Science Part a-Polymer Chemistry 37(7) (1999) 1017-1026.

[5] T. Gunji, Y. Iizuka, K. Arimitsu, Y. Abe, Preparation and properties of alkoxy(methyl)silsesquioxanes as coating agents, Journal of Polymer Science Part a-Polymer Chemistry 42(15) (2004) 3676-3684.

[6] K. Yamamoto, J. Ohshita, T. Mizumo, M. Kanezashi, T. Tsuru, Preparation of hydroxyl group containing bridged organosilica membranes for water desalination, Separation and Purification Technology 156 (2015) 396-402.

Chapter 5: Highly Durable Antifogging Polysilsesquioxane Film Containing Tetraethylene Glycol Chains

1. Introduction

In Chapter 4, the PSQ-OH film exhibited a high scratch resistance, antifogging properties, and transparency. For the practical applications of PSQ-OH, the author conducted a durability test on the PSQ-OH film by keeping the film under humid and dry conditions repeatedly. From the aforementioned investigation, the PSQ-OH films revealed the following problems: (1) a decrease in the water uptake (WU) and (2) the formation of cracks in the PSQ-OH film were observed during the durability test. The author hypothesized that the decrease in WU and formation of cracks were due to the polycondensation reaction between residual silanol groups in the PSQ-OH film during repeated exposure to high and low humidity.

To address these problems, the author studied bridged PSQ prepared from organically bridged trialkoxysilanes, $[(RO)_3Si–R–Si(OR)_3]$ [1, 2], in which each silanol group is sterically separated by the organic bridges, i.e., the polycondensation reaction of the residual silanol groups might be prevented by their space effect. In the present study, we employed hydrophilic ethylene glycol chain as the spacer, expecting that its high hydrophilicity would not affect the antifogging property. The preparation of high-performance antifogging films based on poly(ethylene glycol) (PEG) has been reported, although their mechanical stability is low [3].

In Chapter 5, the effect of introducing ethylene glycol chains into a PSQ-OH film on the antifogging property and durability of the diol-containing film is described. PSQs with diol groups and tetraethylene glycol units were prepared by a sol–gel reaction. Their antifogging property, mechanical property, and durability are compared with those of the PSQ-OH film.

2. Experimental

2.1 Materials

3-Glycidyloxypropyltrimethoxysilane (GPTMS), tetraethylene glycol, allyl bromide, and triethoxysilane were purchased from Tokyo Chemical Industry Co., Ltd (Tokyo, Japan) and used as received. In addition, tetraethyleneglycol diallylether (TEGDAE) and tetraethylene glycol bis(triethoxysilylpropyl)ether (BTESP-EG) were synthesized according to the previous study [4-6]. Super dehydrated methanol; tetrahydrofuran (THF); toluene; *N,N*-dimethylformamide (DMF); hexane (super dehydrated); 2-propanol; 6-mol/L hydrochloric acid (HCl); 1-mol/L sulfuric acid (H_2SO_4); and potassium hydroxide (KOH) were purchased from Fujifilm Wako Pure Chemical Co., Ltd (Osaka, Japan) and used as received. Sodium hydride (60% dispersion in mineral oil) and platinum(0)-1,3-divinyl-1,1,3,3-tetramethyldisiloxane complex solution (Karstedt's catalyst, in xylene, Pt ~2%) were purchased from Sigma-Aldrich. Water was purified using a Millipore Mill-Q UV system. The glass substrates were washed using an alkaline solution according to Chapter 3. A Kapton film (thickness, 12.5 μm) was purchased from AZ One Corporation (Osaka, Japan).

2.2 Synthesis of tetraethyleneglycol diallylether (TEGDAE)

TEGDAE was synthesized according to previous studies [4, 5]. Sodium hydride (2.81 g, 70.4 mmol in mineral oil) and hexane (30 mL) were placed in a vacuum-dried 100-mL two-necked flask in a nitrogen atmosphere. The mixture was stirred and allowed to stand, and the supernatant was removed using a syringe. This process was repeated thrice to remove the oil of sodium hydride. A solution of tetraethylene glycol (2.51 g, 12.9 mmol) in DMF (25 mL) was slowly added to the flask, and the mixture was stirred at room temperature for 20 min. Thereafter, allyl bromide (4.37 mL, 51.6 mmol) was added dropwise, and the mixture was stirred overnight at room temperature. The reaction was quenched by the addition of dilute hydrochloric acid (120 mL) in an ice bath. The product was extracted with hexane (50 mL × 3), and the combined hexane solution was washed with water (50 mL

× 3), dried with anhydrous $MgSO_4$, and the solvent was removed under reduced pressure. The product was purified by silica gel column chromatography (eluent: ethyl acetate:hexane = 3:1) to yield TEGDAE as a viscous liquid (75% yield).

^{1}H NMR (400 MHz, $CDCl_3$, ppm): δ= 3.63 (16H, m), 4.02 (4H, m), 5.22 (4H, m), 5.91 (2H, m).

2.3 Synthesis of tetraethylene glycol bis(triethoxysilylpropyl) ether (BTESP-EG)

BTESP-EG was synthesized according to a reported procedure [6]. A mixture of TEGDAE (1.41 g, 5.13 mmol); triethoxysilane (2.11 g, 12.8 mmol); Karstedt's catalyst (7.0 mg); and toluene (10 mL) was placed in a 100-mL two-necked flask equipped with a nitrogen inlet and outlet. The reaction mixture was stirred at 60 °C for 2 h, and the solvent was removed under reduced pressure to provide BTESP-EG as a clear colorless oil.

^{1}H NMR (400 MHz, $CDCl_3$, ppm): BTESP-EG: δ = 0.63 (4H, t, J = 8.4 Hz), 1.22 (18H, t, J = 7.0 Hz), 1.70 (4H, quin, J = 7.0, 8.4 Hz), 3.43 (4H, t, J = 7.0 Hz), 3.59 (4H, m), 3.65 (14H, m), 3.82 (12H q, J = 7.0 Hz); byproduct: δ = 1.56 (1.4H, m), 3.70 (1.1H, m), 3.87 (1.3H, m), 4.36 (0.4H, m), 4.77 (0.2H, m). 5.98 (0.2H, m), 6.25 (0.2H, m).

2.4 Synthesis of poly(glycidyloxypropyl-co-tetraethylene glycol)silsesquioxane (PSQ-Gly/EG)

GPTMS (0.709 g, 3.00 mmol); BTESP-EG (0.603 g, 1.00 mmol); and methanol (1.28 g, 40.0 mmol) were added in a 100-mL flask equipped with a mechanical stirrer and nitrogen inlet and outlet. The rotation speed and nitrogen flow rate were fixed at 150 rpm and 360 mL/min, respectively. The mixture was stirred at ice-water bath temperature for 10 min. Afterward, 0.0407 g (5.50 mmol) of water and 0.0730 g of 6 mol/L HCl were slowly added and successively stirred at ice-water bath temperature for 10 min. The polycondensation reaction was conducted at room temperature for 5 h to yield PSQ-Gly/EG. The obtained PSQ-Gly/EG was dissolved in THF to a 50 wt% solution and stored in a refrigerator until use. PSQ-Gly/EG with different feed ratios of GPTMS and BTESP-EG were also

similarly prepared and denoted by PSQ-Gly_x/EG_y, where x and y indicate the feed ratios of GPTMS and BTESP-EG.

2.5 Preparation of poly[3-(2,3-dihydroxypropoxypropyl)-co-tetraethylene glycol]silsesquioxane (PSQ-Diol/EG) film

PSQ-Diol/EG films were prepared according to the method described in Chapter 4. First, a 50-wt% PSQ-Gly/EG–THF solution was coated onto a cleaned glass substrate using an applicator (clearance gap of 50 μm) and heated at 80 °C and 150 °C for 1 and 0.5 h, respectively. The polymer-coated glass substrate was immersed in 0.5-mol/L H_2SO_4 for 9–15 h at room temperature to convert the epoxy group into a diol group. The obtained PSQ-Diol/EG film on the glass substrate was washed with water several times and dried at 60 °C for 1 h.

2.6 Measurements

^{1}H and ^{29}Si nuclear magnetic resonance (NMR) measurements were performed using Varian 400 and 500 MHz spectrometers using deuterium chloroform ($CDCl_3$) as a solvent and tetramethylsilane as an internal standard. Gel permeation chromatography was performed using a Shimadzu LC-20AD equipped with CTO-20A and RID-10A detectors and TSKgel G6000H/G4000H/G2000H columns at 40 °C with THF as an eluent at a flow rate of 1 mL/min. Fourier transform infrared (FT-IR) spectroscopy was performed using a Shimadzu IRAffinity-1 spectrometer on a sample-coated silicon wafer in transmittance mode. To measure the water uptake (WU) of the PSQ-Diol/EG film, a PSQ-Diol/EG film was prepared on the Kapton film, and the PSQ-Diol/EG-coated Kapton film was placed in a temperature and relative humidity (RH)-controlled chamber and weighed after exposure to 20% or 95% RH at 30 °C for 2 h. The detailed calculation for WU is described in Chapter 3. Indentation and scratch tests were performed to evaluate the elastic modulus and scratch resistance of the PSQ-Diol/EG film, respectively, using a Nano Indenter G200. The detailed procedure is available in Chapter 2.

3. Results and discussion

3.1 Synthesis of PSQ-Gly/EG by hydrolysis/polycondensation reaction

The author investigated ethylene glycol chains as bridges for improving the durability of the PSQ-OH film. According to previous studies [4-6], BTESP-EG containing a hydrophilic tetraethylene glycol unit was synthesized in two steps including the allylation of tetraethylene glycol and hydrosilylation reaction of the allylation product in a total yield of 65% **(Scheme 1)**. After the hydrosilylation reaction, BTESP-EG was obtained as a clear colorless oil by the evaporation of solvent and the unreactive triethoxysilane even without removal of Karstedt's catalyst because the amount of Karstedt's catalyst was low for the hydrosilylation reaction. The chemical structure of BTESP-EG was verified by its ^{1}H NMR spectrum. Although small impurity peaks attributed to side reaction such as the isomerization of allyl ether were observed, the main peaks were assigned to BTESP-EG by comparison with the literature data [6].

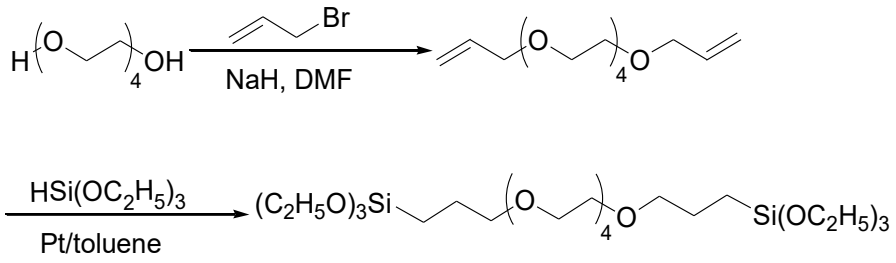

Scheme 1. Synthesis of tetraethylene glycol bis(triethoxysilylpropyl) ether (BTESP-EG).

PSQ-Gly/EG with different ratios of diols and tetraethylene glycol chains was synthesized from GPTMS and BTESP-EG via hydrolysis/polycondensation using the nitrogen flow method (**Scheme 2**) [7]. The results for PSQ-Gly/EG are shown in **Table 1**. When the polycondensation was conducted at 50 °C–80 °C at a feed molar ratio of GPTMS and BTESP-EG = 3/1, the formation of gel was observed during the polycondensation reaction (Entries 1–2 in **Table 1**). The high network structure was easily formed by the addition of BTESP-EG because of the bridged alkoxysilane containing six alkoxy groups. Oppositely, the polycondensation reaction at room temperature afforded a highly viscous product that was soluble in typical organic solvents, such as THF and chloroform after 5 h (entry 3 in **Table 1**). The obtained PSQ-Gly_3/EG_1 possessed a low weight-average molecular weight (M_w) of 800 and polydispersity index (M_w/M_n) of 1.7 (entry 3 in **Table 1**). The ^{1}H NMR spectrum of PSQ-Gly_3/EG_1 is shown in **Figure 1**. The broad signals at 0.73 and 1.8 ppm were attributed to propylene units at α- and β-positions to Si, respectively. Signals attributed to other protons of the glycidyloxypropyl unit were observed in the same regions as those of the PGPS, as described in Chapter 4. The signal attributed to the methylene adjacent to the oxygen of tetraethylene glycol was observed at 3.7 ppm. Peaks of residual ethoxy groups were observed at 1.2 and 3.8 ppm. Based on the integration of the methylene proton of Si-CH_2 and the ethoxy proton, 85% of the ethoxy groups were calculated to be consumed by the hydrolysis/polycondensation reaction. The ^{29}Si NMR spectrum of PSQ-Gly_3/EG_1 is shown in **Figure 2**, along with those of GPTMS, PGPS, and BTESP-EG. Four kinds of peaks attributed to T^0, T^1, T^2, and T^3 were observed in ranges of –40.4 to –42.8 ppm, –49.0 to –51.4 ppm, –57.4 to –59.8 ppm, and –66.0 to –69.0 ppm, respectively, in the PSQ-Gly_3/EG_1 spectrum. BTESP-EG exhibited a sharp signal at –45 ppm, which completely disappeared after the polycondensation reaction, as shown in ^{29}Si NMR spectrum of PSQ-Gly_3/EG_1. Contrarily, the T^0 signal of GPTMS remained or was slightly shifted. In the ^{29}Si NMR spectra of PSQ-Gly_3/EG_1 and PGPS, the positions of the peaks derived from the T^1 and T^2 structures were slightly shifted. Overall,

the tetraethylene glycol chain was introduced into PSQ-OH, and PSQ-Gly_3/EG_1 was successfully synthesized by the copolymerization of GPTMS and BTESP-EG.

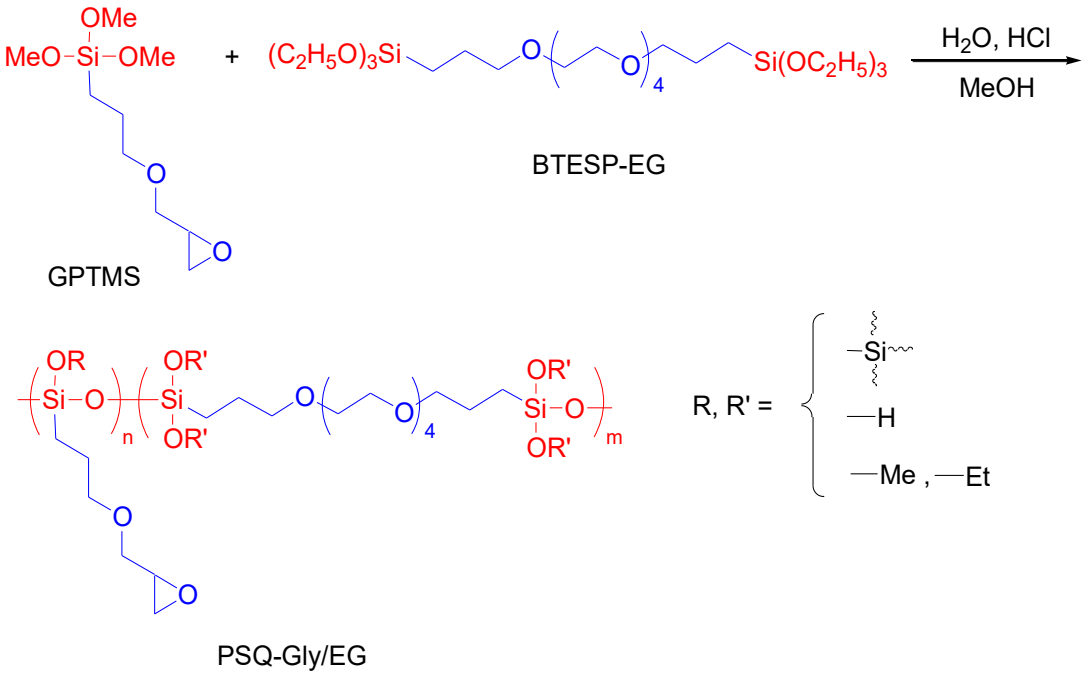

Scheme 2. Preparation of poly(glycidyloxypropyl-co-tetraethylene glycol)silsesquioxane (PSQ-Gly/EG) using the sol–gel method.

Table 1. Results of the synthesis of poly(glycidyloxypropyl-co-tetraethylene glycol)silsesquioxane (PSQ-Gly/EG)

Entry	Copolymer	Feed molar ratio of GPTMS:BTESP-EG:H_2O	Temperature (°C)	Time (h)	M_w	M_w/M_n
1	PSQ-Gly_3/EG_1	3.0:1.0:5.5	80	3		
2	PSQ-Gly_3/EG_1	3.0:1.0:5.5	50	3		
3	PSQ-Gly_3/EG_1	3.0:1.0:5.5	r.t.	5	800	1.7
4	PSQ-Gly_1/EG_1	2.0:2.0:5.0	r.t.	5	700	1.6
5	PSQ-Gly_1/EG_3	1.0:3.0:4.5	r.t.	5	680	1.5

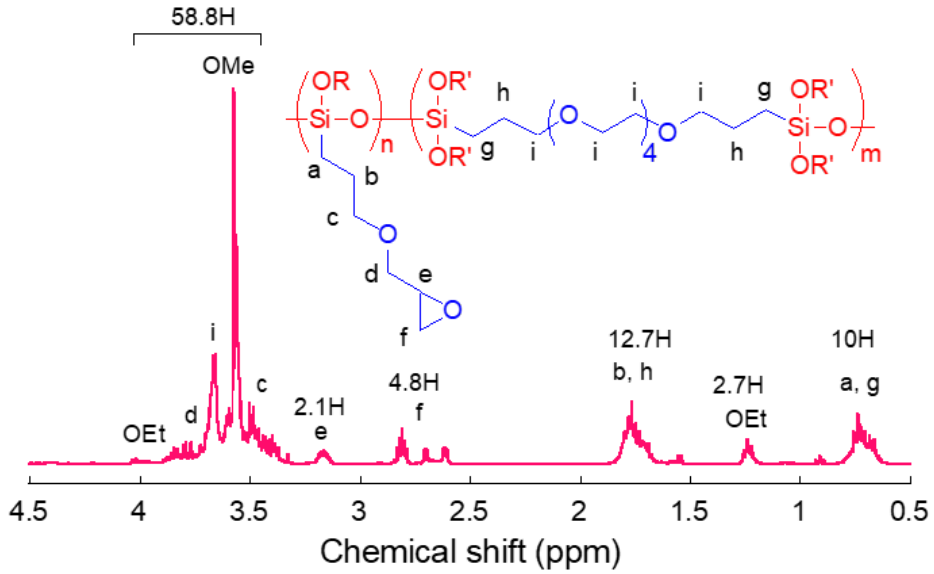

Figure 1. The ^{1}H NMR spectrum of poly(glycidyloxypropyl-co-tetraethylene glycol)silsesquioxane (PSQ-Gly_3/EG_1) in $CDCl_3$.

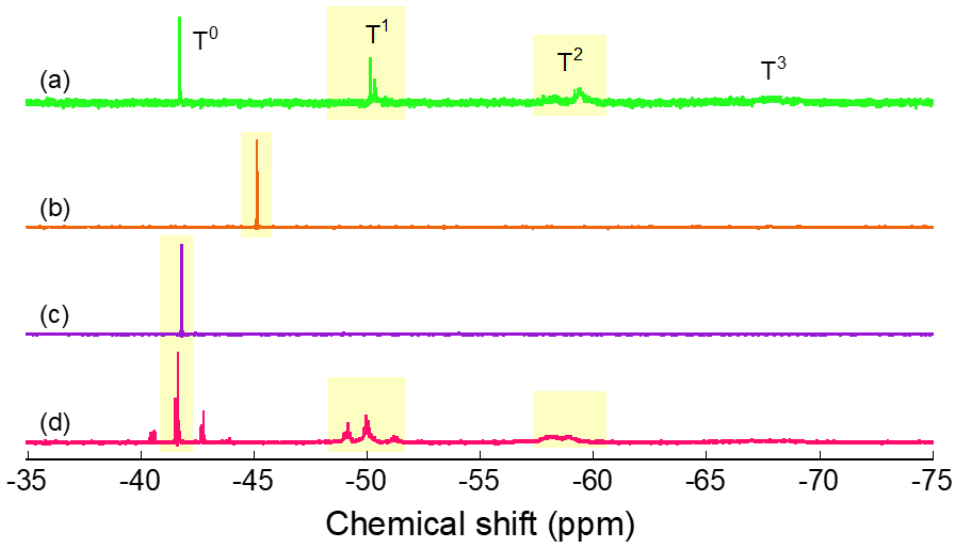

Figure 2. The ^{29}Si NMR spectra of (a) poly(glycidyloxypropyl)silsesquioxane (PGPS), (b) tetraethylene glycol bis(triethoxysilylpropyl)ether (BTESP-EG), (c) 3-glycidyloxypropyltrimethoxysilane (GPTMS), and (d) poly(glycidyloxypropyl-co-tetraethylene glycol)silsesquioxane (PSQ-Gly$_3$/EG$_1$) in $CDCl_3$.

Similarly, PSQ-Gly/EG with different feed ratios of GPTMS and BTESP-EG were prepared with their M_w and M_w/M_n ranged from 680–700 and 1.5–1.6, respectively (Entries 4–5 in **Table 1**). Unfortunately, the storage stability of PSQ-Gly/EG was extremely low, and the M_w of PSQ-Gly/EG increased from 800 to 11000 after 8 days even under storage in a refrigerator. Therefore, to ensure the repeatability of the film preparation, the PSQ-Gly/EG films were prepared within one day after the synthesis of PSQ-Gly/EG. No significant changes of the polymer molecular weights and the NMR spectra were found within one day.

3.2 Preparation of PSQ-Diol/EG film

The ring-opening reaction of epoxy groups in the PSQ-Gly/EG film prepared on the glass substrate was conducted by immersion in sulfuric acid to prepare the PSQ-Diol/EG film (**Scheme 3**). To

investigate the progress of the ring-opening reaction of the epoxy groups, a THF solution containing PSQ-Gly_1/EG_1 containing the same amount of epoxy group and tetraethylene glycol chain was coated onto the silicon wafer and heated at 80 °C and 150 °C for 1 and 0.5 h, respectively. Thereafter, the resultant PSQ-Gly_1/EG_1 films on the silicon wafer were immersed in a 0.5-mol/L H_2SO_4 aqueous solution for 9 and 15 h. The FT-IR spectrum of the PSQ-Gly_1/EG_1 film exhibited a peak around 1100 cm^{-1} corresponding to the Si–O–Si bonding (**Figure 3**). When the film was immersed in H_2SO_4 (aq) for 9 h, the peak intensity of the hydroxyl groups around 3000–3600 cm^{-1} increased. It took 15 h for the PSQ-OH film to wholly convert the epoxy group into a diol group under the same conditions. However, for PSQ-Gly_1/EG_1, no evident changes in the FT-IR spectrum were observed after further immersion of the film for an additional 6 h (**Figure 3**(c)). To obtain additional information for the ring-opening reaction, the surface property was investigated with respect to the water contact angle, which drastically changed prior to and after the ring-opening reaction of the epoxy group. The PSQ-Gly_1/EG_1 pristine film exhibited a water contact angle of 71°. After immersion for 15 h, the water contact angle decreased to 59°. This means that the epoxy groups were wholly converted into diol groups after immersion in H_2SO_4 (aq) for 15 h. Furthermore, the PSQ-$Diol_1/EG_1$ films prepared by immersion in H_2SO_4 (aq) for 9 and 15 h exhibited similar WU (vide infra). The surface of the PSQ-$Diol_1/EG_1$ film prepared on the glass substrate was smooth and free of pinholes, and the root-mean-square (rms) was determined to be 0.15 μm by laser microscopy even after immersion in H_2SO_4 (aq), indicating the formation of a crack-free, transparent, and tack-free PSQ-Diol /EG film using the immersion method.

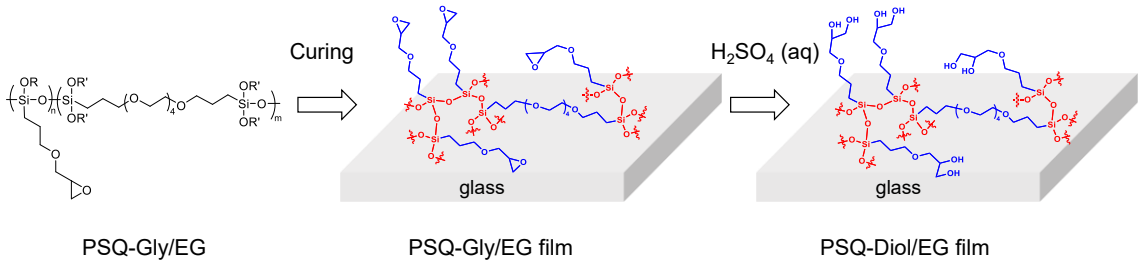

Scheme 3. Preparation of the poly[3-(2,3-dihydroxypropoxypropyl)-co-tetraethylene glycol]silsesquioxane (PSQ-Diol/EG) film.

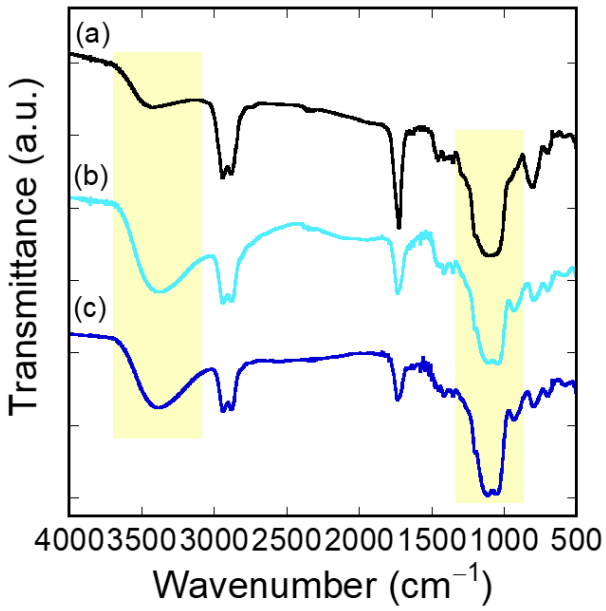

Figure 3. FT-IR spectra of the (a) poly(glycidyloxypropyl-co-tetraethylene glycol)silsesquioxane ($PSQ\text{-}Gly_1/EG_1$); (b) poly[3-(2,3-dihydroxypropoxypropyl)-co-tetraethylene glycol]silsesquioxane ($PSQ\text{-}Diol_1/EG_1$) (immersion for 9 h); and (c) $PSQ\text{-}Diol_1/EG_1$ films (immersion for 15 h).

3.3 Antifogging and mechanical property of PSQ-Diol/EG film

To investigate the antifogging and mechanical properties of the PSQ-Diol/EG films, the WU, scratch resistance, and elastic modulus were evaluated and are summarized in **Table 2**. The WU of the PSQ-Diol/EG films was practically independent of the amount of tetraethylene glycol units, ranging from 15% to 19%, and these values were similar to those of the PSQ-OH films (WU of 12–19%). Similar water contact angles were observed for the PSQ-OH and PSQ-$Diol_1$/EG_1 films (63° and 59°, respectively) immersed in a 0.5-mol/L H_2SO_4 aqueous solution for 15 h, despite the decrease in the number of hydroxyl groups in the PSQ-Diol/EG film, compared with the PSQ-OH film. This indicated that the tetraethylene glycol chains contributed to retaining the hydrophilicity of the film. The contact angle of the PGPS and PSQ-Gly/EG films without hydroxyl groups were 82° and 71°, respectively. The smaller contact angle of the PSQ-Gly/EG film indicated that the tetraethylene glycol chains endowed the film with hydrophilicity. A glass substrate and a PSQ-$Diol_1$/EG_1 film on a glass substrate prepared by immersion in a 0.5-mol/L H_2SO_4 aqueous solution for 15 h were exposed to water vapor at 50 °C for several seconds. The glass substrate rapidly fogged, and the PSQ-$Diol_1$/EG_1 film on the glass substrate maintained its transparency (**Figure 4**). This indicated that the PSQ-$Diol_1$/EG_1 film exhibited antifogging properties.

Table 2. Antifogging and mechanical properties of the poly[3-(2,3-dihydroxypropoxypropyl)-co-tetraethylene glycol]silsesquioxane (PSQ-Diol/EG) film

	Immersion time (h)	WU (%)	Scratch resistance	Elastic modulus (GPa)
PSQ-OH	9	12	2.7	1.5
PSQ-OH	15	19	2.7	1.1
PSQ-Diol$_3$/EG$_1$	15	15	3.3	1.2
PSQ-Diol$_1$/EG$_1$	9	19	3.5	1.2
PSQ-Diol$_1$/EG$_1$	15	18	2.4	1.1
PSQ-Diol$_1$/EG$_3$	15	16	3.2	1.2
PVA		27	0.5	9.0

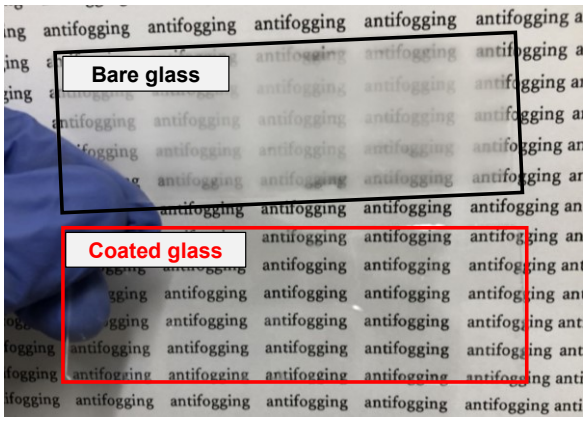

Figure 4. Photograph of the glass substrate (upper) and poly[3-(2,3-dihydroxypropoxypropyl)-co-tetraethylene glycol]silsesquioxane (PSQ-Diol$_1$/EG$_1$) film on the glass substrate (immersion for 15 h) (lower) exposed to water steam.

The PSQ-OH film exhibited a high scratch resistance of 2.7–3.6, which was 5–7 times higher than that of the PVA film. The scratch resistance of PSQ-Diol/EG films ranged from 2.4 to 3.5, comparable to that of PSQ-OH. In the scratch profile of the PSQ-Diol$_1$/EG$_1$ films prepared on glass substrates by the nanoindenter scratch test (**Figure 5**), the profile during scratching (ramped scratch) deformed to approximately 4500 nm in displacement into the surface. Oppositely, the postscratch profile was nearly identical to the prescratch profile because of the recovery from the deformation during scratching. The high elasticity recovery of the flexible siloxane bond appeared to assist the recovery from deformation, as described in Chapter 2. These results indicated that the tetraethylene glycol chains did not decrease the scratch resistance, and the PSQ-Diol/EG films were highly scratch-resistant.

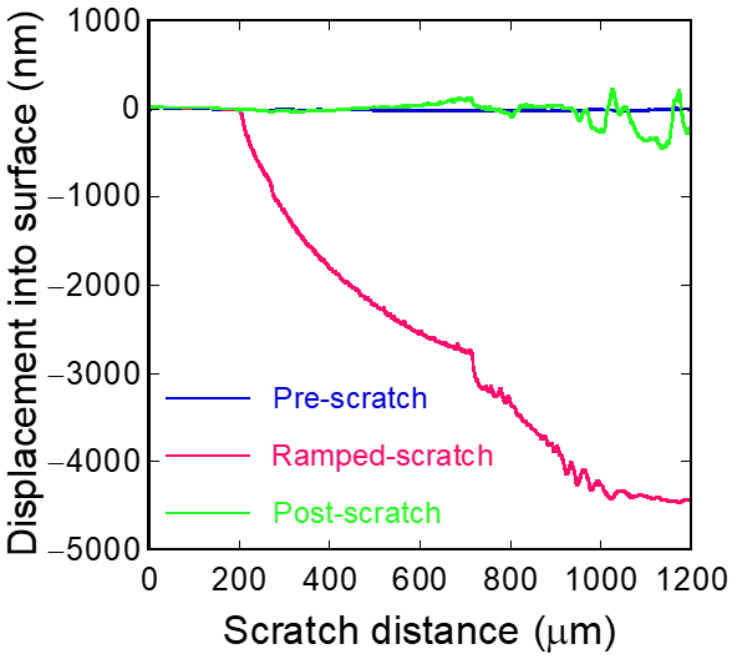

Figure 5. Scratch profile of the poly[3-(2,3-dihydroxypropoxypropyl)-co-tetraethylene glycol]silsesquioxane (PSQ-Diol$_1$/EG$_1$) film (immersion for 9 h).

3.4 Durability of PSQ-Diol/EG film on humidity and temperature change

If an automobile windshield is coated with an antifogging film, the coated film prevents fogging by absorbing water droplets that condense on the windshield surface. However, fogging occurs when the antifogging film is saturated with water (over WU), i.e., the water droplets that cannot be absorbed by the antifogging film form on the film surface. Therefore, the absorbed water in the film must be dried by a heater, such as a defogger system, before reaching saturated water absorption. In addition, considering the atmospheric conditions in said automobile, antifogging films must maintain their antifogging ability, surface smoothness, and transparency even after repeated moisture absorption and desorption. Therefore, after repeated exposure to humid and dry air, the change in WU was monitored to investigate the durability of the antifogging property, surface smoothness, and transparency of the PSQ films through the repeated absorption and desorption of water vapor.

(1) Effect of tetraethylene glycol chain on the antifogging property through repeated testing by changing the humidity

The author performed repeated testing of moisture absorption and desorption on the PSQ-$Diol_1$/EG_1 and PSQ-OH films. The change in WU was monitored during five repeated cycles at 20% and 95% RH at 30 °C (**Figure 6**). The WU of the PSQ-OH film at 95% RH gradually decreased from 16% to 14% after the fifth cycle. Conversely, the WU of the PSQ-$Diol_1$/EG_1 film did not exhibit a change even after the fifth cycle. In Chapter 2, the WU of the PAEAPS films decreased from 52% to 22% with an increase in the heating time at 180 °C from 0.5 to 2 h. The decrease in WU was due to the formation of a highly crosslinked siloxane network when the heating time was increased from 0.5 to 2 h. Similarly, the author considered that the decrease in WU of the PSQ-OH film after repeated exposure to high and low humidity was due to the formation of a crosslinked siloxane network by the polycondensation reaction of the residual silanol groups. In preparation method, silanol groups were formed in the PSQ-OH and PSQ-Diol/EG films by the hydrolysis reaction of residual alkoxy groups

in the films during the ring-opening reaction of the epoxy group. In the course of desorption testing, the remaining silanol groups in the film reacted with each other to form a siloxane bond by the polycondensation reaction. Thus, the decrease in the WU of the PSQ-OH film was observed after repeated absorption and desorption cycles. Contrarily, the PSQ-Diol$_1$/EG$_1$ film contained tetraethylene glycol chains between the silicon atoms, which provided space between the siloxane backbone and the distance between the silanol groups to prevent a further polycondensation reaction of the silanol groups.

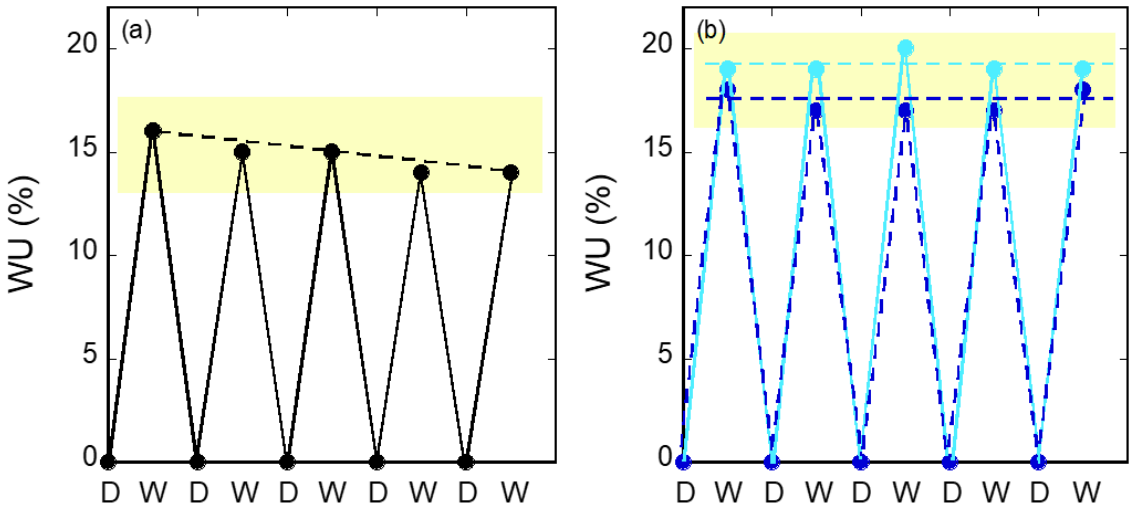

Figure 6. Water uptake (WU) of the (a) poly[3-(2,3-dihydroxypropoxypropyl)]silsesquioxane (PSQ-OH) film prepared by immersion in 0.5-mol/L sulfuric acid for 15 h (black circles). (b) Poly[3-(2,3-dihydroxypropoxypropyl)-co-tetraethylene glycol]silsesquioxane (PSQ-Diol$_1$/EG$_1$) film prepared by immersion in 0.5-mol/L sulfuric acid for 9 h (light blue circles) and 15 h (blue circles) after placing the films at a relative humidity (RH) of 20% (D) and 95% (W), respectively, for 2 h at 30 °C.

(2) Effect of tetraethylene glycol chain on the surface smoothness through repeated testing by changing humidity and temperature

The PSQ-OH and PSQ-Diol$_1$/EG$_1$ films were exposed to water vapor at 50 °C at 95% RH for 1–7 days to investigate their durability regarding surface smoothness. Their appearance was observed using a laser microscope under atmospheric conditions. For the PSQ-OH film, the formation of cracks was partially observed, and a part of the PSQ-OH film was peeled off from the glass substrate after 1 day at 50 °C and 95% RH. Overall, the formation of cracks and the peeling of the PSQ-OH film from the glass substrate occurred after 2 days at 50 °C and 95% RH. Oppositely, the PSQ-Diol$_1$/EG$_1$ film did not exhibit cracks or a detachment of the film from the glass substrate even after 1 week at 50 °C and 95% RH; it possessed a smooth surface (**Figure 7**). Contrarily, the laser microscope image of the PSQ-OH film shows the rough surface due to the formation of cracks and the peeling of the film from the glass substrate. The time-dependent change in the rms roughness at 50 °C and 95% RH was monitored by laser microscopy (**Figure 8**). The rms roughness of the PSQ-OH film increased from 0.16 μm, exceeded 1.5 μm after 1 day at 50 °C and 95% RH, and exceeded 3.0 μm after 2 days. The PSQ-Diol$_1$/EG$_1$ film maintained the initial rms roughness within 0.18 μm even after 1 week under the same conditions. Any changes in the chemical structure were undetected by FT-IR or other methods after exposure to water vapor at 50 °C and 95% RH for the PSQ-OH and PSQ-Diol$_1$/EG$_1$ films. When water-absorbing antifogging films are exposed to high humidity, the films usually swell and expand in volume, owing to the absorption of water. Thus, the drying process under atmospheric conditions during the laser microscopy caused the film to shrink. Simultaneously, the polycondensation reaction of the residual silanol groups also promotes the shrinkage of film. The repeated swollen and drying processes were accompanied by large volume changes that led to the formation of cracks and peeling of the PSQ-OH film. In addition to the inhibition of polycondensation reaction of silanol groups, the flexibility of the tetraethylene glycol chains in the PSQ-Diol$_1$/EG$_1$ film may have prevented the formation of cracks by relaxing the internal stress during the swelling and drying conditions.

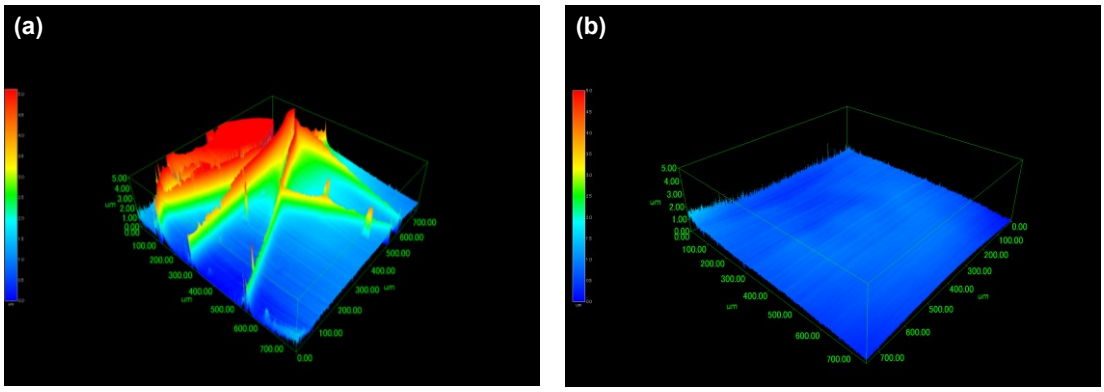

Figure 7. Laser microscopy image of the (a) poly[3-(2,3-dihydroxypropoxypropyl)]silsesquioxane (PSQ-OH) film (immersion for 15 h) after exposure at 50 °C and 95% relative humidity (RH) for 1 day and the (b) poly[3-(2,3-dihydroxypropoxypropyl)-co-tetraethylene glycol]silsesquioxane (PSQ-Diol$_1$/EG$_1$) film (immersion for 15 h) after exposure at 50 °C and 95% RH for 1 day.

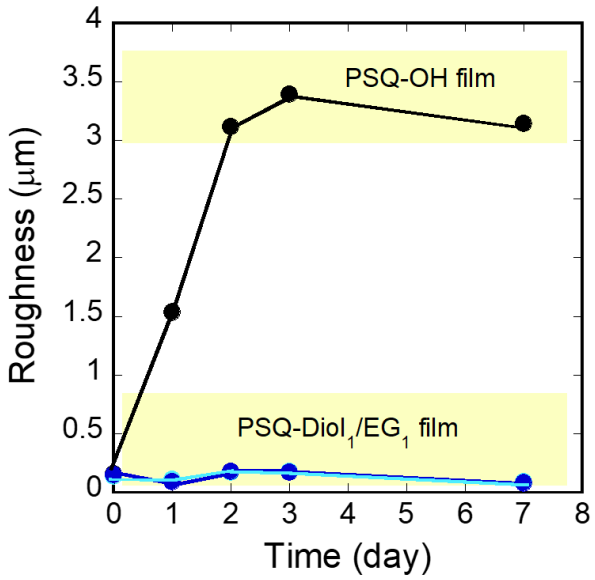

Figure 8. Time-dependent change in the root-mean-square roughness at 50 °C and 95% relative humidity (RH) of the poly[(3-(2,3-dihydroxypropoxypropyl)]silsesquioxane (PSQ-OH) film (immersion for 15 h) (black circles), poly[3-(2,3-dihydroxypropoxypropyl)-co-tetraethylene glycol]silsesquioxane (PSQ-Diol$_1$/EG$_1$) film (immersion for 9 h) (light blue circles), and PSQ-Diol$_1$/EG$_1$ film (immersion for 15 h) (blue circles).

(3) Transparency of PSQ-Diol$_1$/EG$_1$ film after exposure to water vapor at high temperature

Transparency is also desired for antifogging materials for practical safety; therefore, the transmittance of the PSQ-Diol$_1$/EG$_1$ film was measured. The transmittance of the PAEAPS film prepared at 180 °C for 1 h was 91% at 400 nm (**Figure 9**). The low transmittance of the PAEAPS film may have been due to denaturation, such as the oxidation of the amino groups on the side chains. The PSQ-Diol$_1$/EG$_1$ film on a glass substrate exhibited over 99% of transmittance in the wavelength range of 400−800 nm. This indicates that the hydroxy groups and tetraethylene glycol in the PSQ-Diol$_1$/EG$_1$ film were thermally stable and oxidation-resistant at high temperatures.

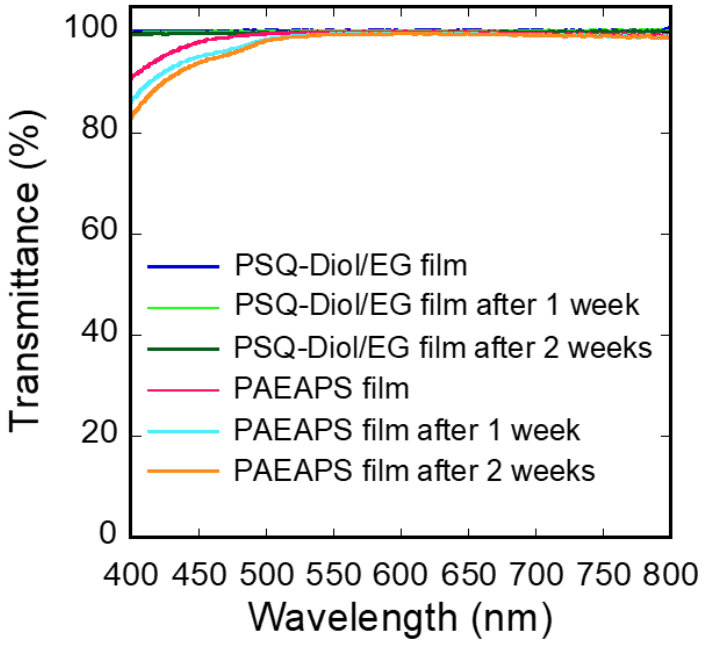

Figure 9. UV–visible spectra of the poly[3-(2,3-dihydroxypropoxypropyl)-co-tetraethylene glycol]silsesquioxane (PSQ-Diol$_1$/EG$_1$) film (immersion for 15 h), poly[3-(2-aminoethylaminopropyl)]silsesquioxane (PAEAPS) film prior to and after exposure at 50 °C and 95% relative humidity for 1–2 weeks.

Changes in transparency under high humidity conditions were investigated. The transmittance at 400 nm of the PAEAPS film decreased from 91% to 86% and 83% after exposure to water vapor at 50 °C and 95% RH for one and two weeks, respectively. Conversely, the PSQ-$Diol_1$/EG_1 film retained a transmittance exceeding 99% at 400 nm even after exposure to the water vapor at 50 °C and 95% RH for two weeks. As discussed, the color change of the PAEAPS film was derived from the oxidation of amino groups. Under high humidity conditions, the oxidation of amino groups might have accelerated in the wet state. In contrast, the PSQ-$Diol_1$/EG_1 film showed high oxidation resistance.

4. Conclusions

The PSQ-Diol/EG film was successfully prepared for the application of antifogging materials. The PSQ-Diol/EG films exhibited a high WU of 15%–19%, which was similar to that of the PSQ-OH film. From the WU and contact angle measurements, it was observed that the tetraethylene glycol chains of the PSQ-Diol/EG film were sufficiently hydrophilic to exhibit antifogging abilities. The PSQ-Diol/EG film on the glass substrate remained transparent when exposed to water vapor. For the mechanical properties, the PSQ-Diol/EG film exhibited a high scratch resistance of 2.4–3.5, which was similar to that of PSQ-OH film. It was concluded that the introduction of tetraethylene glycol chains did not decrease the WU and mechanical properties. For durability, the WU of the PSQ-OH film decreased by repeated exposure to dry and wet conditions at 20% and 95% RH, respectively, at 30 °C, and the formation of cracks was observed by leaving the film to stand at 50 °C and 95% RH. The WU of the PSQ-Diol/EG film did not decrease, and the formation of cracks was not observed. The space effect of the tetraethylene glycol chains inhibited the residual silanol groups from being condensed, and the flexible chain effect provided film stability upon volume changes during the repeated swelling–drying processes. Overall, PSQ-Diol/EG exhibited antifogging, scratch resistance, and humidity resistance.

5. References

[1] K.J. Shea, D.A. Loy, Bridged polysilsesquioxanes. Molecular-engineered hybrid organic-inorganic materials, Chemistry of Materials 13(10) (2001) 3306-3319.

[2] D.A. Loy, K.J. Shea, BRIDGED POLYSILSESQUIOXANES - HIGHLY POROUS HYBRID ORGANIC-INORGANIC MATERIALS, Chemical Reviews 95(5) (1995) 1431-1442.

[3] E. Nam, E.H.H. Wong, S. Tan, Q. Fu, A. Blencowe, G.G. Qiao, Antifogging Surface Facilitated by Nanoscale Coatings with Controllable Hydrophobicity and Cross-Linking Density, Macromolecular Materials and Engineering 302(1) (2017) 1600199.

[4] C. Zona, G. D'Orazio, B. La Ferla, Controlled-Length Efficient Synthesis of Heterobifunctionalized Oligo Ethylene Glycols, Synlett 24(6) (2013) 709-712.

[5] R. Guterman, A.R. Kenaree, J.B. Gilroy, E.R. Gillies, P.J. Ragogna, Polymer Network Formation Using the Phosphane-ene Reaction: A Thiol-ene Analogue with Diverse Postpolymerization Chemistry, Chemistry of Materials 27(4) (2015) 1412-1419.

[6] A. Bouvet-Marchand, C. Chatard, A. Graillot, G. Boutevin, C. Loubat, D. Grosso, Influence of experimental parameters on the side reactions of hydrosilylation of allyl polyethers studied by a fractional factorial design, Reaction Chemistry & Engineering 3(5) (2018) 696-706.

[7] T. Gunji, Y. Iizuka, K. Arimitsu, Y. Abe, Preparation and properties of alkoxy(methyl)silsesquioxanes as coating agents, Journal of Polymer Science Part a-Polymer Chemistry 42(15) (2004) 3676-3684.

Chapter 6: Summary

In summary, the author developed PSQ antifogging materials with hydrophilic groups to achieve a high level of water uptake and scratch resistance in antifogging materials. In addition, considering the practical application of PSQ antifogging materials, the improvement of environmental resistance by designing hydrophilic groups was also investigated.

In Chapter 1, the overview of previous studies on antifogging materials and PSQ was given to clarify the purpose of the thesis.

In Chapter 2, the author investigated whether PSQ films with hydrophilic groups have the potential as coating materials with both high water uptake and scratch resistance. The PSQ antifogging materials poly(3-aminopropyl)silsesquioxane (PAPS) and poly(3-(2-aminoethylaminopropyl)silsesquioxane) (PAEAPS) were prepared by sol-gel reactions that are self-catalyzed by the amine moieties of the monomers. The PAPS and PAEAPS films exhibited high water uptakes of 34% and 42%, which are 1.2- and 1.5-times that of the typical antifogging film of PVA, respectively. PAEAPS films exhibited high transparency under humidified conditions. Furthermore, the PAEAPS film exhibited a scratch resistance 6–7 times higher than that of PVA, as determined by a nanoindenter experiment. The mechanical property measurement using a nanoindenter indicated that a characteristic feature of polysiloxanes whereby flexible Si-O bonds induce recovery from the deformation and thus enhance scratch resistance.

In Chapter 3, the author focused the talk on the amine hydrochloride salt as a hydrophilic group in PSQ, because the ion is expected to possess stronger interaction with water than neutral polar functional groups to develop the high-performance-antifogging materials. The poly[3-(2-aminoethylamino)propyl]silsesquioxane hydrochloride (PAEAPS-Cl) films containing amine hydrochloride salt were prepared by immersing the PAEAPS film in 0.5 mol/L HCl methanolic

solution. FTIR, ^{13}C solid-state NMR and SEM-EDX analysis indicated that the amino group was converted to the amine hydrochloride salt upon immersion in 0.5 mol/L HCl methanolic solution for 1 h. The PAEAPS-Cl films showed no cracks or pinholes, and chlorine atoms were homogeneously distributed on the surface of the PAEAPS-Cl film. The PAEAPS film showed a water uptake and scratch resistance of 22% and 3.2, respectively. The introduction of the amine hydrochloride salt into the PAEAPS film increased its antifogging property and surface hardness, and the water uptake and scratch resistance of the PAEAPS-Cl film were improved to 29% and 4.3, respectively. However, the amine hydrochloride salt sometimes induced the morphological change of the PAEAPS-Cl film owing to strong hydration, and cracks and dimples were observed after exposure to water vapor at 40 °C and 95% for 1 h. In contrast, the poly[3-(2-aminoethylamino)propyl-co-methyl]silsesquioxane (P(AEAP-co-Me)S-Cl) film exhibited a water uptake of 17%, which was lower than those of the PAEAPS and PAEAPS-Cl films, but the cracks and dimples were not observed for the P(AEAP-co-Me)S-Cl films even after exposure to water vapor at 40 °C and 95% RH for 1 h. The introduction of the amine hydrochloride salt structure did not decrease transparency. These findings provides the information for further design and development of antifogging materials with high-performance.

Chapter 4 is focused on hydroxyl groups as hydrophilic groups in PSQ, aiming to develop a colorless antifogging film. Poly(glycidyloxypropyl)silsesquioxane (PGPS) was successfully synthesized by hydrolysis and polycondensation of 3-glycidyloxypropyltrimethoxysilane using the nitrogen flow method. To prepare poly(3-(2,3-dihydroxypropoxypropyl)silsesquioxane) (PSQ-OH) film, PGPS was coated on a glass substrate and immersed in a 0.5 mol/L sulfuric acid for 1–15 h at room temperature, producing a diol group. The water uptake of the PSQ-OH film increased from 5% to 19% with increasing immersion time. The PSQ-OH film exhibited a high scratch resistance of 2.7–3.6, similar to that of a PAEAPS film. The PSQ-OH film was transparent and colorless and exhibited a high

transmittance of >90% in the wavelength range of 400–800 nm. Unlike the amino-containing PSQ films, the PSQ-OH film was stable at high temperature and no coloration was observed.

In Chapter 5, the author deals with organically bridged PSQ synthesized from 3-glycidyloxypropyltrimethoxysilane and tetraethylene glycol bis(triethoxysilylpropyl)ether (BTESP-EG), aiming to suppress degradation under high humidity conditions. A poly[3-(2,3-dihydroxypropoxypropyl)-co-tetraethylene glycol]silsesquioxane (PSQ-Diol/EG) film was prepared via the sol–gel reaction of 3-glycidyloxypropyltrimethoxysilane (GPTMS) and BTESP-EG. From the water uptake and contact angle measurements, it was concluded that the tetraethylene glycol chains of the PSQ-Diol/EG film were sufficiently hydrophilic not to suppress the antifogging abilities of PSQ-OH. For the mechanical properties, the PSQ-Diol/EG film exhibited a high scratch resistance of 2.4–3.5, which was similar to that of PSQ-OH film. It was demonstrated that the introduction of tetraethylene glycol chains did not decrease the water uptake and scratch resistance. For durability, the water uptake of the PSQ-Diol/EG film did not decrease, and the formation of cracks was not observed. The space effect of the tetraethylene glycol chains inhibited the residual silanol groups from being condensed, and the flexible chain effect provided film stability upon volume changes during the repeated swelling–drying processes.

In this thesis, the author demonstrates that the development of PSQ antifogging materials with both water uptake and scratch resistance are at high level could be achieved by the choice of appropriate hydrophilic groups. In addition, the author clarified that organically bridged PSQ could improve environment resistance. In the future, PSQ will enable the design of new antifogging materials.

List of publications

1. T. Maeda, T. Hamada, S. Tsukada, D. Katsura, K. Okada, J. Ohshita, Antifogging Hybrid Materials Based on Amino-Functionalized Polysilsesquioxanes, ACS Applied Polymer Materials 3(5) (2021) 2568-2575. (Chapter 2)

2. T. Hamada, T. Maeda, K. Kawashima, T. Sugimoto, A. Tanaka, Y. Tanaka, D. Katsura, S. Mineoi, Y. Kaneko, J. Ohshita, Effect of the Amine Hydrochloride Salt on the Antifogging Properties of Amino-Functionalized Polysilsesquioxane, ACS Applied Polymer Materials 5(2) (2023) 1596-1605. (Chapter 3)

3. T. Hamada, T. Sugimoto, T. Maeda, D. Katsura, S. Mineoi, J. Ohshita, Robust and Transparent Antifogging Polysilsesquioxane Film Containing a Hydroxy Group, Langmuir 38(18) (2022) 5829-5837. (Chapter 4)

4. T. Maeda, T. Sugimoto, T. Hamada, D. Katsura, S. Mineoi, J. Ohshita, Highly Durable Antifogging Materials Based on Polysilsesquioxane with Double Hydrophilic Groups: Effect of Bridged Tetraethylene Glycol Chains in Polysilsesquioxane Films, ACS Applied Polymer Materials 4(10) (2022) 7599-7606. (Chapter 5)

Acknowledgments

This thesis is a summary of the author's studies from 2020 to 2023 under the direction of Professor Joji Ohshita at Hiroshima University.

I would like to express my gratitude to my supervisor Professor Joji Ohshita for his advice and warm encouragement. I am also grateful to Lecturer Takashi Hamada for helpful and careful advises. I would like to thank Professor Toshinori Tsuru, Associate Professor Ichiro Imae, Assistant Professor Yohei Adachi. I would like to thank Dr. Kazuaki Kawashima, Mr. Susumu Mineoi, Ms. Yuko Tanaka, Mr. Katsuhiro Horata, Mr. Daiji Katsura, Ms. Sakino Takase, Mr. Sun Weipeng, Ms. Wang Conghuan, Mr. Takashi Kai, Mr. Keigo Kawakami, Mr. Kei Oshima, Ms. Maho Kurihara, Mr. Mitsuru Sakabe, Mr. Tetsuya Sugimoto, Mr. Kohei Yamada, Mr. Arata Tanaka, Mr. Takumi Hasegawa, Mr. Tsubasa Yoshio, Mr. Lin Zhixin, Mr. Shota Terao, Mr. Ryuji Matsuura, Mr. Ryuto Miyazaki for their kindness and collaboration.